TECHNISCHE UNIVERSITÄT WIEN
Vienna University of Technology

DIPLOMARBEIT

URBAN HEAT ISLAND AND MITIGATION STRATEGIES FOR STUDY CASE

VIENNA

**ausgeführt zum Zwecke der Erlangung des akademischen Grades
einer Diplom-Ingenieurin
unter der Leitung von**

Univ. Prof. Dipl.-Ing. Dr. techn. A. Mahdavi

E 259-3 Abteilung für Bauphysik und Bauökologie

Institut für Architekturwissenschaften

eingereicht an der Technischen Universität Wien

Fakultät für Architektur und Raumplanung

von

Blagovesta Dimitrova

Matrikelnr. 1027621

Wien, am

TABLE OF CONTENTS

Abstract

The aim of this work is to give useful information to urban planners and architects concerning the interactions between buildings and climate change on a micro-scale level, or the so called *urban heat island* (UHI). Recent long term measurements from different weather stations in Vienna are summarized and discussed to create an overview of the spatial, daily and seasonal distribution of this phenomenon. In order to support and narrow the analysis to a more detailed level two urban canyons are chosen for field surveys with the aid of mobile measurements. The obtained data serve as a base for the proposition of mitigation strategies for the chosen case studies. The proposed approaches are simulated with computational fluid dynamics software in order to predict the magnitude of potential UHI reduction. The study confirms the importance and necessity for climate-adaptation procedures in the building stock, building codes and urban planning regulations of Vienna.

Zusammenfassung

Das Ziel dieser Arbeit ist es, nützliche Informationen den mikroklimatischen Wandel oder die so genannte *städtische Wärmeinsel* betreffend, an Stadtplaner und Architekten zu geben. Um einen Überblick von der räumlichen, täglichen und jahreszeitlichen Verteilung dieses Phänomens zu bekommen, wurden kürzliche Langzeitabmessungen von verschiedenen Wetterstationen in Wien zusammengefasst und diskutiert. Zur Unterstützung und Detaillierung der Analyse wurden zwei Straßenschluchten in der Stadt gewählt. Untersuchungen vor Ort wurden mit Hilfe von mobilen Wetterstationen durchgeführt. Die erhaltenen Daten dienten als Basis für Vorschläge zur Abschwächungsstrategien für die Fallstudien. Die vorgeschlagenen Methoden wurden mit einem numerischen Strömungsmechaniksoftware simuliert um das Ausmaß für potenzielle Abschwächung des urbanen mikroklimatischen Wandels vorauszusagen. Die Studie bestätigt die Wichtigkeit und Notwendigkeit von Klimaanpassungsverfahren in dem Gebäudebestand, den Bauvorschriften und den Städtebauverordnungen der Stadt Wien.

Acknowledgements

1. INTRODUCTION

1.1 Objective

The aim of this research is to ascertain the urban heat island of Vienna, to study the factors that are influencing it and to try finding most appropriate methods for mitigating this phenomenon. Numerous studies have been done before to define this occurrence for other urban places all over the world (Oke 1981; Montavez et al. 2000; Ferguson et al. 2008; Kolokotroni and Giridharan 2008). Despite the outlines that can be drawn as a conclusion from them, a significant fact is noticed - the elements that influence micro-environment are different according to the urban context. The factors that have a positive impact in one place can have a negative one in another. They alter with the specific geographic location, atmospheric conditions, urban properties and population (Oke 1987). These circumstances evoke a demand for a deeper research of local characteristics. Once a proper description of micro climate is drawn for the city of Vienna the correct methods can be applied to assure rational energy management, human comfort and create a more sustainable living environment.

1.2 Motivation

The steady growth of cities and increasing density of urban fabrics cause substantial changes to urban climates (Oke 1981). Soil and vegetation are constantly replaced with man-made structures, altering this way natural air-flow, surface properties, water, energy and mass balances (Oke 1987). The phenomenon of heat island, considered to be the result of such metropolitan developments, aggravates the situation further. Its main properties - increased air temperatures and consequently altered air humidity levels – give rise to an unhealthy and often pernicious outdoor environment and excessive cooling energy use indoors. Nevertheless, through better understanding of UHI and its influencing factors the appropriate methods for mitigating can be found and applied. Detrimental consequences can be reduced to a minimum and habitability of cities increased.

Alleviating the main characteristic of UHI – increased temperatures - is followed by series of benefits for urban residents and their environment (Figure 1.1). It improves outdoor thermal comfort by reducing heat stress in hot summers and hence decreasing cases of heat-related morbidity and mortality (Matzarakis et al. 2011). Favourable thermal environment improves quality of life and provides people with psychological and physiological health (Harlan and Ruddell 2011). Lowering the air temperatures also reduces the amount of absorbed heat by urban surfaces which prolongs their life-expectancy and saves resources

on production, maintenance and disposal (Scholz and Grabowiecki 2007). Further economic benefit of decreased outdoor temperatures is the reduced cooling energy demand of buildings (Akbari et al. 2001). This improves their ecological performance by reducing emissions from power plants and ameliorates the financial state of building users.

Adding of greenery and water bodies is an important mitigation method aiming mainly reduced temperatures, reduced carbon dioxide and balanced humidity levels through the process of evapotranspiration (Oke 1987). Trees have positive influence on the human psyche, lower pollution levels and also can reduce the energy use in buildings providing wind shielding in winter and sufficient shading in summer (Doshi et al. 2005).

According to OECD statistical data for 2003 the building sector – both commercial and residential – contributed to 60% of the total net electricity consumption in these countries (OECD 2012). The same situation is valid for developing countries as well. Additionally, cooling electricity demand in OECD-countries increased by 13% for a period of 10 years – 1990 to 2000 (OECD 2012). These facts underline the immense necessity for change in building energy codes and urban planning regulations, and emphasize the enormous potential of building sector for alleviating the urban climates. That is why research on possible mitigation strategies has a significant role in creating a sustainable living environment. The outlines that are drawn with the aid of this study can give an important knowledge to architects and urban planners and make them responsive and supportive in the process of providing habitants with healthy outdoor conditions and increasing quality of life in urban settlements.
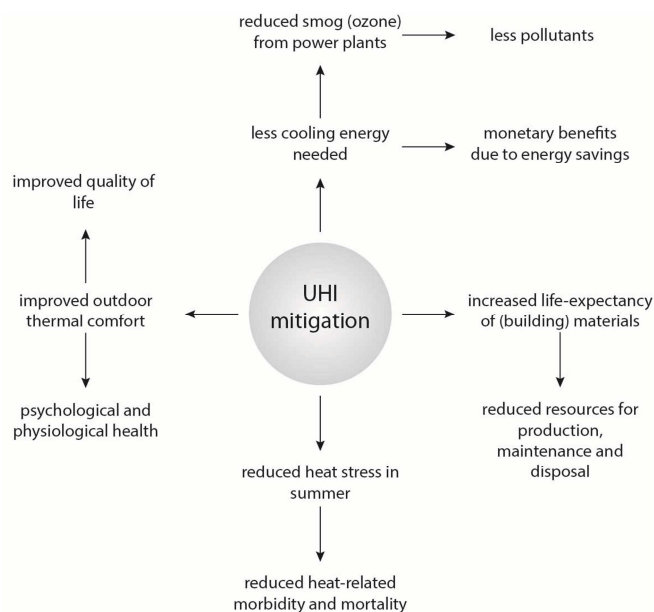
Figure 1.1 Beneficial consequences of mitigating the UHI

2. BACKGROUND

2.1 Urban heat island: state-of-the-art

2.1.1   What is UHI?

The rapid urbanization in the last decades has caused meaningful changes in urban climates. Almost 80% of the people in the European Union are living in cities and spend 50% of their free time outdoors (Drlik 2010). Increased population density and growth of impermeable surfaces replacing vegetated ones is related to aggravation of air quality, increased anthropogenic heat release and series of other environmental issues. Higher temperatures during summer periods are the reason for increased cooling electricity demand in buildings, leading not only to costs - related problems for the users but also to serious air pollution from power plants. These problems are causing human discomfort and unhealthy outdoor as well as indoor conditions. That is why places with increased human concentration require more detailed assessment.

The issues listed above are considered the main reason for the occurrence of the phenomenon *urban heat island* (Howard 1818, Oke 1987, Akbari et al. 1990). This term has gained a lot of interest among scientists in the past decades. It is described as the positive difference between urban temperatures and surrounding rural and suburban ones. The intensity of this occurrence is observed to be the highest in city centers, where human concentration is higher and impermeable surfaces prevail, and decreasing to the city boundaries. When this intensity is plotted above a city cross section the form resembles an island, where its name comes from (Figure 2.1). The following formula is used for the calculation of UHI intensity (UHII) in this study:

$$\Delta T_{u\text{-}r} = T_u - T_r \text{ [K] (Oke 1987), (2.1)}$$

where T_u is the air temperature in the urban center, and T_r – air temperature in the reference rural location.
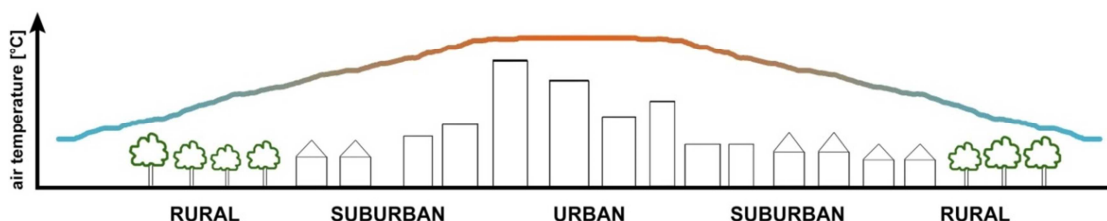

Figure 2.1 Cross section of a typical UHI

2.1.2 First observations

First observations about urban climate are made by Luke Howard in 1818. His documentations from 1833 indicate clear temperature differences between the metropolitan part of London and its rural surroundings (Howard 1833). Almost three decades later these interpretations are confirmed by another scientist Emilien Renou for the city of Paris. A pioneer of this field for the city of Vienna was the biometeorologist Wilhelm Schmidt. In the beginning of 20th century he used meteorological equipment attached to a vehicle in order to make point measurements in the near-surface atmosphere, which became the standard way for such measurements for the next 50 years (Mitchell 2011).

2.1.3 Causes and characteristics

The theories of these scientists point out several main causes for the formation of heat islands in developed areas – reduced evaporation, increased heat storage and net radiation, reduced convection and increased anthropogenic heat. These causes are affecting the natural energy balance in different ways. The reduced evaporation for example is caused by the lack of vegetation and the usage of impermeable surfaces in cities (Akbari et al. 1990). According to Akbari et al. (1990) most of these surfaces have higher thermal diffusivity values, which is the reason for increased heat storage. The authors state that a raise in the net radiation is observed as a consequence of low solar reflectance of urban materials, higher levels of air pollution and higher quantity of urban fabrics. Dense urban structures are entrapping heat and slowing down wind speed that leads to reduced convection (Akbari et al. 1990). All these factors are causing also increase in energy use followed by higher anthropogenic heat releases. UHIs are characterized by higher air and surface temperatures, and thermal inversions (Oke 1987). They are also observed to have larger effects in a clear and calm, cloudless weather, when short-wave radiation can reach urban surfaces completely unhindered (Gartland 2008).

2.1.4 Key studies

Properties of UHI and causes for its formation in different urban contexts are intensively studied. It is concluded that effects of the same UHI reduction strategies could be positive for one place and negative for another, depending on local topology, regional climate conditions, human perception or the particular urban geometry and morphology situation (Oke 1981). The surrounding micro climatic conditions should be therefore carefully investigated, so that appropriate strategies can be assigned. An overview of different

aspects of the heat island phenomenon and approaches for its mitigation is presented in the following sections.

2.1.4.1 Human comfort

Human thermal comfort and physical well-being depends to a larger extent on the surrounding meteorological conditions. Extremely high temperatures for example, or heat stress, are found to cause serious health problems and irritate already existing diseases. Exposure in an extreme hot weather can cause heat syncope, cardiovascular stress, thermal exhaustion or even heat stroke (Kleerekoper et al. 2012). Another consequence of heat stress is the enhancing effect on ground - level ozone formation in cities, which is considered to cause or worsen cardio - respiratory diseases, like for example cardio-pulmonary disease (Kleerekoper et al. 2012). Akbari et al. (1990) show the correlation between daily maximum ozone levels and temperatures for Los Angeles (Figure 2.2). It can be seen from the graph that smog levels are within the acceptable range (according to NAAQS) when temperatures do not exceed 74°F (23.33°C). Above 90°F (32.22°C) ozone levels reach a critical stage.

As stated in many studies city inhabitants are at greater risk of mortality from ambient heat exposure than individuals living in the surrounding rural places (Conti et al. 2005). Usually the more vulnerable part of population – old people, people with medical conditions and children under 5 - is affected by extreme weather conditions and UHI impact (Shahmohamadi et al. 2011). This phenomenon keeps temperatures in hot summer at higher levels even after sunset, when human body needs its regeneration. A severe heat wave in European cities in the summer of 2003, that caused thousands of deaths mainly among the elderly population, serves as an evidence for this statement and raises the public concern about aggravation of urban climates (Conti et al. 2005). A mitigation of the heat stress is therefore of great importance for human health and comfort. Alleviating high summer temperatures and taking of measures against high heat accumulation in urban structures is able to reduce heat-related morbidity and mortality risks. According to Hoyois et al. (2007) an outdoor temperature of 17°C is put in relation with the lowest mortality.

Different thermal indices like for instance PMV (Predicted Mean Vote) or PET (Physiological Equivalent Temperature) are developed to access and evaluate thermal environment and energy exchange between human body and its surroundings. These indices find an important application in rating the heat island impact on urban residents. With their help extreme thermal conditions like extreme cold or heat stress are quantified and more easily comprehended. PET index has nine levels of thermal perception (Table 2.1). Examples of
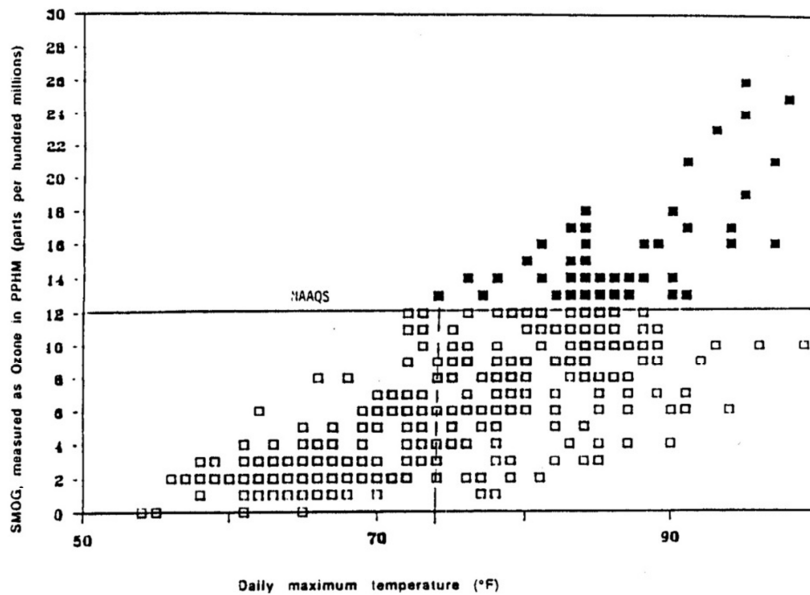
Figure 2.2 Correlation between ozone levels and temperature in Los Angeles, CA, 1985 (Akbari et al. 1990)

PET values for different weather conditions are given in Table 2.2.

Mean radiant temperature is another parameter referred to human thermal comfort and one of the most important objective dimensions for its evaluation. It is described as the "*uniform temperature of an imaginary enclosure in which the radiant heat transfer from the human body equals the radiant heat transfer in the actual non-uniform enclosure*" (ASHRAE 2001). Humidity levels and air velocity are determinant for this dimension. Despite of the mean air temperatures being comfortably warm, an individual may experience a great discomfort if seated in a shaded place with very strong winds and same mean air temperatures. This is the reason this parameter is taken into account in almost every study about human thermal comfort.

Understanding of such parameters is very important in order to provide city inhabitants with healthy and comfortable environment. Along with the human body the human psychology is also affected by higher heat-loads. Hot summer temperatures aggravate quality of open urban spaces and therefore enhance social isolation (Nikolopoulou and Lykoudis 2006). Efficient changes in the built environment and alleviating high temperatures in summer can increase physical activity, which also leads to improved mental health for urban dwellers (Harlan and Ruddell 2011).

Table 2.1

PET ranges for different grades of thermal perception (Matzarakis et al. 2011)

PET	THERMAL PERCEPTION
4°C	Very cold
8°C	Cold
13°C	Cool
18°C	Slightly cool
23°C	Comfortable
29°C	Slightly warm
35°C	Warm
41°C	Hot
	Very hot

Table 2.2

Examples of PET values for different weather conditions (Gulias et al. 2006)

EXAMPLES	T_a [°C]	T_{mrt} [°C]	WS [m/s]	VP [hPa]	PET [°C]
Winter, sunny	-5	15	0.5	2	-1
Winter, shade	-5	-5	5.0	2	-13
Summer, sunny	30	60	1.0	21	43
Summer, shade	30	30	1.0	21	29

T_a – air temperature; T_{mrt} – mean radiant temperature; WS – wind speed; VP – vapour pressure

2.1.4.2 Vegetation

Human perception of comfort is often closely related to greenery (Kleerekoper et al. 2012). Same authors underline that except for cooling down temperatures, it prevents also the ground-level ozone formation, affects positive the human psyche, forms a habitat for fauna, and makes cities more attractive. Adding vegetation in urbanized areas is therefore an efficient method for alleviating heat islands. As reported by Oke (1987) this strategy restores snow cover distribution and duration, and decreases storm water runoff – both of them detrimental consequences from removal of vegetation. According to Kleerekoper et al. (2012) there are four main types of urban vegetation: urban parks, street trees, private greenery and green facades or roofs. Their effects in a non - rural environment are described more detailed in the following part.

City parks

City parks, also known as urban forests, are vegetated areas within an urbanized environment (Kleerekoper et al. 2012). They can vary in size, type and amount of vegetation. Small green areas between residential buildings for example are mainly used for relaxation of dwellers. They influence surrounding temperatures only to a limited extent

because of their small size, but are preferred for the shading opportunities and psychological comfort. Furthermore they reduce CO_2 concentration (Oke 1987).

Larger green parks, often exceeding 1 ha (10 000 m^2), provide urban inhabitants with place for social interactions, sports and aesthetics, depending on the equipment of the park (Drlik 2010). The size of the area and bigger amount of vegetation affects temperatures, humidity and CO_2 to a much greater degree than small residential parks. Through efficient shading and process of evapotranspiration such landscaped areas build the so called *cool islands* within the cities, where temperatures are observed to be lower (Drlik 2010). Characteristic for cool islands is the expansion of their influence even outside the park area (Kleerekoper et al. 2012). A study about the cooling behavior of green spaces and its extension to the surroundings concludes that city parks can spread their cooling effect up to 200 - 300 m from their edge during night hours throughout all four seasons (Hamada and Ohta 2010). In the same study from August until October this extension during daily hours was even more than 300 m, reaching a maximum difference of 1.9°C compared to non-green urban locations. For that reason the authors suggest a rather scattered positioning of green areas. In this way their influence can be spread wider and more parts of the city can experience the positive micro-climate alteration. However, this beneficial impact may differ in another urban context. Surrounding high-rise buildings or heavy traffic level may affect and diminish the impact of a green park (Hamada and Ohta 2010).

Street trees

Another way to reduce CO_2 amount and air temperatures is planting trees along urban streets. Because of their dispersion their impact on air temperatures is not as significant as from green parks. Nevertheless, the evapostraspiration process of a tree on a sunny day is found to cool with a power of 20 - 30 kW, which is comparable to the power of more than 10 air-conditioning units (Kleerekoper et al. 2012). Moreover, street trees control luminosity and solar radiation, preventing it from reaching paved surfaces with high capacity of heat accumulation. Hence long-wave radiation from pavements is reduced and so is near - surface temperature.

Private greenery

Buildings owners can contribute to the cooling of urban temperatures through planting additional vegetation in their private plots. Except for reducing heat stress and CO_2 amount within cities, strategic positioning of shade trees and shrubs can substantially decrease building's energy use, and thus air pollution from power plants. Hence this method has an enormous potential to mitigate UHIs.

Trees can affect energy use and smog directly, as well as indirectly (Akbari et al. 1990). As reported by the same authors, urban trees directly provide buildings with shading and reduce this way the solar heat gain through building parts. Radiant heat gain is also decreased because of lower view factor and shading. In addition, evergreen trees prevent the wind coming to the building and with this shielding effect they reduce the infiltration in winter. Deciduous trees are advantageous because they allow the incoming short-wave radiation in wintertime, and provide sun protection with their foliage in summertime. Gartland (2008) underlines the importance of planting shade trees to the west and east of a building, because of the lower position of the sun in the morning and evening hours. Gartland also states, that when south-west and west facing windows are shaded with trees the building cooling energy use can drop down by 7 to 40%. The author suggests, that trees should be planted at least 1.5 - 3m away from the building and less than 10 - 15m, in order to provide their maximum protection. In addition, trees to the north of a building are effective in blocking cold winds in winter. Gartland reports further the results of a survey of Lawrence Berkeley National Laboratory about annual cooling and heating energy savings for a typical residential building in US. Providing that one tree is planted on the west and another one on the south side of the house, annual cooling energy savings can reach 18%, and annual heating savings - 2 to 8% (Figure 2.3). Nevertheless, it has to be noted, that energy savings from shade trees are higher for residential buildings than for commercial ones (Akbari et al. 2001). The authors mention also an important detriment of some types of shade trees – the capability to emit volatile organic compounds (VOCs). Because of this reason they must be chosen very carefully.

Akbari et al. (1990) point out also the indirect benefits of tree vegetation. Along with the reduced rate of outside air infiltration because of increased surface roughness and decreased wind speeds, trees cool down ambient air temperatures through the process of evapotranspiration. In this way they reduce heat gain of buildings. In hot summer days for instance, trees constitute natural "evaporative coolers" using big amount of water every day and creating the above mentioned cool islands. Buildings located near such cooler environments have lower cooling electricity demand (Akbari et al. 1990).

Additionally to the environmental and economic benefits, tree vegetation increases the value of properties and provides protection against floods through decreased rain run-off water (Akbari et al. 2001). It also adds aesthetics to the urban environment and plays an important role for the human psychology (Doshi et al. 2005).
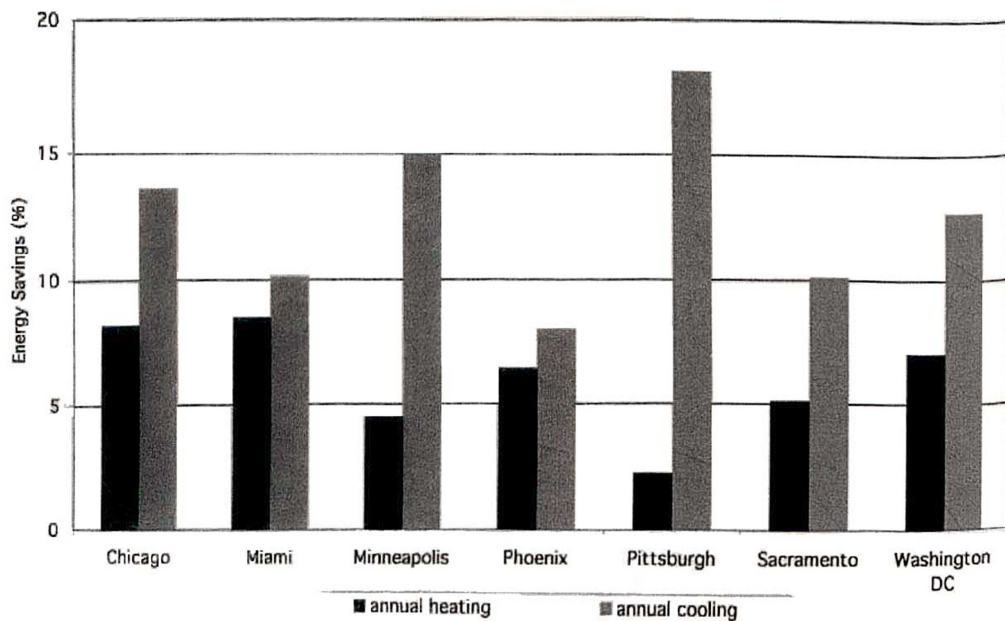
Figure 2.3 Predicted energy savings due to planted trees on the west and south of residential buildings (Gartland 2008)

Green facades

Another way to add greenery in cities is to cover facades with vegetation. The benefits of that measure are pointed out in a lot of research (Ottele et al. 2011; Alexandri and Jones 2008). Besides mitigating the UHI, increasing the biodiversity and improving the air quality, which is valid for all types of greenery, a "vertical garden" provides the dwellers also with better acoustical and thermal insulation, and can decrease building's energy use (Ottele et al. 2011). The authors differentiate two main categories of vertical greening considering their growing method: green facades and living wall systems (LWS). In the first case climbers planted in the ground, at the base of the building, are used as vegetation type (Figure 2.4). They can be either attached directly to the building surface, or supported by steel cables or trellis. Vertical gardens of the second category have their own soil in modular panels or other growing medium (Figure 2.5). They are more expensive than the first type and constitute a higher environmental burden due to maintenance requirements, materials production and difficulties with recycling. However, they have the advantage of the prefabrication as opposed to green facades that may need several years to cover the whole building surface. A disadvantage of the first category is also the limited height of growth to a maximum of 25m.

Regardless of its type, a vegetated facade protects the building materials from overheating in summer. Through shading and the process of photosynthesis a green façade catches

10

most of the sun light and this way less of it is absorbed by the building envelope. Positive consequences are observed in both directions – outdoors as well as indoors. In the first case reflected heat back to the surroundings is diminished and so is ambient outside temperature. In the second case building cooling electricity demand becomes lower and emissions from power plants are reduced. Both cases contribute to the improvement of air quality and UHI mitigation. The same result is observed also in winter time. Evergreen plants slow down air velocity near the building surface and decrease its convective heat loss. Hence, less heating energy is needed. Ottele et al. (2011) calculated that the additional thermal resistance of direct and indirect greening systems is nearly 0.09 Km2/W. After comparing all four types of green facades listed above, it was also concluded that the highest energy saving for heating is observed by the LWS based on planter boxes.
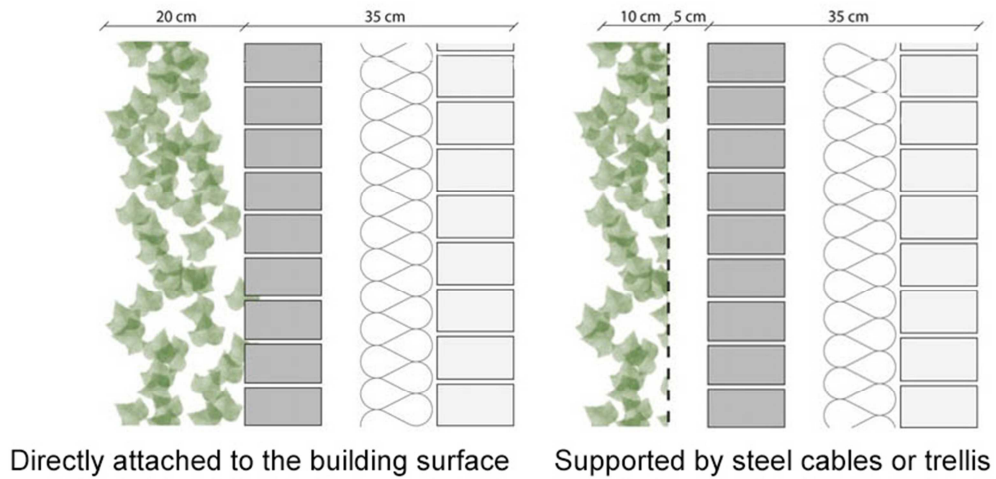

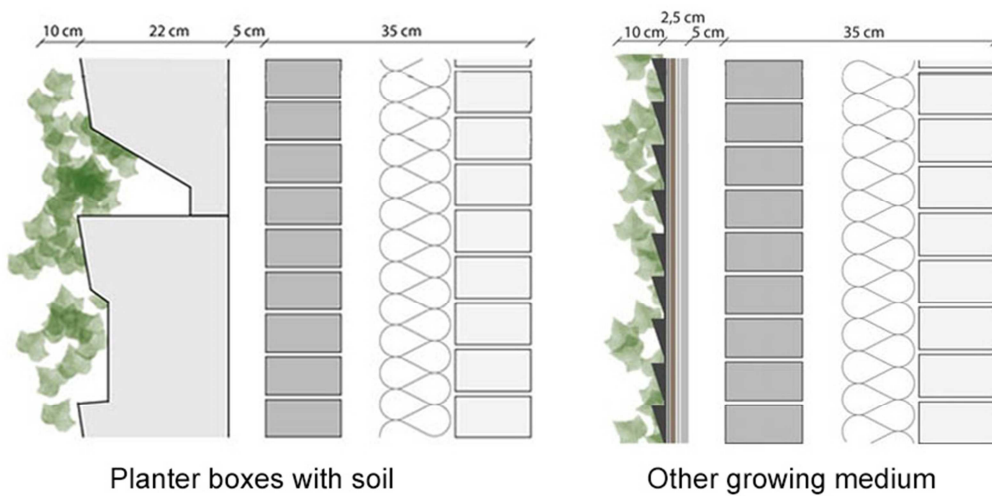*Figure 2.4 Green facades (Ottele et al. 2011)*

Figure 2.5 Living wall systems (Ottele et al. 2011)

Despite some of the negative aspects of the LCA of green facade systems, e.g. transport and waste, greening the building envelope is always a sustainable option when considering all other benefits that it provides.

Green roofs

Vegetating a roof surface is another opportunity to add greenery on a building. Generally there are two types of green roofs: extensive and intensive one (Kosareo and Ries 2007; Gartland 2008). The first type is lighter in weight with soil depth of up to 10cm. Plants species are restricted to grasses, mosses or wild flowers that need almost no human interference (Gartland 2008). A favorable property of these systems is that they can be applied even to inclined roofs with slopes of up to 30°. The second type of vegetated roofs, which constitutes a real garden, often including trees, can be used by the building occupants or it is even accessed by the public. Its soil depth can reach 25cm or more and can host much wider variety of plants than the extensive system. Because of its bigger weight an intensive green roof requires additional load-bearing structure below, which should be able to support the whole system even when fully saturated. This is not the case when referring to extensive systems. They need little or often no extra support. Intensive green roofs require higher initial costs and regular maintenance, whereas extensive ones require almost no human intervention after the plants are established.

The principle structure of a green roof remains similar, regardless of its kind (Figure 2.6). Both types need a growing medium for the plants and a drainage system under it. A thicker water proofing membrane than the traditional one is installed below, and finally the roof construction with its insulation constitutes the undermost layer of the system (Kosareo and Ries 2007).

The positive impact of vegetated rooftops on storm water runoff, air quality and UHI is proved in series of studies (Doshi et al. 2005, Kosareo and Ries 2007, Zinzi and Agnoli 2012). The rainfall in urban areas usually collects chemicals, heavy metals, oils and other pollutants from the impermeable surfaces on its way to the city drainage systems. Green roofs are a sustainable opportunity to prevent this polluted stream. An extensive green roof for instance can capture 10 to 75% of the rainfall that normally would become a runoff (Gartland 2008). An intensive one could capture all of the fallen rain water.

Vegetation directly influences air quality through production of oxygen and usage of CO_2 for
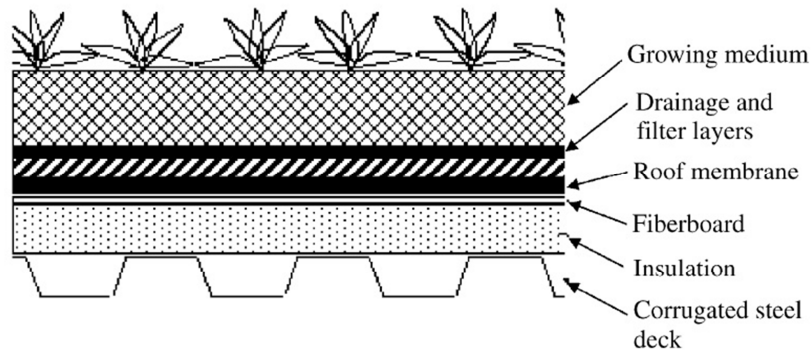
Figure 2.6 Cross section of a typical green roof (Kosareo and Ries 2007)

its biological processes, as mentioned before. Doshi et al. (2005) report an urban forestry study that found out that 2000m^2 of green roof area with unmowed grass could remove around 4000kg of particulate matter from surrounding air by trapping it on its foliage. Akbari et al. (2001) point out the potential indirect effect of plants on urban air. They claim that by reducing surrounding air temperature and surface temperature of the roof, vegetation is able to decrease the building peak cooling demand and consequently emissions from power plants.

The benefits gained due to green roof treatments concerning the UHI phenomenon are discussed by many scientists (Oke 1987; Doshi et al. 2005; Alexandri and Jones 2008). Removal of vegetation in cities and its replacement by impermeable surfaces disturbs natural snow cover and rain water distribution. Naturally it would be stored in the soil and vegetation layers as moisture and this moisture will evaporate and create a cooling effect for the surrounding temperatures. In areas, where such stored moisture is absent and water is not able to soak through the impermeable urban covers, this evaporative cooling does not take place. Surface temperatures remain heated and radiate this heat to the surrounding air temperatures (Doshi et al. 2005). Therefore, installment of additional green areas in cities, like for example on building roofs, is vital for recovering these natural processes and alleviate heat islands.

An additional effect of vegetated rooftops is the protection against thermal and ultraviolet degradation of the materials below (Doshi et al. 2005). The result of this is reduced resources for production, maintenance and disposal of building materials. Further outcome of these systems is the improvement of building energy performance (Doshi et al. 2005). Energy savings of up to 49% were observed for both, cold and hot seasons, in a nursery school in Athens after the application of a green roof (Zinzi and Agnoli 2012). Another survey in Brazil, reported by Zinzi and Agnoli, indicated a reduction of 92 - 97% in the heat

flux through a green roof compared to a ceramic and a metallic roof. All these study cases lead again to the conclusion that green roofs contribute to the improvement of air quality in urbanized areas and the mitigation of UHIs.

2.1.4.3 Water bodies

Water surfaces almost completely absorb long-wave radiation from the atmosphere without any substantial reflection or transmission (Oke 1987). The reflectivity of this natural element is nearly 3% and it can absorb up to 80% of the radiation (Radhi et al. 2013). Because of its high thermal capacity and the ability to evaporate at its surface, water preserves surrounding temperatures cooler than these over engineered covers, as demonstrated by Radhi et al. (2013) in their examination of UHI in Bahrain. They found out that temperatures over water bodies were 2.5 – 3.5°C lower compared to these over concrete and hard surfaces. The difference increased to almost 5°C when water and vegetation were combined.

These properties of water serve as a prerequisite for efficient heat island mitigation approaches. They can be used in the design of urban parks for instance. Kleerekoper et al. (2012) point out the importance of water bodies for cooling down the air temperatures in densely built-up areas. In their study a stronger cooling effect was identified when water had larger surface or it was dispersed like from a fountain. It was also discovered that this cooling effect was spread to a distance of about 30m from the water body. Accordingly, adding of fountains in small green areas or artificial lakes in bigger city parks influences positive the surrounding thermal environment. Smart fountain or artificial lake designs could be used even in winter time for other purposes.

2.1.4.4 Pavements

Pavements take high percentage of land cover in cities – usually between 25 and 50% (Gartland 2008). Typical paving materials are impermeable and dark in color. Both of these features enhance heat islands: the first characteristic reduces evaporation and induces storm water run-off issues, and the second one is responsible for increased absorption of heat and its release during the day and mostly during the night. Pavements structure has therefore a significant impact on the urban micro climate, as well as on the pedestrian thermal comfort. Indicators like permeability, thermal conductivity, solar reflectance, emissivity, porosity, convective heat transfer and heat capacity have to be considered for the assessment of pavements performance. Improving these physical characteristics could not only reduce the heat island effect but also enhance outdoor thermal comfort.

Gui et al. (2007) report that hot pavement temperatures are one of the major reasons for smog production. Application of paving materials with high thermal conductivity allows the heat gain from the solar radiation at the surface to be transferred away rapidly and consequently absorbed into the ground. Thus the conduction acts as a heat sink. Harvesting this conducted heat energy and its utilization could be a sustainable option for reducing the effect of UHI. Such novel approach is proposed by Mallick et al. (2009). Their concept involves a piping system with flowing water under asphalt pavements for removing the stored heat through convective heat transfer and using it in buildings. The computer simulations made during the study indicated 10 to 20°C difference between surface temperatures of conventional black asphalt and black asphalt with pipes underneath. Another key point of the survey is the improving of overall pavement conductivity through adding of aggregates with higher conductivity (e.g. quartzite). The authors state that if these modifications are implemented there would be significant savings in building energy consumption and reduction of ozone concentration, which also contributes to the mitigation of the UHI phenomenon.

Another recent approach made by Guan et al. (2011) proposes a mixture of phase - change materials (PCM) and asphalt aggregates to reduce the impact of surface temperatures on the environment. The exploration showed a significant improvement of the thermo-physical characteristics of the asphalt mixture. The thermostat effect is achieved through absorption and release of heat with the aid of PCM.

According to Gartland (2008) pavement solar reflectance, also called albedo, and its permeability are the properties with the greatest impact on pavements surface temperature. Solar reflectance is discussed in detail in the next section. Examinations of the second property are described below.

As reported by Liu et al. (2011) underground temperatures in urban areas are higher with around 3 - 4°C, and soil moisture content is much lower in comparison to these under suburban areas. Soil thermal properties are changed mainly because of insufficient rain infiltration and modifications in these properties raise a concern about stability of engineered structures (Liu et al. 2011). Hence, permeability of urban covers is a key factor to consider when referring to UHI reduction strategies. It enables water exchange between the ground cover and the deeper soil layers and in this way evaporation is able to take place.

Investigations in the field of permeable pavement systems (PPS) are made by Scholz and Grabowiecki (2007). They define permeability as the ability of water to flow through a

material. In their study a typical permeable pavement system is described and depicted (Figure 2.7). Its function is to collect storm water, to store it and treat it with geotextiles under the base of the pavement. The water is then used for recharging of groundwater. This part of the water that evaporates serves as a cooling mechanism of the material and the temperatures above it. The authors present also an improvement proposition for PPS. They suggest the installment of heating/cooling system underneath the sub-base, followed by a recycling process. The heated water could be utilized in buildings and save energy costs. The survey shows that geotextiles help prevent the transfer of pollutants into the base of PPS. A reduction of suspended solids by up to 64% and lean up to 79% is observed. Nevertheless, the long-term impact of PPS on the environment is still unclear.

Porosity is another important quality of paving materials. The degree of porousness is defined from the amount of water a material can hold (Scholz and Grabowiecki 2007). Likewise permeable materials, the use of porous ones is found to be very advantageous for lowering of surface and ambient air temperatures because of enabling the process of evaporative cooling. A study by Nakayama et al. (2010) about water-holding pavements showed an increased evaporation after rainfall leading to cooling effect. The air temperature at 1 m above the water-holding block dropped down with 1-2°C more than that above a lawn surface. Both types – permeable and porous systems, contribute also to better storm water management. However, porous materials have the disadvantage to be prone to clogging. Once their void spaces are clogged these systems have to be entirely removed and replaced, which makes them expensive and inconvenient in terms of environmental burden. Permeable covers are therefore preferred when considering pavements eco - performance.

Despite the various benefits of advanced and reflective pavement systems, decision making processes are still highly influenced by initial costs. Black asphalt requires about
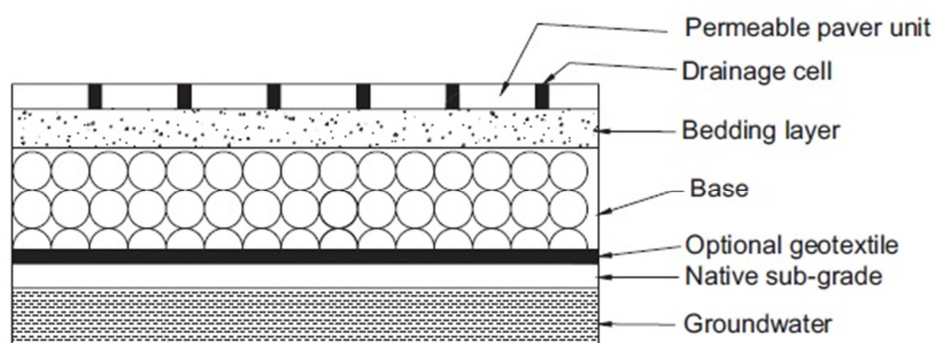

Figure 2.7 A typical permeable paving system (Scholz and Grabowiecki 2007)

33% less installation costs than concrete, but needs more maintenance and lasts only from 6 to 20 years, as opposed to concrete that has a life span between 13 and 35 years, tends to support heavier traffic loads and has equal or even less life-cycle costs (Gartland 2008). However, most developers of paving materials are not considering their LCA and prefer instead to have lower initial costs.

2.1.4.5 Cool materials

Cities are largely covered with sealed surfaces and this aspect makes them a major factor to study and to consider in UHI mitigation procedures. Improving their thermal performance is found to have plenty of beneficial consequences for the micro environment. Such type of advanced materials that have gained a lot of interest among scientists recently is *cool materials*. They are mainly defined as materials with high solar reflectance and high thermal emittance (Gartland 2008). However, the definition of "cool" can be extended by other properties like for instance permeable, porous or vegetated. These physical characteristics keep material surface temperatures lower, which leads to expanded material durability. In this way temperatures near them are also affected because of the decreased long-wave radiation. Further, air-quality is improved due to decreased summertime urban temperatures. Some studies about permeable and porous pavements even prove that rougher road surfaces absorb and hence decrease traffic noise (Gartland 2008).

An essential term referred to cool materials is solar reflectance, or the so called *albedo*. It is described as the ratio of reflected to incoming light and has a value between 0 and 1 - absolute absorption and total reflection, respectively (Akbari et al. 2001). By reflecting higher amount of the incident light instead of absorbing it, the material surface remains cooler and long-wave radiation to the surroundings is decreased. Taha et al. (1992) for example have studied different surface albedos and their relation to ambient air temperatures. They reported that a material with solar reflectance of 0.61 was only 5°C warmer than the ambient air. This difference rose to 30°C by conventional gravel with an albedo of 0.09. Doulos et al. (2004) provide a thermal image of sample materials that shows the essential difference between dark and light coloured materials and their surface temperatures (Figure 2.8).

Cool materials show positive influence not only during the day but also during the night. Oke (1987) states that at night there is no difference between high albedo surface and a lower one, but the coolness of the lighter surface is retained after sunset. These materials are used also for reduction of cooling energy loads in buildings which reduces the need for
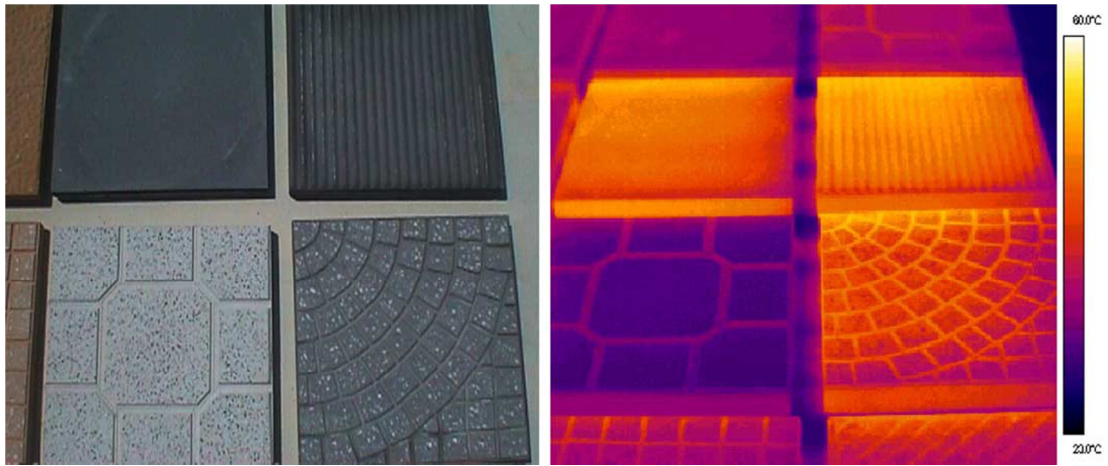
Figure 2.8 Visible and infrared image of selected materials (Doulos et al. 2004)

power generation and consequently emissions from power plants. Such characteristics of reflective materials underline their huge potential to moderate UHI effects.

Thermal emittance of surfaces is another important feature of cool materials. Emissivity, which is the measure of thermal emittance, is defined as the ability of a material to emit heat to the environment (Oke 1987). Similar to surface albedo, it is a value between 0 and 1. The higher the value, the cooler is the surface. Oke (1987) provides examples of albedo and emissivity for different construction materials (Table 2.3).

Paved and roofed surfaces typically take up to 60%, or sometimes in densely populated cities even more, of the total urban surfaces (Akbari et al. 2009). Their material and thermal characteristics are determinant for the micro climate. Akbari et al. (2009) estimated the potential net energy savings from increasing the albedo of roofs from 0.1 - 0.2 to 0.6 in U.S. cities. The cooling energy savings minus heating energy penalties accounted to 1 billion dollars per year. Combined with increased reflectivity of pavements and the consequent air-quality improvement, these potential savings raised to 2 billion dollars. Several approaches for effective increase in the reflectivity of roofs and pavements are presented below.

Pavements

Determinant for cool pavements is their albedo value. It is related to pavements maximum surface temperatures, as opposed to emissivity that is related to their minimum temperatures. Thermal emittance is considered to have less influence on pavements temperatures since most of the paving materials have primarily high emittance values. That is why ongoing research focuses mostly on solar reflectance.

Table 2.3

Solar reflectance and thermal emittance of some construction materials (Oke 1987)

SURFACE	ALBEDO	EMISSIVITY
Asphalt	0.05-0.20	0.95
Concrete	0.10-0.35	0.71-0.90
Brick	0.20-0.40	0.90-0.92
Stone	0.20-0.35	0.85-0.95
Wood	-	0.90
Tar and gravel	0.08-0.18	0.92
Tile	0.10-0.35	0.90
Slate	0.10	0.90
Corrugated iron	0.10-0.16	0.13-0.28
Clear glass (zenith angle less than 40°)	0.08	0.87-0.94
Clear glass (zenith angle 40 to 80°)	0.09-0.52	0.87-0.92
Paint: white, whitewash	0.50-0.90	0.85-0.95
Paint: red, brown, green	0.20-0.35	0.85-0.95
Paint: black	0.02-0.15	0.90-0.98

There are several common ways to make pavements cool. Porosity and permeability for example prevent accumulation of heat in the surface layers of a material. As mentioned before, elevated water content allows the process of evaporative cooling and keeps surface and ambient temperatures lower. Mixing light colored aggregates with conventional paving materials is another way to raise their reflectivity. A paving material with typical albedo value of 0.15 could raise its reflectivity up to 0.45 if mixed with lighter aggregate (Gartland 2008). Adding vegetation to sealed surfaces could also be an effective way to turn them into cool. Although it is a sustainable strategy, its application is limited because of particular use requirements. Parking lots for instance are a suitable place to apply this method.

Existing paved surfaces can also be turned into cool. They can be made more reflective by covering them with white toppings or pigments. Currently such methods are intensively studied, since they require less investment compared to fully replacement of pavements. Regular cleaning is another important action to maintain reflectivity - not only of painted surfaces, but also of conventional concrete pavements.

Akbari et al. (2001) studied the effects of changing the albedo of existing pavements in California, U.S. The results showed that an increase by only 0.25 in the albedo can lower the pavement surface temperature by up to 10°C. Excluding the electric power savings, the smog savings for the city of Los Angeles from cooler surfaces are estimated to be around 360 million dollars annually. Another examination conducted by Santero et al. (2011) concluded that if the albedo of a pavement is increased from 0.05 to 0.3 the ambient air temperature decreases with 0.6°C.

An important aspect when studying reflective materials is their correct application. A lot of literature points out the advantages of high albedo materials for the decrease of air temperatures (Taha et al. 1992; Akbari et al. 2001; Ferguson et al. 2008). Estimations of the reduced CO_2 levels because of albedo changes are stating indeed very positive results. However, only few of the existing investigations have studied the negative impacts of reflectivity. Glare problems, reducing the visibility of white line during driving, toxicity of white toppings and their harmful effect on the underlying soil after precipitation, increased buildings heating load in winter or human discomfort are rarely discussed in land cover related research. Furthermore, solar reflectance of surfaces decreases over time, because of factors like traffic or human pollution. For these reasons alternatives of high reflective pavements worth to be examined more detailed. Such innovative alternative is for example the one proposed by Kinouchi et al. (2004) – a paint coating applied on conventional asphalt that satisfies both - high albedo and low brightness. The material is less reflective in the visible part of the spectrum and high reflective in the near-infrared (NIR) spectrum. Experiments showed that the maximum surface temperature of the painted asphalt is 15°C lower than that of the conventional asphalt pavement.

Another proposal is made by Wan et al. (2009). A dark colored pavement coating with high albedo has been studied. Characteristic for the material are its NIR reflectance of 81%, low heat conductivity of 0.25 W/mK and high emissivity value of 0.83. The studies indicated up to 5°C lower surface temperatures for the tested coating compared to concrete slabs and up to 17°C compared to conventional asphalt.

Roofs

Roofs of buildings are the hottest spots seen in thermal images of cities and represent about 20% of the urban covers (Gartland 2008). Their surface temperature can reach 65 - 90°C. Cool roofing materials have two main characteristics that can mitigate the UHI – they have high solar reflectance and high thermal emittance: over 85%.

Direct and indirect energy and smog reductions are observed after applying a cool roof as reported in a study by Akbari et al. (2001). These effects started almost immediately by changing the surface albedo. The results show that building energy use, affected directly, and urban air temperatures, and thus smog, affected indirectly, are significantly decreased. An additional benefit of cool roofs is the limited absorption of ultraviolet light due to the lighter colour, which slows down the deterioration of materials and expands their use life.

Cool roofs provide cooling energy savings in buildings and decrease greenhouse gas (GHG) emissions and pollution at the local level. Two commercial buildings in Hyderabad,

India were examined to study the influence of different roof coatings on the energy consumption (Xu et al. 2012). Both had a flat concrete roof with an area of 700m^2 and experienced the same weather conditions lying next to each other – one to the west and one to the east. The roofs were not shaded by any neighbor buildings or trees. The investigation was divided into three phases – pre-coating from January to March, post-coating from March to July and post-coating from August to December. In the first phase both concrete roofs had an albedo value of 0.3. In the second phase the western building roof was painted in white (albedo of 0.7) and the eastern one in black (albedo of 0.1). In the third phase both roofs were coated white with reflectance of 0.7. The measured roof-surface temperatures clearly show the huge influence of surface solar reflectance on energy savings. The estimations indicated a potential for an annual energy use reduction of 10-19% for this particular location when a concrete roof is coated white. The GHG emissions related to these savings are approximately 11-12kg CO_2/m^2 of flat roof area per year. In order to establish such conclusions for another location and building type, a lot of field work has to be done. Influencing factors would be then also building design and operation, occupancy, surrounding structures, etc.

In predominantly cold-weather climates the increasing of albedo can have a negative effect on the environment, because it can increase the prevailing annual heating load. In such regions the elevated urban temperatures influence positively the electricity demand of surrounding buildings (Santero et al. 2011). Because of such assertions changes in pavement components should be made with the corresponding estimations and region-based research and simulations.

2.1.4.6 Urban geometries

Sustainable architecture is a complex term, combining responsibility not only for building users but also for pedestrians. A uniform part of this term is energy efficient performance, depending very strongly on geometry. It is the form of a building that defines to a great extent its indoor climate as well as its surrounding outdoor environment and consequently the surrounding behaviour of UHI. According to Oke (1987) UHI is fundamentally controlled by urban structures. They provide constant shading, produce heat, absorb and emit large amount of radiation. Additionally, they alter natural air flow. A correlation between UHII and air velocity was discovered in a study by Vardoulakis et al. (2013). Measurements in the city center of Agrinio, Greece indicated that stronger air velocities offer a substantial cooling effect for densely built-up and high populated urban areas (Figure 2.9). Nonetheless, there
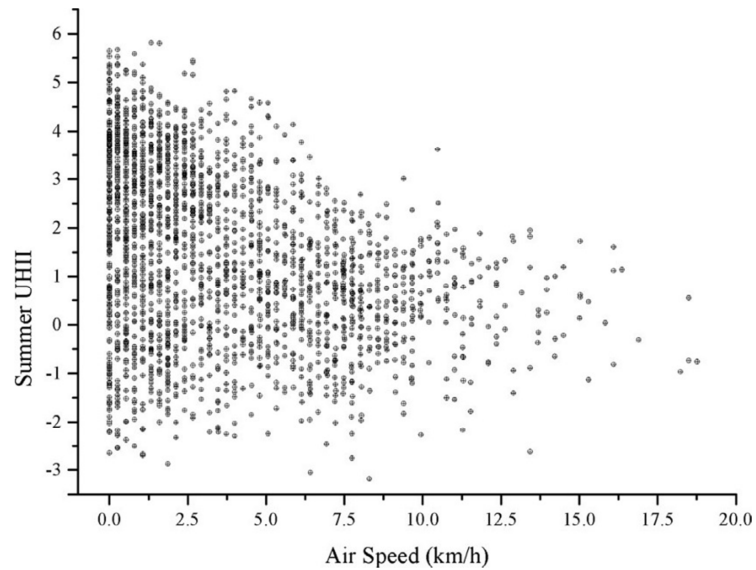
Figure 2.9 Correlation between summer UHII and air speed (Vardoulakis et al. 2013)

are also urban areas with very low air velocities where shading provides considerable protection in hot summer days due to high density of buildings (Andreou 2013).

Essential term related to urban geometries is sky view factor (SVF). It is a parameter used by urban climatologists to define energy and heat exchanges for a given place, considering the obstruction of the sky by the surroundings, compared to a place with no obstructions of the horizon (Holmer 1992). SVF of locations is a value between 0 and 1 or it is expressed as a percentage and indicates a relevant role for both - heat islands and outdoor thermal comfort. A case study in Curitiba, Southern Brazil demonstrated that places with less obstruction of the sky, i.e. high value of SVF, on days with higher temperatures are mostly perceived as uncomfortable due to overheating (Krüger et al. 2011). Nevertheless, same locations can provide comfortable outdoor environment on days with lower temperatures. Oke (1987) developed a formula for calculating the maximum UHI intensity at a location taking into account its SVF.

$$\Delta Tmax = 15.27 - 13.88 \; SVF \; (Oke \; 1987), \; (2.2)$$

Street canyons

Street canyon is a term used for streets restricted from both sides by buildings. It is often characterized by compromised pedestrian thermal comfort due to higher pollution levels, altered ventilation rates and elevated temperatures. Urban canyons are trapping heat as a consequence of higher obstruction of the sky and thus limited long-wave radiative heat loss from buildings. Street orientation, street morphology and height/width (h/w) ratio are found to be most important for evaluating thermal comfort conditions in street canyons. Andreou

(2013) compared different variances of these parameters for a hot period of time. In this work it was concluded that a street with an orientation E-W has the worst comfort conditions for all the h/w ratios, compared to a N-S oriented street. PET value levels for such streets with h/w ratios from 0.6 to 2.0 were outside the comfort zone for most of the day. Another objective of the study was a comparison between a contemporary straight street canyon with low h/w ratio and a traditional one with higher h/w ratio, and more organic form, but compact design of the buildings. It was discovered that despite the lower wind speeds, the comfort levels were higher in the traditional site due to increased shading.

Air quality and pollutants dispersion are a prime issue related to urban canyons. Some studies (Gromke and Ruck 2007; Ali-Toudert and Mayer 2007) declare that pollutants concentration depends mostly on wind direction and canyon aspect ratio h/w. A perpendicular direction of the wind to the canyon axis is taken usually as the worst scenario case for pollution dispersion in experiments. Contrary to the general assumptions, that vehicle traffic adds additional stress in air pollution, it can have a positive influence in the context of a street canyon. When traffic motion has been added in a laboratory experiment by Gromke and Ruck (2007) pollution levels decreased in comparison to standing but exhaust emitting traffic. It was inferred that traffic motion is an effective way to carry pollutants out of the canyon. In the same study the impact of trees for air quality in urban streets was also examined. The results showed that when tree crowns overtopped the canyon roof level, pollution concentrations at pedestrian level increased. A relation between crown diameter and air quality was also observed – the larger the tree crown, the more aggravated was air quality within the canyon, because of hindered natural ventilation. Additionally, tree spacing was examined. It was found that pollution levels decreased with increasing tree spacing.

Another laboratory study that explored vegetation impact in urban streets was made by Alexandri and Jones (2008). Green walls and green roofs in nine cities – all of them with different climatic conditions, were the subject of this work. In all nine cases decreases in canyon air and surface temperatures were observed due to vegetation. Asphalt surface temperatures decline of 0.9°C was noticed due to radiative cooling from green walls even for colder cities like Moscow, Russia, which has lower insolation and continental cool summer. The highest decline of 2°C was assessed in Riyadh, Saudi Arabia. Further, it was discovered that air masses enter the canyon much cooler, when green roofs are present and cause greater decrease in canyon temperatures, compared to the green walls case, where air masses enter the canyon already heated by the unvegetated roofs that absorb significant amount of summer insolation. PET values were examined when both cases were

combined. Levels improved in all nine locations. For the warmer cities Riyadh and Athens, Greece, they changed from "hot" to "slightly warm" and "comfortable" during the day, reaching "slightly cool" in the early morning, when greenery was applied.

According to many studies (Oke 1981; Akbari et al. 2001; Papadopoulos 2001) urban canyon models are most appropriate for evaluating how urban climate affects energy use in buildings. Surrounding weather conditions determine the operational system of a building, but often this system cannot satisfy the expressed summer heat island. A necessity for the installation of additional air-conditioning units is provoked. They are usually attached to the building's façade and the rejected heat from the compressor units contributes to the rise of air temperatures within the canyon. The UHI effect intensifies even more, buildings cooling energy demand grows and the process is back to initial position, where more air conditioning units are needed. In order to avoid such vicious circles, proper urban planning rules should be developed and energy management must be strongly considered when designing a building (Papadopoulos 2001). An appropriate solution is presented by Alexandri and Jones (2008). After the application of greenery on walls and roofs in urban canyons in several cities significant cooling load declines are observed (Figure 2.10). Ranging from 32% to 100% the displayed energy savings underline the effectiveness and importance of vegetation for the building performance and for the mitigation of heat islands in urban areas.

Building design

Canyon shape and building design are decisive for surrounding micro-climate. Different approaches are developed to ensure outdoor comfort and to minimize the impact of heat islands on buildings and vice versa. An example for such approach dates from the ancient Greeks that used porticos to provide sufficient shading at the ground levels of a building. This solution is used also in contemporary architecture in the form of street galleries. Ali-Toudert and Mayer (2007) examined and compared street galleries, overhanging facades and asymmetrical vertical profiles in urban canyons with different orientations (Figure 2.11). For E-W oriented canyons it was concluded that galleries are an effective way to ameliorate pedestrian comfort in hot summer days. Overhanging facades were most efficient for N-S streets. Asymmetrical canyon geometry has higher SVF, which allows higher amount of short-wave radiation, but also permits easier radiative heat loss after sunset. For N-S oriented canyons this option improved the thermal situation significantly between 14 and 17h. Another design solution used very often in modern architecture are adjustable building shading panels that can be closed for incoming sun radiation in summer and opened or
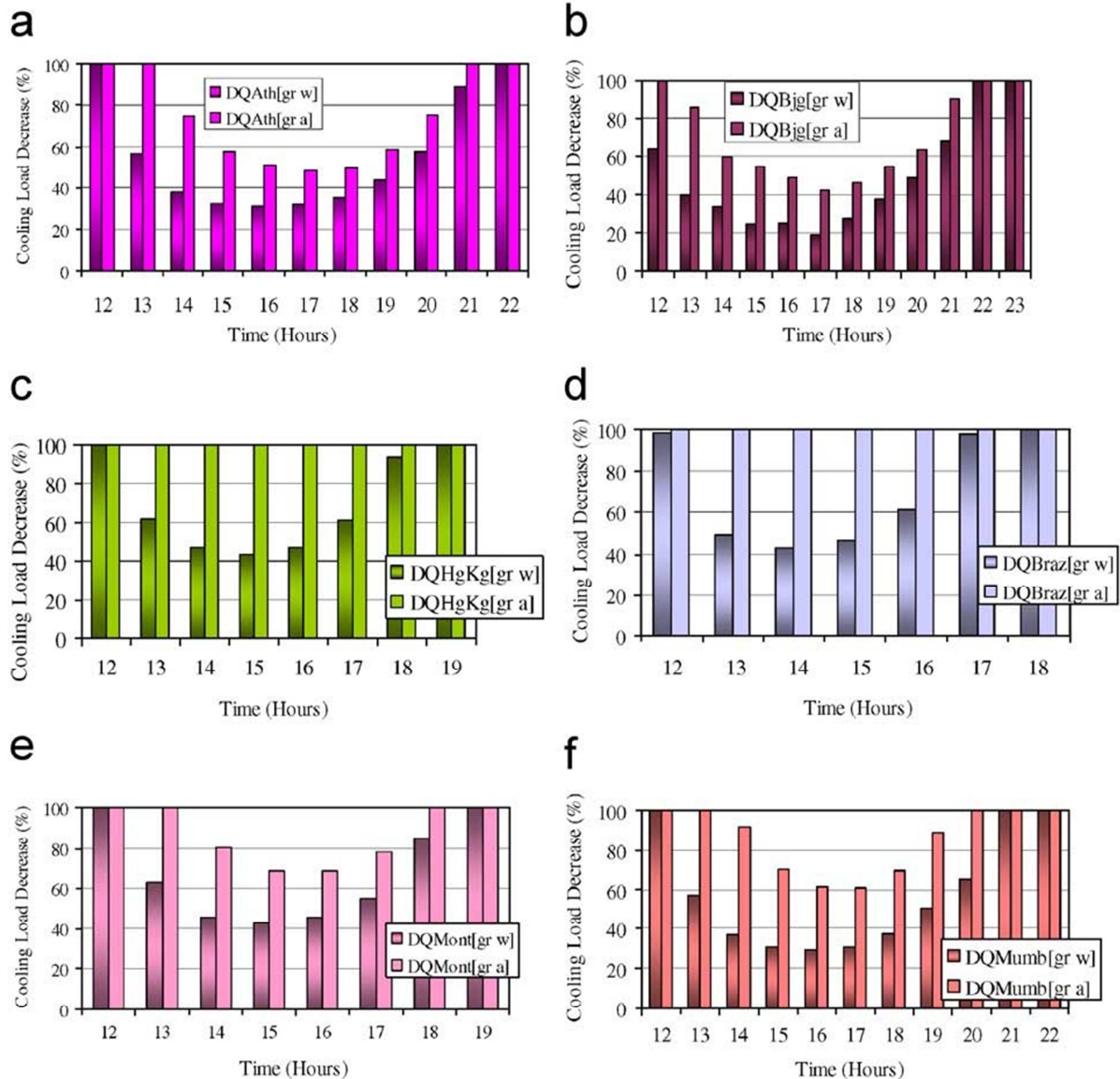
Figure 2.10 Cooling load decreases (%) for (a) Athens, (b) Beijing, (c) Hong Kong, (d) Brasilia, (e) Montreal and (f) Mumbai. "Gr w" refers to green wall case, and "gr a" to green wall combined with green roof case (Alexandri and Jones 2008)

completely removed in winter (Figure 2.12). Vegetated trellises can be also an efficient opportunity for pedestrian areas.

Development of urban areas is often related to vertical expansion of structures. Tall buildings, representative for big cities, successfully alter the surrounding micro climate. Once built, they become a constant shading source for ambient structures, absorb and emit large amount of solar radiation. In addition, air speed and turbulence at the base of high buildings is increased significantly. This creates an uncomfortable environment for pedestrians increasing their body heat loss in winter days and rendering a sudden change
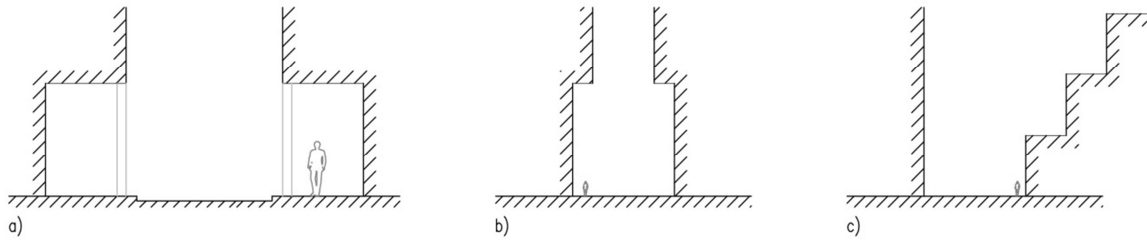
Figure 2.11 Design solutions for urban canyons: a) street galleries; b) overhanging facades; c) asymmetric vertical geometry
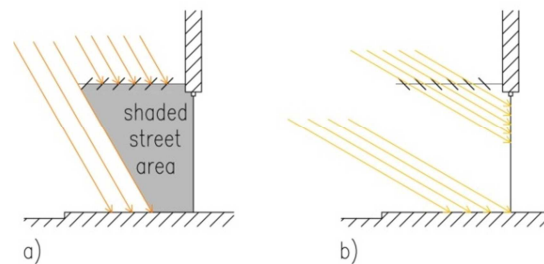
Figure 2.12 Adjustable shading panels: a) closed in summer and protecting pedestrians from direct sun light; b) opened in winter to allow short-wave radiation into buildings and pedestrian areas
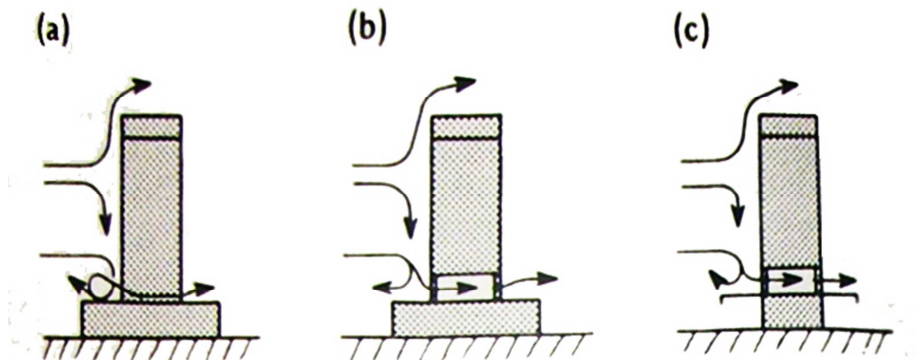
Figure 2.13 Design solutions for high buildings: a) larger ground level; b) open space between ground level and main building part combined with larger fundament; c) open space between ground level and main building part combined with a roof canopy (Oke 1987)

in temperatures in summer days. Oke (1987) proposes several design opportunities for high buildings to alleviate undesirably enhanced wind flow at the pedestrian level (Figure 2.13).

2.2 Situation in Vienna

As mentioned before local research of demographic and climatic properties is fundamental for the heat island analysis of a particular region. Knowing the area conditions in detail

constitutes a prerequisite for proper heat island surveys and mitigation approaches. Therefore a short background of study case Vienna is provided below.

Vienna is located in northeastern Austria in the Vienna Basin in the easternmost part of the Alps. Highest point above sea level is at 543 m, and deepest one - 151 m (Stadt Wien 2012). In accordance with Köppen-Geiger climate classification the city lies within the climate class *Dfb*: *temperate continental climate / humid continental climate* (World Maps of Köppen-Geiger Climate Classification 2012). Average temperatures in summer are between 22 and 26°C (ZAMG 2012). Winter periods are cold, with snowfall mostly from December until March, and autumn and spring seasons - mild. Predominant winds in spring and summer months are coming from western and north-western directions, whereas in autumn and winter from south-eastern directions (Schwab and Steinicke 2003). The region has moderate precipitation reaching its maximum in June and July. Danube River passes through the city and represents the only large water body.

Austria's capital has experienced a significant growth in the last century. For a period of 20 years population of Vienna increased with more than 12% and the steepest increase is in the last 10 years (Appendix: Figure 9.1). The population in 2012 accounts to nearly 1.737 million inhabitants as reported after the last census (Statistik Austria 2012). An adequate rise in the quantity of dwellings followed. More than 24 000 new residential dwellings are completed just in the years 1999 and 2000 (Appendix: Table 9.1). The degree of sealed surfaces around the center of the city became between 50 and 70%, and in the very central part - Innere Stadt, more than 70% (Schwab and Steinicke 2003). Buildings use outside the center is mostly residential and partly for services. Emissions in this area are from traffic and domestic sources, whereas in the center traffic emissions are prevailing and buildings use is mostly for services (Schwab and Steinicke 2003).

These facts represent a reasonable precondition for a transformation in the city micro-climate. Inevitable growth in electricity generation is observed with the rising numbers of new buildings. Ascent in smog levels and in degree of sealed surfaces modifies local atmospheric conditions and forces the effect of UHI. Differences between air temperatures within the city and around it gradually increase. A comparison of air temperatures was conducted between two locations in Vienna - one of them in the city center – Innere Stadt, and another one at the very boundary of the city, within the Vienna Woods – Neuwaldegg (Schwab and Steinicke 2003). The results showed that evening air temperatures in the inner part of the city are cooling down more slowly than in the suburbs. This fact is a reason for a night overheating in the city center. In the same study another two weather stations are compared - one in the center – Schottenstift, and one in the outskirts – Mariabrunn. The

measurements showed that the highest temperature differences occur in the early morning between 6:00 and 7:00, and in the evening after 19:00 CET (Figure 2.14). The lowest differences are observed in the middle of the day – between 10:00 and 14:00 CET. Formayer et al. (2007) also explored micro climate in Vienna. It was confirmed that UHI is most intensive at night in the city center – Innere Stadt, and state that in this central part the days of heat – the so called "Hitzetage", are 40% more than in the outskirts. The days of frost are less - around 60, than in the surrounding suburban areas where they are 80.

These atmospheric alterations and the pronounced UHI effect produce very often extreme conditions for the human body. Heat stress is one of them. Matzarakis et al. (2011) studied the relationship between heat stress and mortality in Vienna on the basis of the PET index. The analysis of long-term data from 1970 to 2007 indicated an increase in the air temperatures between April and October, and consequently an increase in the days of heat stress. Their exploration revealed a tendency – relative mortality rose on days with strong (PET ≥ 30°C) and extreme (PET ≥35°C) heat stress reaching values of 5.6% and 12.3%, respectively. This relationship raises a concern about the impact of UHI on human well-being and confirms the demand for a climate adaptation plan and detailed examination of local solution opportunities to provide healthy environment for Vienna citizens.
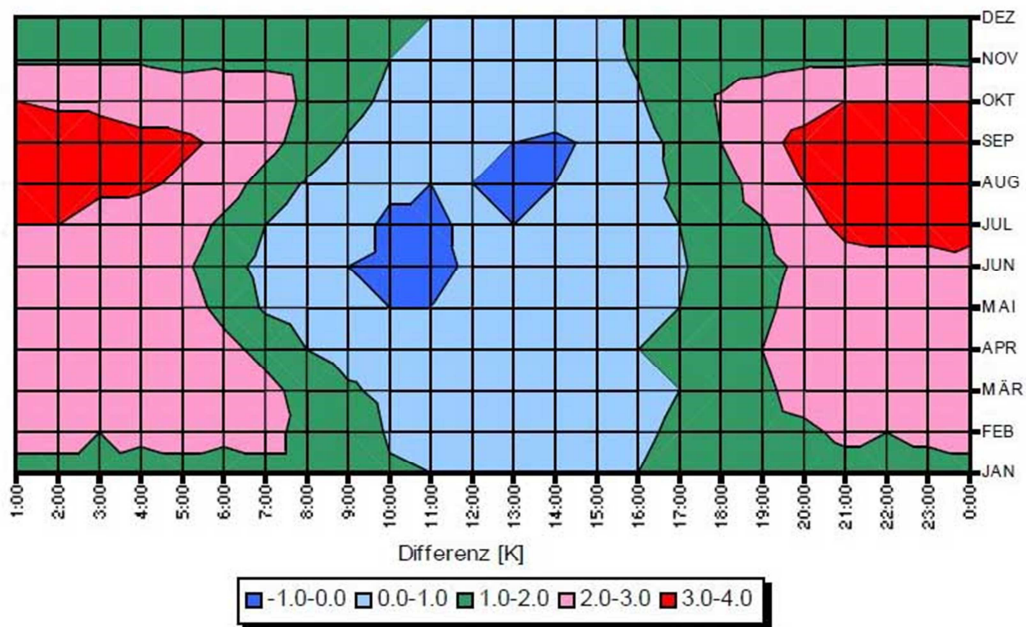
Figure 2.14 Average hourly air temperature differences between the stations Vienna-Schottenstift and Vienna-Mariabrunn, 1951-1980 (Schwab and Steinicke 2003)

3. METHODOLOGY

The structure of the proceedings for this study consists of three main components. The first one is the analysis of long-term weather measurements from four weather stations in Vienna and one rural station near the city, used as a reference location. The second part focuses on a single study-case examination with the aid of mobile weather measurements. The third part of the methodology constitutes computer simulations of proposed UHI reduction strategies for the study-case. Central European Time (CET) is used as a time format in the study.

3.1 Analysis of long-term weather data

First step of the methodology is the analysis of long-term weather data obtained from the Central Institution for Meteorology and Geodynamics (Zentralanstalt für Meteorologie und Geodynamik or ZAMG). Hourly values for five weather stations are summarized to provide

Table 3.1

Description of ZAMG weather stations and mobile measurements

WEATHER STATION	ABBREVIATION	HEIGHT ABOVE SEA LEVEL [M]	TYPE OF AREA	AVAILABLE DATA
Innere Stadt	U1	171	City center; densely built urban area with all kinds of traffic sources; main use of buildings for services and partly residential	12.1984 – 06.2012
Hohe Warte	U2	198	Loosely built residential area with big amount of vegetation	01.1984 – 06.2012
Donaufeld	U3	161	north-east from the center of the city; densely built-up area near Danube river	08.1996 – 06.2012
Groß - Enzersdorf	R1	154	18 km eastern from the city center; agricultural character	04.1994 – 06.2012
Seibersdorf	R2	185	Rural area to the south of the city; nearly half of the area is forested	06.1982 – 06.2012
Mobile Measurements	MM	-	Densely built-up urban area; 2.5km to the west of the center; mainly residential buildings with 4 to 5 storeys	Short-term data: 17. July, 7. - 9. August and 19. - 22. August 2012

Figure 3.1 Map of Austria with location of Vienna; position of Seibersdorf (R2) according to Vienna; exact location of used ZAMG weather stations and location of mobile measurements in the city

a more comprehensible view of the heat island distribution in Vienna. Available measured parameters from ZAMG are: air temperature, relative humidity, wind velocity and global solar radiation. The primal dimension used for the analysis is air temperature.

Three urban – Innere Stadt, Hohe Warte and Donaufeld, and two rural places – Groß – Enzersdorf and Seibersdorf, are chosen for the examination. A short description of the type of each area can be seen in Table 3.1. Their location in and around the city is shown on the map in Figure 3.1. The year 2011 is chosen for a deeper survey of the available measurements. Seasonal, monthly and hourly distributions of temperatures and UHI intensity are plotted. The hottest week of the same year is taken for a more detailed investigation.

3.2 Field surveys

3.2.1 Description

Mobile weather measurements constitute the second part of the methodology. According to many authors (Oke 1981; Montavez et al. 2000; Papadopoulos 2001) canyon geometry and its thermal properties are among the most important factors for UHI formation. As representatives of the urban environment in Vienna two densely built-up street canyons are chosen as case studies: Koppstrasse and Herbststrasse (Figure 3.2). Both streets are

Figure 3.2 Koppstrasse on the left and Herbststrasse on the right (picture by M. Vuckovic)

parallel, lying next to each other and located at about 2.5km to the west of the city center in the heavily built-up 16th municipal district Ottakring. Their orientation is south east – north western with an average h/w ratio of 1. Main properties of the case studies are summarized in Table 3.2.

Koppstrasse is a street with two car lanes and heavy traffic level during the whole day. It has high trees on both sides – nearly 12 to 14 m high, but it does not have a lot of soil area. Instead of whole stripes of soil, there are parking areas between the small soil spots where the trees are planted. The area of parking places takes around 15% of the studied location. There are no water bodies. Paving material is black asphalt for the car lanes and concrete for the pedestrian areas. Buildings type is the typical "Gründerzeit" style, made of plastered bricks – mostly 4 or 5-storey with an attic and light coloured plastered façade. Pitched roofs with red tiles define the top layer of the street. The average sky view factor is very low during the summer period because of the tree vegetation: 0.13. Width of the street is 18 m (Figure 3.3).

Herbststrasse is a street with two car lanes, parking places on both sides of the road and without any vegetation, water bodies or soil. The traffic level can be defined as a middle one and therefore a little bit more quite than its parallel street. The parking places take up to 20% of the investigated street section. Paving material is black asphalt for the car lanes and concrete for the sidewalks with a width of 12 m and 3 m, respectively (Figure 3.4). The surrounding buildings have the same style like at Koppstrasse. The roofs are pitched with typical dark-red roofing tiles. Because of the lack of trees and width of the street of 18 m the average SVF throughout the year is relatively big: 0.45.

Table 3.2

Main properties of the examined streets

PROPERTY	KOPPSTRASSE	HERBSTSTRASSE
Orientation	SE - NW	SE - NW
Street width [m]	18	18
Buildings height [m]	16 - 20	16 - 20
Building materials	Plastered bricks	Plastered bricks
Façade colors	Light colors (albedo 0.3 – 0.4)	Light colors (albedo 0.3 – 0.4)
Paving materials	Black asphalt, cement concrete	Black asphalt, cement concrete
Vegetation	Trees (12 - 14m high)	None
Parking places [%]	15	20
Mean SVF [%]	13	45
Traffic level	High	Middle

Figure 3.3 Dimensions Koppstrasse (in meters), crown diameter max. 8m

Figure 3.4 Dimensions Herbststrasse (in meters)

⊗ Measurement spot
🏠 Gemeindebau

Figure 3.5 Exact place of mobile measurement spots on the streets

The street sections that were taken for mobile measurements are both approximately 210 m long with a crossing unvegetated street between them - Kirchstetterngasse. Multiplied by the street width of 18 m, each of the studied street parts has an area of 3780 m^2.

Patterns of human activities are the same for both streets. There are no benches, green parks or other rest areas where people can stop for a longer time. That is why both locations can be considered as transitional for pedestrians. Highest stream of people is in the morning, from 7:00 until 9:00 CET, when most of the people are going to work, and in the late afternoon, between 16:00 and 18:00 CET, when they are on their way back. The periods for the mobile measurements were chosen exactly during these hours, so that the conditions when most people and vehicles are present can be studied. On each street three approximately parallel spots were chosen – one by the crossing and another two, representative for these streets. The parameters that were measured for every spot are: air temperature, relative humidity, wind velocity, global solar radiation and CO_2 concentration. The duration of measuring was one hour for each street, 20 minutes per spot. The first five minutes at each position were always considered as adaptation time of the equipment, in which the measuring tools reached equilibrium with the environment. Therefore they were not included in the analysis of the results. The exact location of spots for the measurements is shown on Figure 3.5. Their abbreviations used in the analysis can be seen in Table 3.3.

Table 3.4 shows that measurements at each spot are made always at the same time. For example first spot is always measured only from 7:00 to 7:20 and from 17:30 to 17:50 CET;

Table 3.3

Abbreviations of each spot for mobile measurements

ABBREVIATIONS MM	
Koppstrasse Spot 1	K1
Koppstrasse Spot 2	K2
Koppstrasse Spot 3	K3
Herbststrasse Spot 1	H1
Herbststrasse Spot 2	H2
Herbststrasse Spot 3	H3

Table 3.4

Exact time of measuring at each spot

TIME		PLACE
Morning MM	7:00 – 7:20 h	1. Spot
	7:20 – 7:40 h	2. Spot
	7:40 – 8:00 h	3. Spot
Evening MM	17:30 – 17:50 h	1. Spot
	17:50 – 18:10 h	2. Spot
	18:10 – 18:30 h	3. Spot

second spot is measured from 7:20 to 7:40 and from 17:50 to 18:10 CET, and so on. Exact dates and values of measurements can be found in Table 11.2 and Table 11.3 in the appendix.

3.2.2 Equipment

HOBO Weather stations were attached to bicycles and were used as monitoring tools (Figure 3.6). Each of them consists of a cup anemometer as a wind measuring tool, a pyranometer for the global solar radiation and temperature and humidity sensors. Frequency interval of measuring of the HOBO equipment was 15 seconds. Fish-eye photographs were taken with a Nikon Coolpix 8400 camera at 1 m height above ground at each measuring spot (Figure 3.7). Nikon UR-E16 Fisheye Lens was attached to the camera and mounted on a tripod with a compass on it, so that hemispherical sky images have north-southern orientation (Appendix: Figure 9.16). The images were then imported in Sky View Factor Calculator (Version 1.0) which computes SVF according to the proceedings described in Holmer et al. (2001). Synotech onset HOBO external data loggers were attached to monitoring tools and collected CO_2 data with frequency interval of 15 seconds (Figure 3.8).

Figure 3.6 HOBO mobile weather stations

Figure 3.7 Fish-eye camera

Figure 3.8 HOBO external data loggers

3.2.3 Data analysis

The monitored air temperature and relative humidity values were used to calculate the absolute humidity, or in this case the humidity ratio W, in gram water vapour per kilogram dry air. A sequence of equations was used to determine this parameter. First the saturation vapour pressure E (Formula 3.1) was used to compute the vapour pressure e (Formula 3.2). The partial pressure of dry air p_a was calculated according to Formula 3.3 in order to find the total pressure P_{tot} (Formula 3.4). The results were then used to calculate the

absolute humidity, or humidity ratio, W through the Formula 3.5. Obtained values were multiplied by 1000 in order to receive g/kg instead of kg/kg dry air.

$$E = 611.2 * \exp\left(17.08085 * T / (234.175 + T)\right) \text{ [Pa]} \qquad (3.1)$$

where E is the saturation vapour pressure and T - the air temperature in °C.

$$e = \varphi * E / 100\,000 \text{ [kPa]} \qquad (3.2)$$

where e is the vapour pressure, φ – the relative humidity, and E – the saturation vapour pressure from equation 3.1.

$$p_a = \rho_a * T / 0.0035 \text{ [kPa]} \qquad (3.3)$$

where p_a is the partial pressure of dry air, ρ_a - the density of dry air, T – the air temperature in K.

$$P_{tot} = p_a + e \text{ [kPa]} \qquad (3.4)$$

where P_{tot} is the total pressure, p_a is the partial pressure of dry air from equation 3.3, and e - the vapour pressure from equation 3.2.

$$W = \epsilon * e / (P_{tot} - e) \text{ [g/kg dry air]} \qquad (3.5)$$

where W is the absolute humidity, or humidity ratio, ϵ is the ratio of molecular weight of water vapour to dry air (ϵ = 621.97), e is the vapour pressure from equation 3.2, and P_{tot} – the total pressure from equation 3.4.

3.3 Computer simulations

The third part of the methodology is 3D-modeling of both urban canyons. The micro-scale models are developed in the Computational Fluid Dynamics (CFD) Freeware program called ENVI-met® (Version 4.0). ENVI-met is a three-dimensional micro-scale model, designed to simulate and analyze short-wave and long-wave radiation fluxes between buildings and their environment, taking into account shading, reflection and radiation (ENVI-met 2013). The typical vertical resolution used is 0.4m and a time frame of 24 to 48 hours with a time step of 10 sec. For the purposes of this study a 24-hour simulation time was taken. This version of ENVI-met calculates wind velocity as a nearly constant value during the whole simulation period. Therefore one average value is extracted as a representative for each simulation case. For a more accurate comparison temperature and relative humidity are considered at a height of 1.8m, since that was the approximate height of the HOBO sensors for mobile measurements. Albedo of facades in the configuration settings

was set to 0.40. The albedo of the dark-red roofing tiles was set to 0.2 (Gartland 2008; Akbari et al. 2009).

Both streets with surrounding buildings, paving materials and vegetation were modeled and receptor points were placed at the exact three positions at each street, where mobile measurements were taken (Figure 3.9 - 3.10). 20th August 2012 is taken for all the simulations since that was the hottest day during the mobile measurements. Differences between real and virtual temperatures on this date were minimized to a maximum of 1K in the simulation of the base case. The calibration of the ENVI-met model is shown in the Figures 3.11 - 3.13. In these graphs "E" refers to ENVI-met and "MM" to mobile measurements. After this calibration several UHI mitigation methods for the current situation are proposed and applied in the computational models, again for the same date and same weather conditions, so that the level of microclimate improvement for both of the study cases can be estimated. Simulated cases with their abbreviations are summarized in

Figure 3.9 Top view of ENVI-met models in base case situation with the exact placement of the receptor points (green spots denote the place of tree trunks)

Table 3.5.

The first improvement proposition for both urban canyons is to replace all the black asphalt pavements with concrete ones. According to many studies (Akbari et al. 2001; Santero et al. 2011) increasing the albedo of pavements is very important at the pedestrian level and leads to lower temperatures through higher reflection of short-wave radiation. This reduces the absorbed and emitted heat, which lowers the air temperatures within the canyon, directly increases use-life of paving materials, preventing overheating, and indirectly reduces cooling demand of the surrounding buildings (Akbari et al. 2001).

Second proposed mitigation method is increased albedo values of building facades. Their reflection value for base case is estimated to be 40%. For this simulation it is increased to 80%. As in the first improvement this is expected to reflect more of the coming short-wave radiation so that facades remain cooler. In this way the energy used for cooling decreases, which contributes to less CO_2 emissions from power plants. Lower surface temperatures of facades are also expected to keep ambient temperatures within the canyon at a more comfortable level.
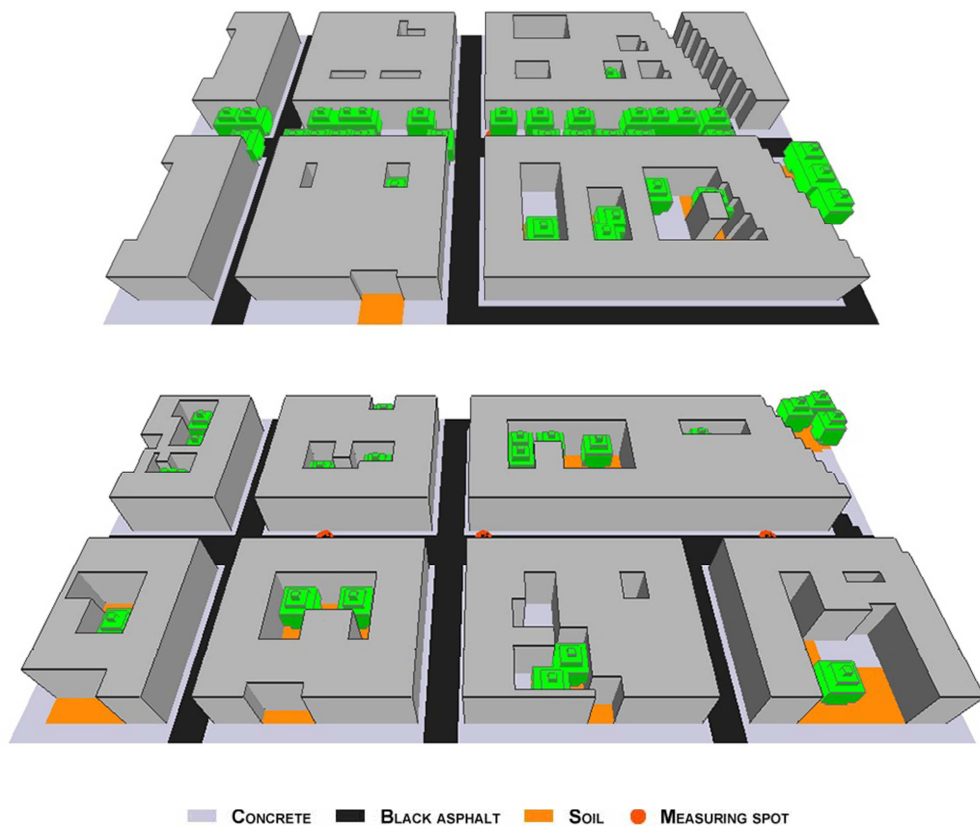
Figure 3.10 Perspective view of the ENVI-met models in base case: Koppstrasse (up) and Herbststrasse (down)
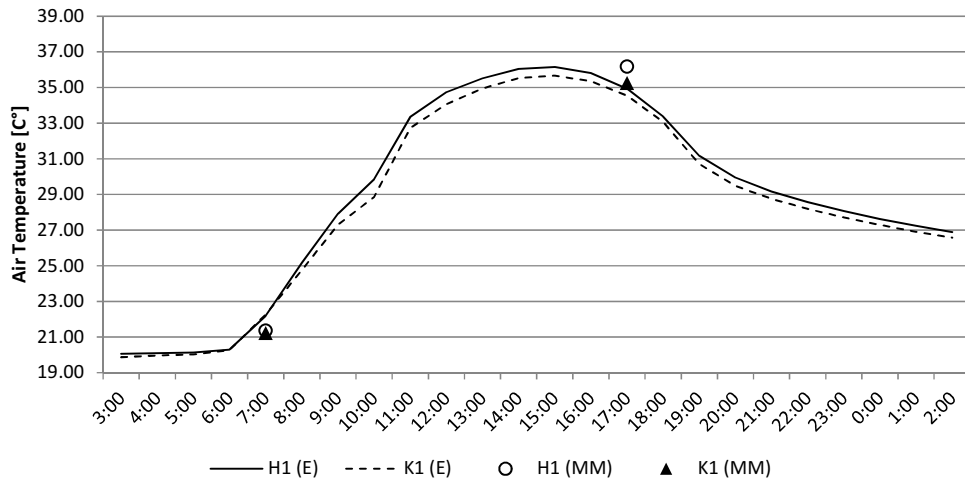
Figure 3.11 ENVI-met calibration: Spot 1
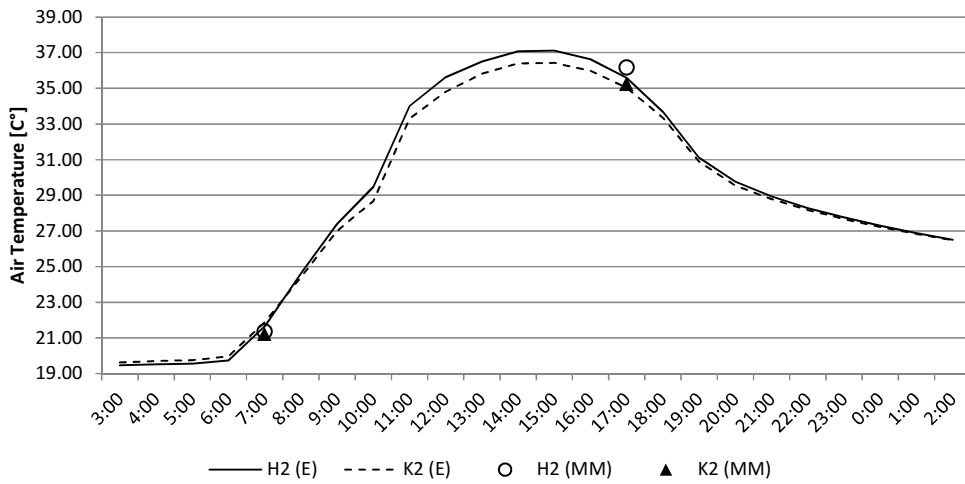
Figure 3.12 ENVI-met calibration: Spot 2
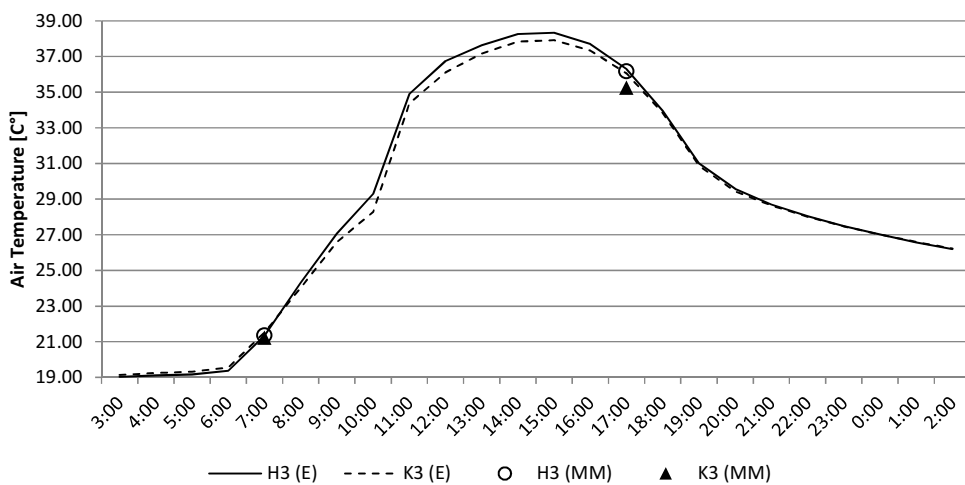
Figure 3.13 ENVI-met calibration: Spot 3

Table 3.5

Simulated ENVI-met cases

SIMULATION CASE	KOPPSTRASSE	HERBSTSTRASSE
Base Case (BC)	Current situation	
Improvement Case 1 (C1)	Black asphalt materials replaced with white concrete	
Improvement Case 2 (C2)	Increased albedo of building facades	
Improvement Case 3 (C3)	Larger tree spacing	Trees added
Improvement Case 4 (C4)	C1, C2 and C3 cases combined	

Third strategy applied in the computational model is adding of tree vegetation at Herbststrasse and making larger distances between trees at Koppstrasse (Figure 3.14). In the first case this method is supposed to lower air temperatures, increase absolute humidity and decrease CO_2 amount. The larger spacing between trees in the second case is expected to improve natural ventilation and consequently lower the temperatures and enhance the dispersion process of harmful particulate matter. In both cases trees are situated at minimum 10 m from street edges to ensure sufficient air flow induced by corner eddies (turbulent vortices of various sizes) entering the street canyon. Distance between tree trunks is kept at a minimum of 20 m and maximum of 30 m.

In the last simulated case all three methods are combined at each street in order to estimate the entire amount of mitigation if these strategies are applied together.

Altering the albedo values of roofs was also simulated. However, it did not have any influence on the examined parameters. Apparently this version of ENVI-met does not consider such alterations. Therefore reflection of roofs is not taken as mitigation option in the computer simulations and remained unchanged in all the cases. Green roofs were also not an option, because of the high inclination of the building roofs in the examined area. Another UHI and building cooling reduction strategy that is not available for application in this version of the software is greening of the building façade. This method is left only for theoretical analysis.

Figure 3.14 Top view of ENVI-met models in case C3 with the exact placement of trees at Herbststrasse and re-spaced trees at Koppstrasse

4. RESULTS AND DISCUSSION

Results from long-term weather data, short-term mobile measurements and ENVI-met simulations are compared and discussed. The potential of the proposed mitigation strategies and probable reduction of UHI intensity in the city of Vienna is analyzed.

All hourly data in the graphs is expressed by means of CET. Formula 4.1 is used for the calculation of mean values in the graphs:

$$y_m = \frac{1}{n} \sum y_i \quad (4.1)$$

where y_m is the arithmetic mean of the data set, n is the number of samples, and y_i is every individual sample.

4.1 ZAMG weather data

The following section presents the obtained summery of weather data divided into seasonal, monthly and hourly distributions of air temperatures and UHI intensities. An overview and a short description of the examined ZAMG weather stations and mobile measurements are provided in Table 4.1.

Mean hourly distribution of air temperatures for each season at all five ZAMG weather stations is depicted in the figures below (Figures 4.1 - 4.4). Seasons are divided by the exact equinoxes and solstices for the year 2011. The values are averaged on an hourly basis according to formula 4.1 and a reference day for each season is created.

Spring in this year began on March 20th and ended on June 21st. Figure 4.1 shows the distribution of air temperatures for the reference day of this period. The highest variance is monitored at the reference station R2 with a difference between maximum (20.63°C at 14:00) and minimum (12.58°C at 5:00) temperatures of 8.05 K. The lowest temperature difference of 5.76 K is measured for U1 with a minimum of 15.33°C at 5:00 and a maximum of 21.09°C at 15:00. Temperature differences between these two stations are the highest compared to the other locations. Small exceptions can be seen in the middle of the day between 10:00 in the morning and 13:00 in the early afternoon when values are almost the same or slightly higher at R2.

The summer of 2011 lasted from June 21st to September 23rd. In comparison to spring season temperatures here have lower ranges (Figure 4.2). Minimum and maximum values are again at 5:00h in the morning and 15:00 in the afternoon, but differences between them

Table 4.1

Description of ZAMG weather stations and mobile measurements

WEATHER STATION	ABBREVIATION	HEIGHT ABOVE SEA LEVEL [M]	TYPE OF AREA	AVAILABLE DATA
Innere Stadt	U1	171	City center; densely built urban area with all kinds of traffic sources; main use of buildings for services and partly residential	12.1984 – 06.2012
Hohe Warte	U2	198	Loosely built residential area with big amount of vegetation	01.1984 – 06.2012
Donaufeld	U3	161	north-east from the center of the city; densely built-up area near Danube river	08.1996 – 06.2012
Groß - Enzersdorf	R1	154	18 km eastern from the city center; agricultural character	04.1994 – 06.2012
Seibersdorf	R2	185	Rural area to the south of the city; nearly half of the area is forested	06.1982 – 06.2012
Mobile Measurements	MM	-	Densely built-up urban area; 2.5km to the west of the center; mainly residential buildings with 4 to 5 storeys	Short-term data: 17. July, 7. - 9. August and 19. - 22. August 2012

Figure 4.1 Mean hourly distribution of air temperatures at ZAMG weather stations for a reference day, Spring period 2011
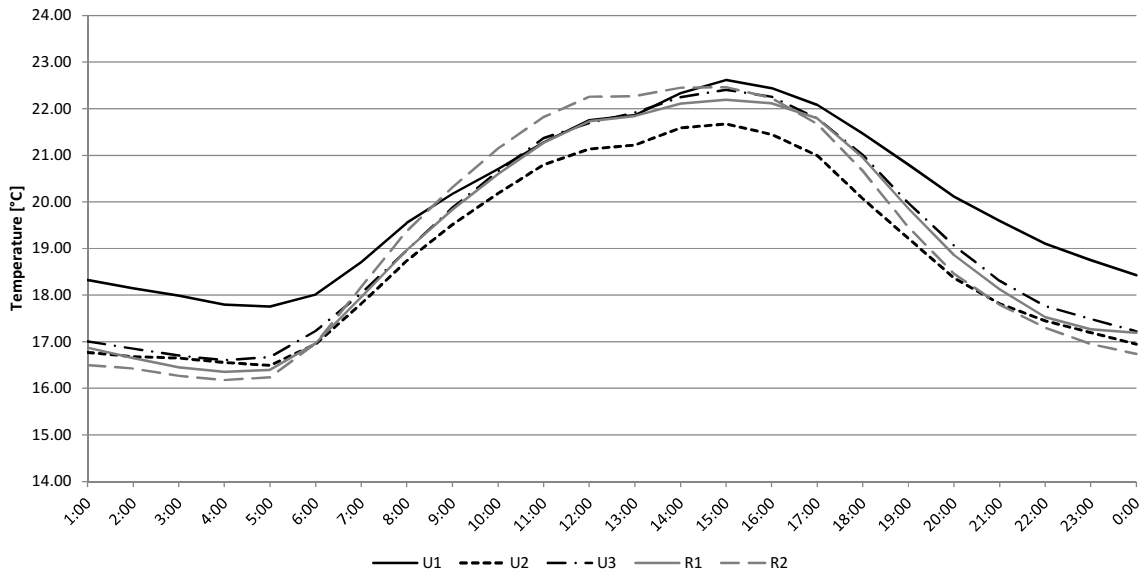
Figure 4.2 Mean hourly distribution of air temperatures at ZAMG weather stations for a reference day, Summer period 2011

are lower. The same occurrence with higher temperatures at R2 in the middle of the day can be seen also in this graph - from 9:00 until 14:00. During the whole day, between 7:00 and 20:00, temperatures at U2 are the lowest. The other four curves at that time are interlacing. During the night the same pattern is observed like for spring months – minimum values are at R2 and maximum ones at U1.

In the graph of the autumn season can be seen that temperatures variety is lower than the previous seasons (Figure 4.3). Differences between maximum and minimum temperatures at U1 amount to 3.1 K and 4.7 K at R2. Differences between the locations are expressed most visible during this season. Vertical order of curves (U1 at uppermost position, followed by U2, U3, R1 and R2 at the undermost position) remains almost the same throughout the day, with small exceptions in the afternoon. Minimum and maximum values are monitored again at R2 and U1, respectively.

Winter in 2011 began on December 22nd and ended on March 20th. Differences between day and night temperatures at each weather station are the lowest compared to the other seasons (Figure 4.4). Air temperatures range from 1.48°C at midnight to maximum 4.71°C in the afternoon for the rural R2 and from 3.29°C to 5.13°C for U1. The vertical disposition of curves from the previous season remains the same.

Seasonal temperatures at R2 – Seibersdorf - are the lowest compared to the other four stations as noticed from the previous graphs. Therefore the rural R2 is taken as a reference
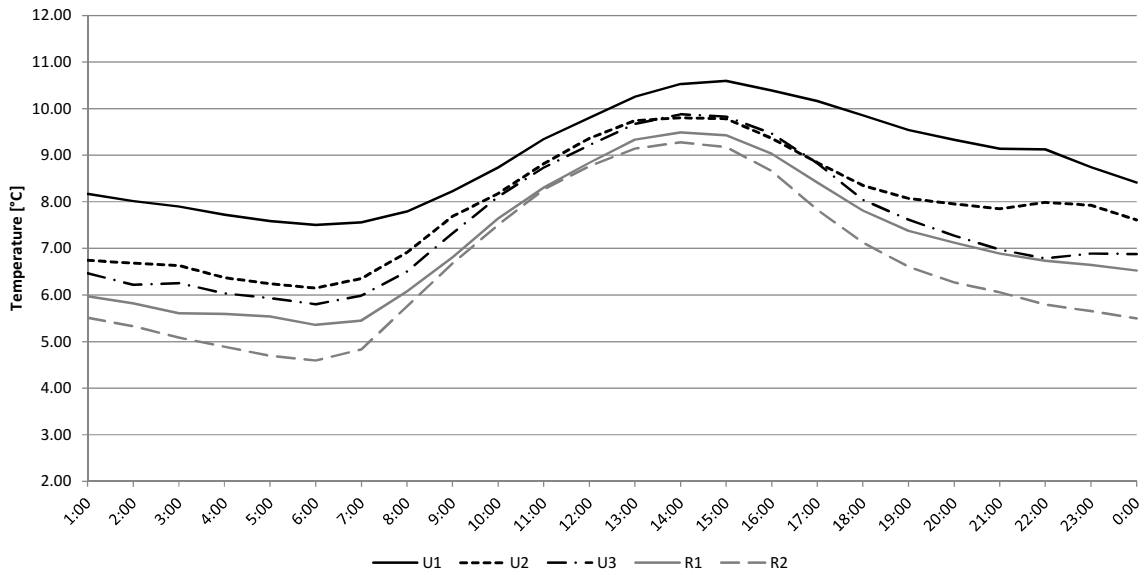
Figure 4.3 Mean hourly distribution of air temperatures at ZAMG weather stations for a reference day, Autumn period 2011
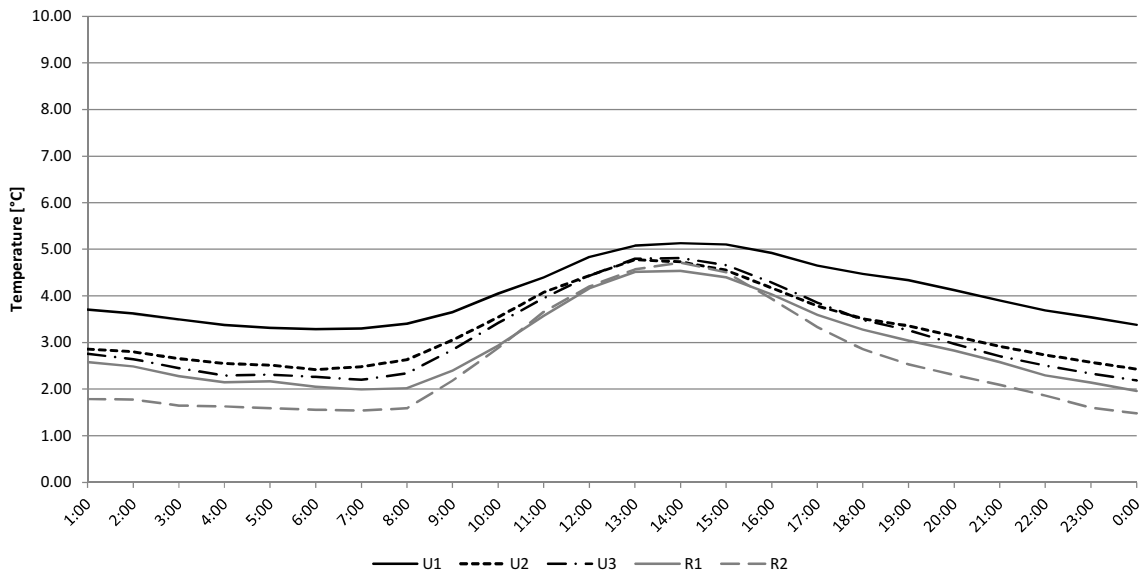
Figure 4.4 Mean hourly distribution of air temperatures at ZAMG weather stations for a reference day, Winter period 2011

location for the calculation of mean hourly UHII for each season in the year 2011 at the urban station U1 according to equations (2.1) and (4.1).

All four curves in the graph depict a rather nocturnal expression of UHII (Figure 4.5). Minimum values are seen in the middle of the day - from 10:00 until 14:00. An important aspect that is noticed is the position of the autumn curve that lies above all other curves
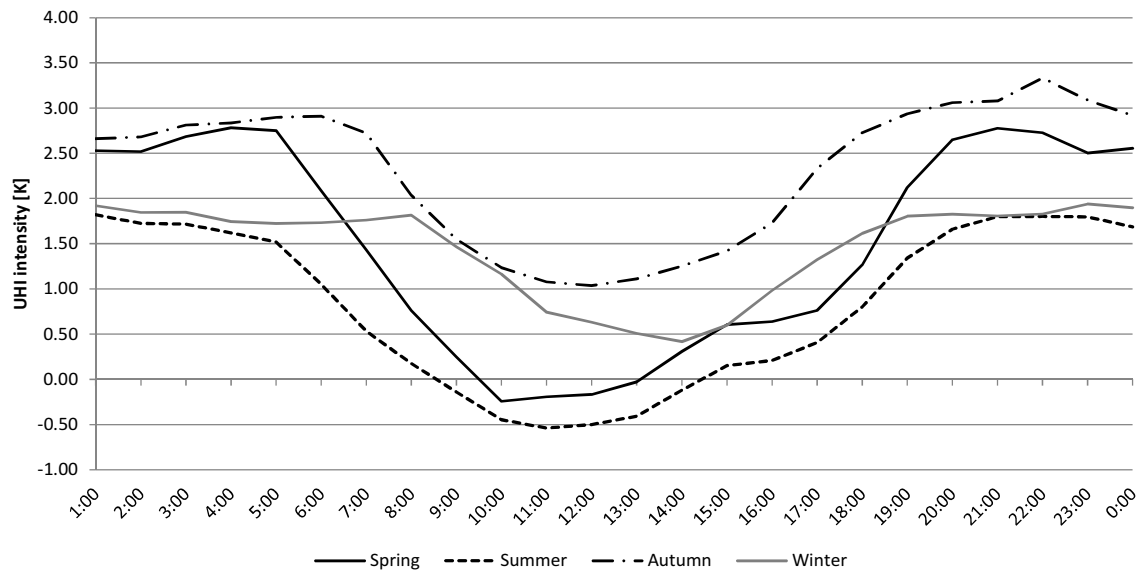
Figure 4.5 Mean hourly UHII for each season: Difference between U1 (Innere Stadt) and R2 (Seibersdorf): 2011

throughout the whole day without any interlacing. Additionally, intensity is always positive in this season, reaching its maximum of 3.3 K at 22:00. Minimum intensity in autumn with a value of nearly 1.0 K can be seen at noon time. While winter UHI distribution remains above the zero line during the whole day, the spring one demonstrates a very high temperature variance – the highest of all the seasons, going both - above and below zero intensity. Its peak values at 4:00h and 5:00 in the early morning are going very close to the peak values of the autumn curve – the season with the highest intensity. On the other hand, its minimum values are close to the minimum ones in summer, the season with the lowest intensity, reaching - 0.24 K at 10:00 in the morning. Winter time appears to be the season with the lowest temperature variance. Heat island intensity here is always positive. Nevertheless, it does not exceed 2 K even in its highest point - around midnight. Lowest intensity of 0.4 K is observed at 14:00 in the afternoon. The lowest position in the vertical order of curves is taken by the summer season. UHI intensity is negative between 9:00 and 14:00. After that the curve goes up, reaching its highest values in the evening from 21:00 until 1:00 at night.

The comparison of different weather stations on a seasonal and monthly basis ascertained an indisputable UHI effect in the city of Vienna. Maximum temperature values are found always at the urban Innere Stadt and minimum ones at the rural Seibersdorf. In autumn and winter periods air temperatures in the center demonstrate constantly higher values than surrounding suburban and rural stations, whereas during spring and summer seasons UHI remains mainly a night-time phenomenon. Disturbed snow cover distribution and duration can be a reason for this particular occurrence. Temperatures at suburban areas showed

values close to the rural ones during the day and slightly higher during night hours. With these facts a spatial distribution of UHI is revealed, establishing the attenuation of UHI effect with the distance from the urban center.

After the examination of seasonal and monthly values the week with the highest air temperatures in this year (21st to 27th August 2011) is chosen for a deeper analysis to ascertain the behaviour of UHI phenomenon in extreme conditions. Distribution of hourly air temperatures at each ZAMG weather station can be seen in Figure 4.6. Noticeable differences between U1 and the other four curves at night and their convergence during the day are observed in the graph. The curves of each weather station start to split up every day at around 19:00 and differences become higher, mostly with a pick around 5:00 in the early morning. After 6:00 they slowly start to gather again. During the night, when temperature differences are the highest, the curve of the urban station U1 lies above all other curves of weather stations, i.e. temperatures at U1 were higher.

Monitored values from this week are summarized and mean hourly air temperatures for the same period (21st – 27th August 2011) are extracted and depicted in Figure 4.7. This average distribution confirms the night expression of temperatures in the urban location U1, Innere Stadt. From 19:00 in the evening until 9:00 in the morning average monitored values at U1 are higher than monitored values at the other ZAMG stations. In the early afternoon, between 14:00 and 15:00, averaged air temperatures at U3 are the highest ones. Between 11:00 and 18:00 air temperatures at U2 are the lowest compared to the other locations.

Cumulative frequency of air temperatures at each weather station for the examined hot period is obtained from the hourly data and presented in Figure 4.8. A significant deviation of the U1 curve from the other four curves can be seen in the graph. Considering the median (the 50% line) of the plot it can be inferred that 50% of the time temperatures in the city center were equal or exceeded 27°C. The place where the median crosses the R2 curve – at 25.25°C, indicates a difference of 1.75 K with the urban station U1. Not only R2, but also all other stations at this level lie to the left of the U1 curve, i.e. their medians are lower than this of Innere Stadt. The average range of temperatures for each set of data, or the so called *inter quartile range* (IQR), is defined between the 25% and 75% lines. This range lies between 24.25 and 30.50°C for U1 and between 21.10 and 29.70°C for R2. The station U3 also appears to have very high temperatures in comparison with the rest of the locations.

Cumulative frequency of UHI intensities for the same period of time (21st – 27th August
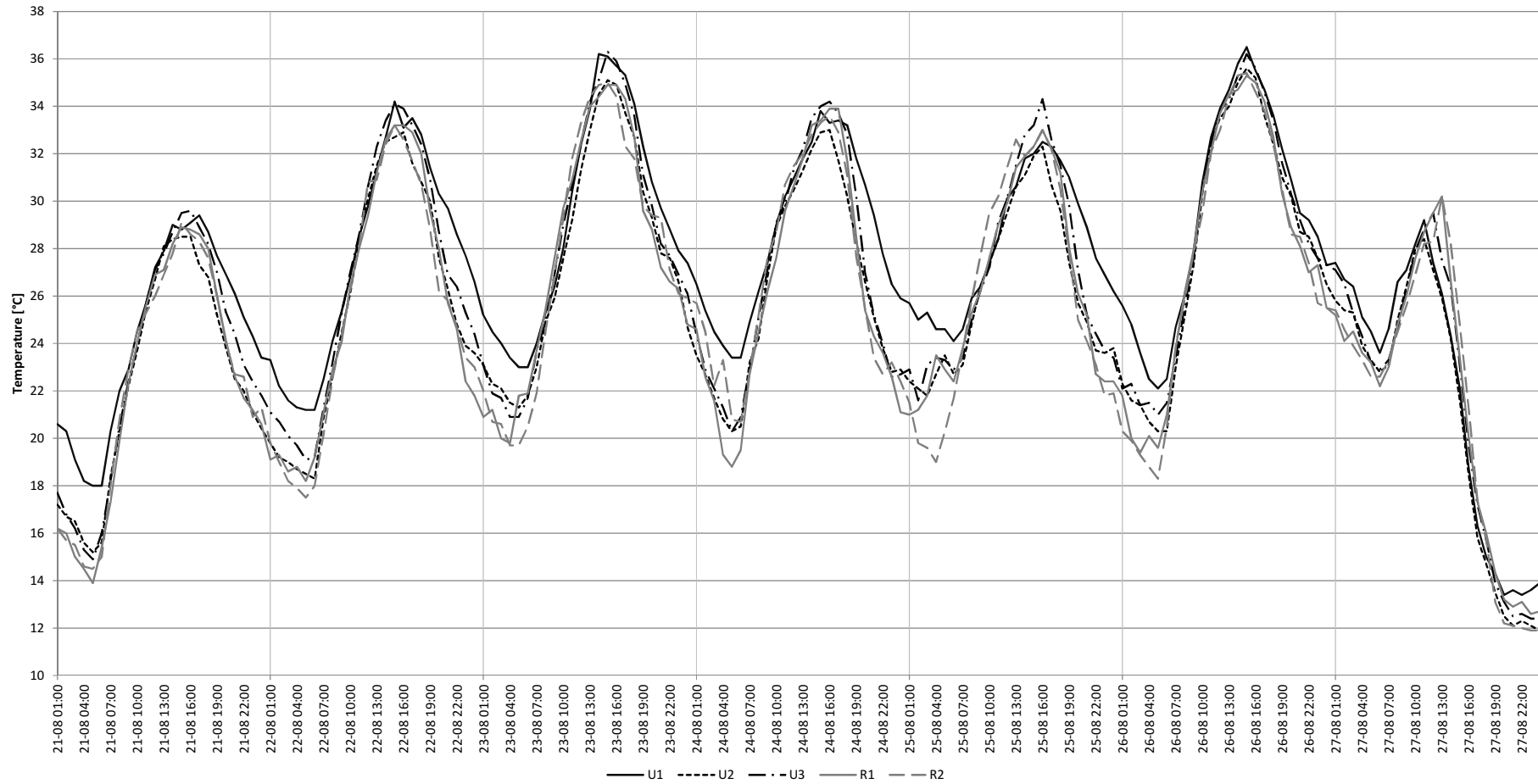
Figure 4.6 Distribution of hourly air temperatures at ZAMG weather stations for the chosen period (21st – 27th August 2011)

Figure 4.6 Distribution of hourly air temperatures at ZAMG weather stations for the chosen period (21st – 27th August 2011)
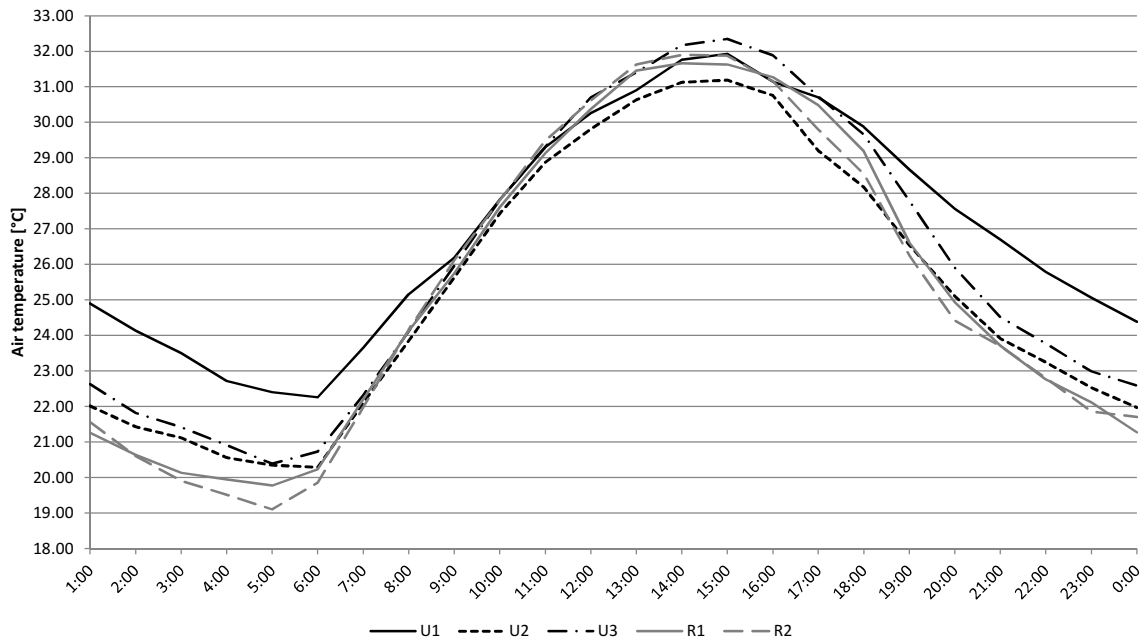
Figure 4.7 Mean hourly air temperatures for the chosen period (21st – 27th August 2011)
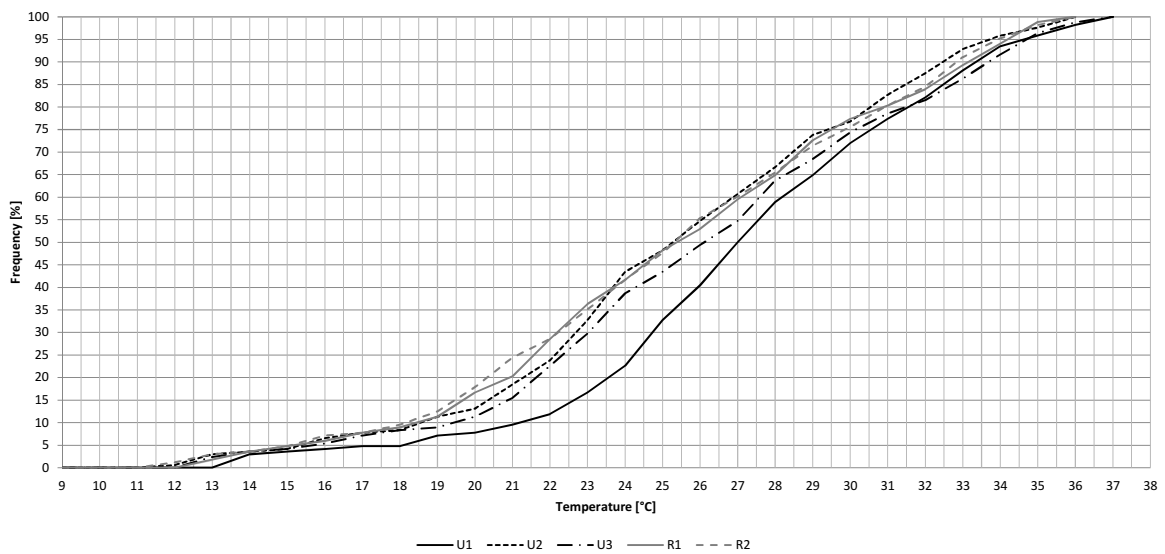
Figure 4.8 Cumulative frequency distribution of air temperatures for the chosen period (21st – 27th August 2011)

2011) is depicted in Figure 4.9. The rural station R2, Seibersdorf, is taken as a reference station for the calculation of intensities according to formula 2.1. It can be noted again that both - the median and the IQR of the urban U1, Innere Stadt, are positioned on the right side of all other medians and IQRs, i.e. hourly intensities at this station were higher more than 75% of the time in the examined period. Lowest intensity can be seen at the rural R1.

Hourly intensity of UHI in the city center for the same hot week period is displayed in Figure
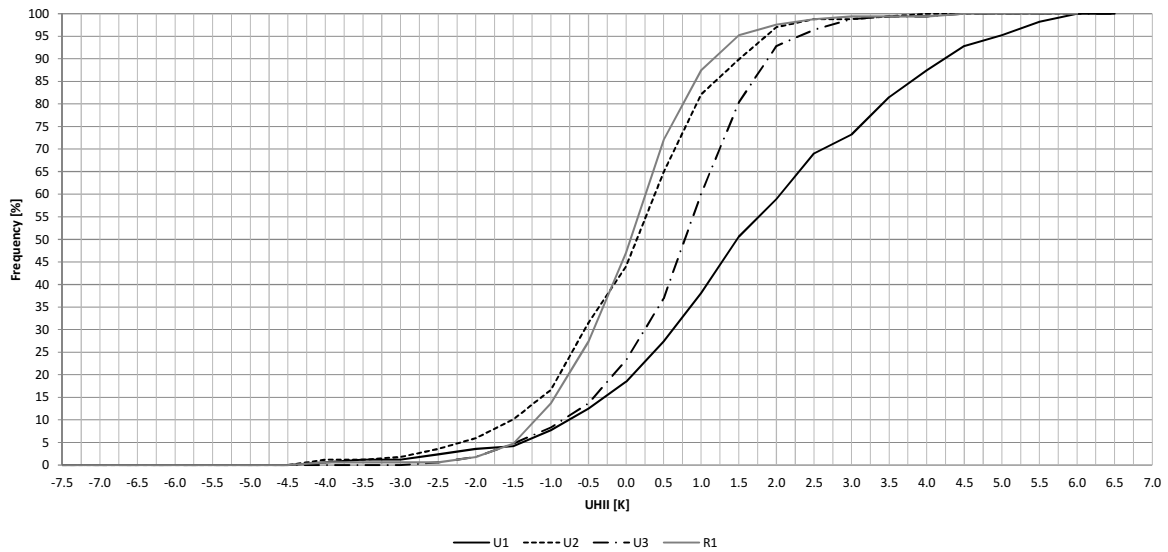
Figure 4.9 Cumulative frequency distribution of UHII for the chosen period (21ˢᵗ – 27ᵗʰ August 2011)

4.10. A certain daily pattern can be identified from this bar graph. Highest values are reached always during the night, approximately between 20:00 in the evening and 7:00 in the morning. Very low and often negative values are seen in the middle of the day between 9:00 and 16:00 with lowest intensities around noon time. The maximum intensity for this week is measured at 21:00 (24th August) reaching 6 K, and the minimum one at 13:00 (27th August) with a value of - 4.1 K.

The UHI intensities from the previous graph are summarized and a box plot of hourly UHII values for the weather station U1 is obtained (Figure 4.11). The values of the medians form a distribution with lowest point at 13:00 in the early afternoon. The UHI intensity at this position has a negative value of -0.73 K. The peak values of the medians are marked by the night hours with a maximum intensity of 3.6 K at 3:00. Adjacent average night time values between 20:00 and 5:00 in the morning are equal or above 3 K, with an exception at midnight. All average values between 12:00 and 13:00 are below the zero line, i.e. the UHI intensity is negative during this time of the day.

The absolute maximum values for this hot week period are either equal or exceed 1 K. Peak absolute maximum value of 6 K is found at 21:00. The lowest values can be seen at 11:00 and 13:00. Highest values are found to be again between 20:00 and 5:00 in the early morning.

Absolute minimum values do not follow the systematic distribution of the maximum and average ones. However, the logic of ascending and descending intensity remains the
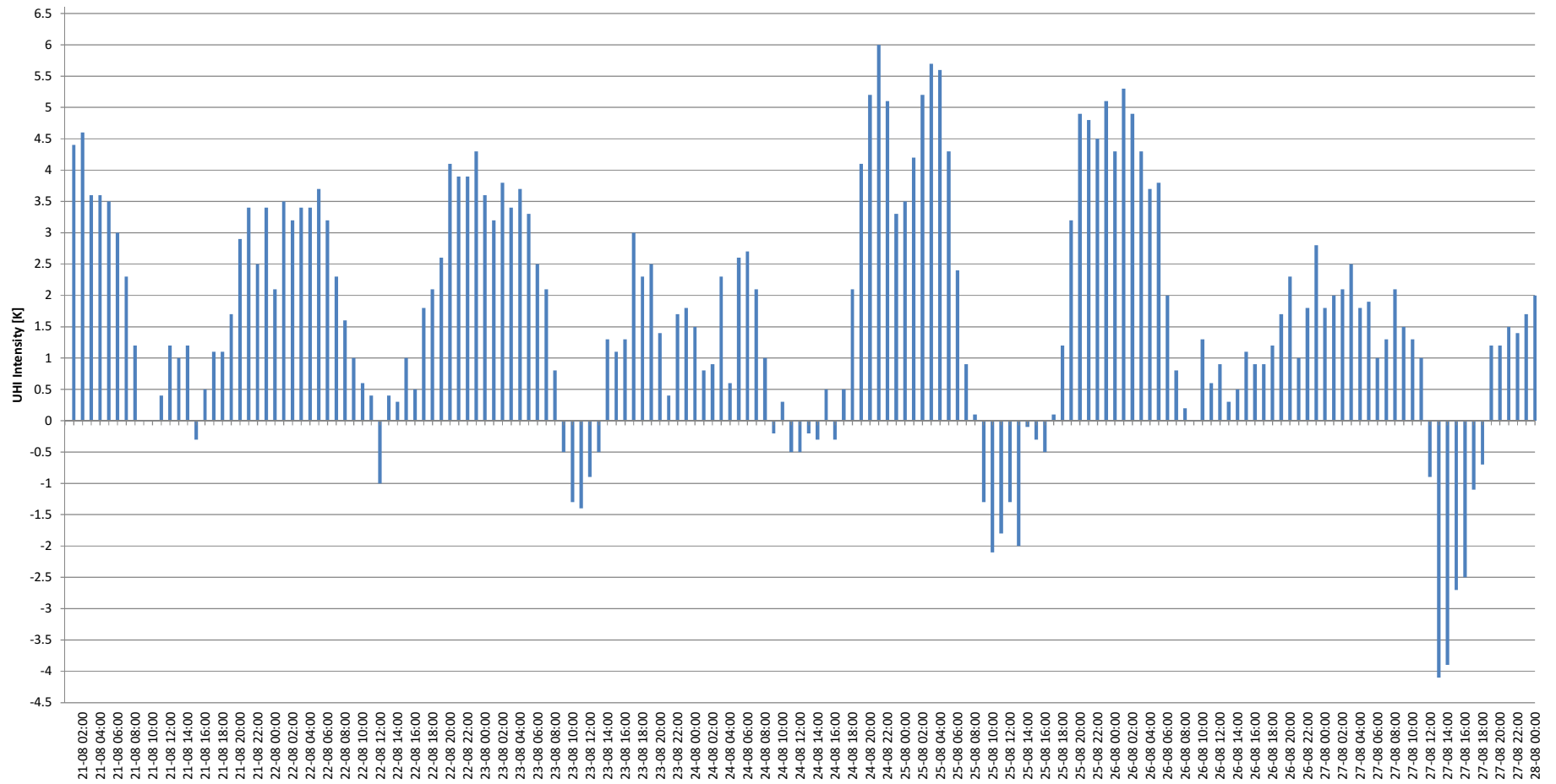
Figure 4.10 Hourly UHII for the chosen period (21st – 27th August 2011): Difference between U1 (Innere Stadt) and R2 (Seibersdorf)

51
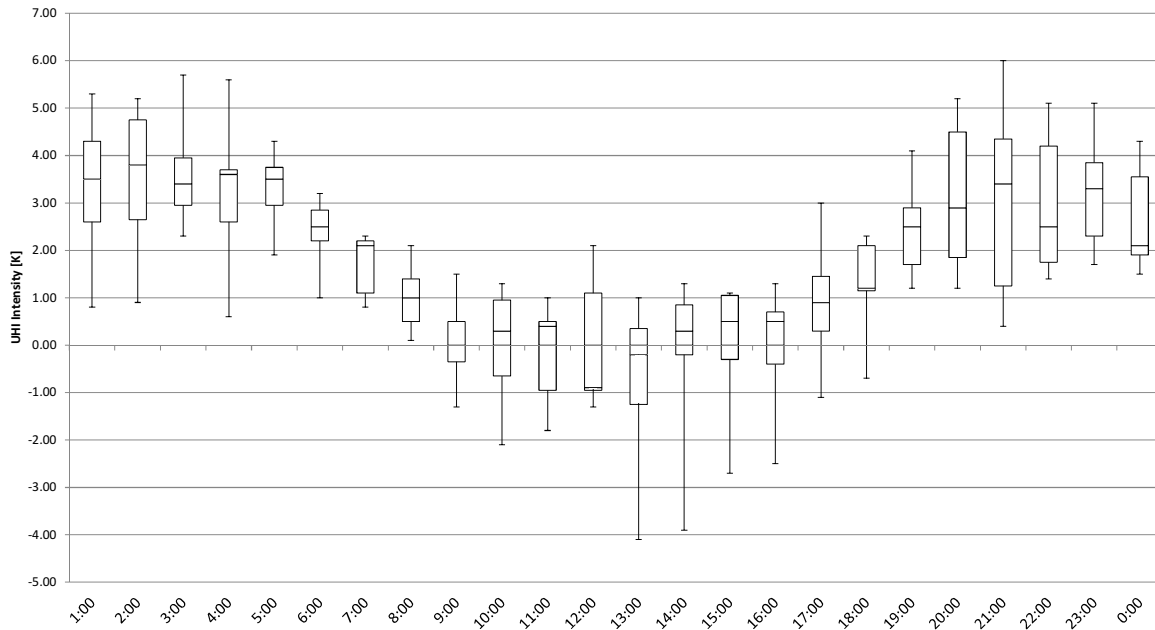
Figure 4.11 Box plot of hourly UHII for the chosen period (21st – 27th August 2011): Difference between U1 (Innere Stadt) and R2 (Seibersdorf)

same: lowest values are found in the middle of the day with -4.1 K and -3.9 K at 13:00 and 14:00 respectively, and highest values at night reaching 2.3 K at 3:00.

The analyzed short summer period with extreme conditions displayed a more detailed behaviour of UHI on an hourly basis. The night time expression of the effect is underlined once again showing maximum values at the urban U1 and U3, and minimum ones at both rural locations – R1 and R2. In this hot week the loosely built residential U2 indicated rather comfortable levels of temperatures with values during some of the days even lower than these at the reference rural location. The lower density of structures, the abundance of vegetation and less traffic appear to have a very advantageous behaviour in extreme summer conditions.

The nocturnal appearance of UHI effect can be comprehended as a delayed response from daily processes. Urban surfaces act like huge heat storages that emit the gathered heat during night hours. In rural places this emitting process is almost absent and that is the reason why temperature differences at night reach their highest values. Permeable surfaces, natural materials with higher solar reflectance and vegetation to permit the process of evapotranspiration prevent extreme conditions and heat stress in suburban and rural places.

4.2 Mobile measurements

Collected data from the mobile measurements is divided into morning and evening values. The measured parameters are averaged for each spot and measuring period so that only one representative value is obtained in the end. The bar graphs below show differences of the averaged data between the street without trees, Herbststrasse, and the street with trees, Koppstrasse (Figure 4.12 - 4.16).

The retrieved mean air temperature differences result only in positive values with a minimum difference amounting to 0.07 K (Figure 4.12). This means that air temperatures at Herbststrasse were higher. Nevertheless, differences do not exceed 0.68 K. Another aspect noticed in the graph is that evening differences are higher at all three spots compared to morning ones.

Next monitored parameter is global solar radiation (Figure 4.13). As in the temperature graph, obtained differences are always positive, i.e. solar radiation at the unvegetated street was higher, and differences in the evening, varying from 167 to 360 W/m^2, are again higher than the morning ones, varying only from 31 to 52 W/m^2.

Compared to the values in the first two charts, absolute humidity differences between both canyons are very low (Figure 4.14). They are positive and vary between 0.07 and 0.10 g/kg dry air in the morning, which may be a result of the absorption of earth under the trees; and negative, between 0.19 and 0.23 g/kg dry air in the evening, i.e. absolute humidity is higher at the vegetated street.

Wind speed differences at all three spots are positive during the whole day, i.e. air velocity on the street without trees is permanently higher, regardless of the fact that it has less traffic than the vegetated street (Figure 4.15). The highest difference values can be seen again in the evening, varying between 0.80 and 1.19 m/s. In the morning wind speed on Herbststrasse is higher with 0.19 to 0.60 m/s.

Carbon dioxide concentration within both canyons is measured in parts per million (ppm). Against the expectations that trees at Koppstrasse contribute to the reduction of CO_2, differences here are negative, which means CO_2 concentration is higher at the vegetated street (Figure 4.16). Their values vary from -59 to -69 ppm in the morning, and from -58 to -68 ppm in the evening. Even if an average error of the HOBO sensors of about 10 to 20 ppm is accepted, differences would have remained negative.
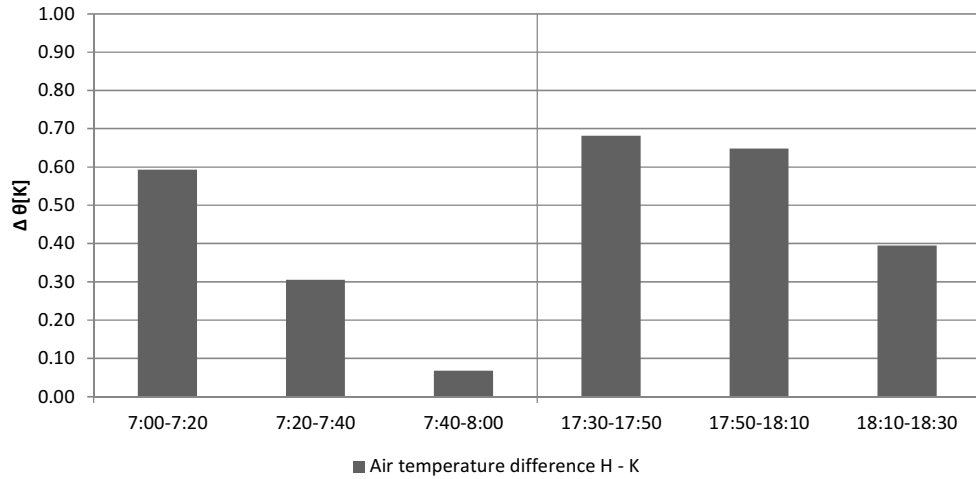
Figure 4.12 Mean air temperature differences between Herbststrasse and Koppstrasse
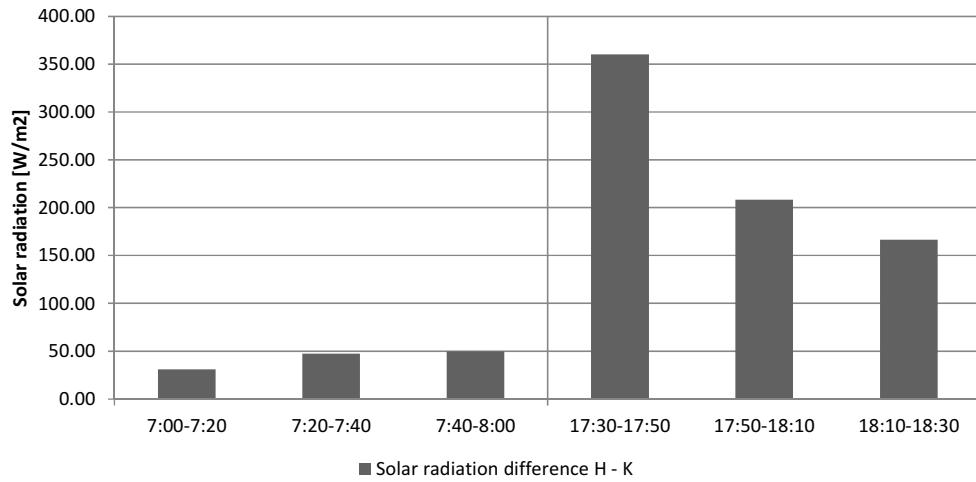
Figure 4.13 Mean solar radiation differences between Herbststrasse and Koppstrasse
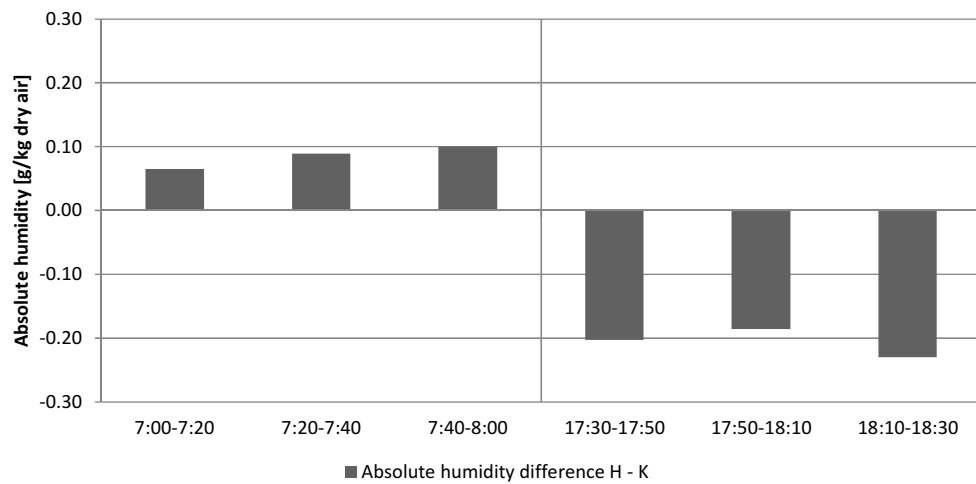
Figure 4.14 Mean absolute humidity differences between Herbststrasse and Koppstrasse
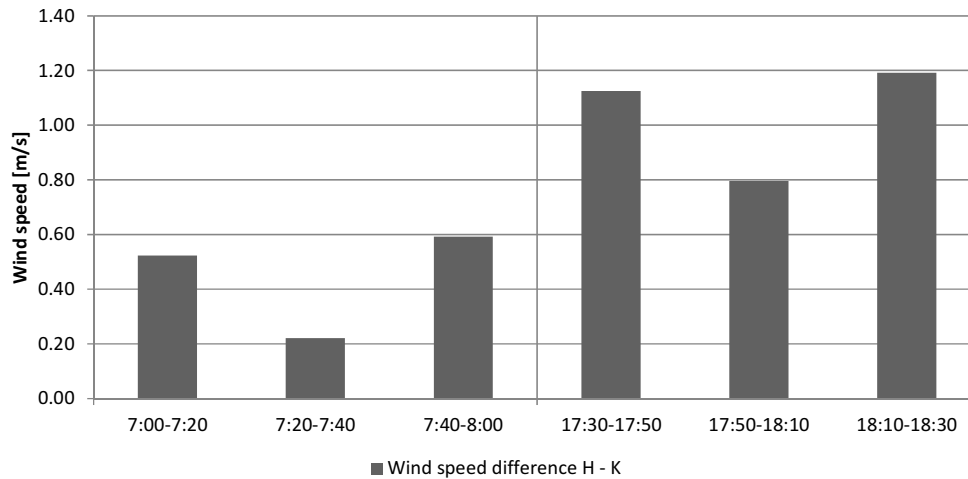
Figure 4.15 Mean wind speed differences between Herbststrasse and Koppstrasse
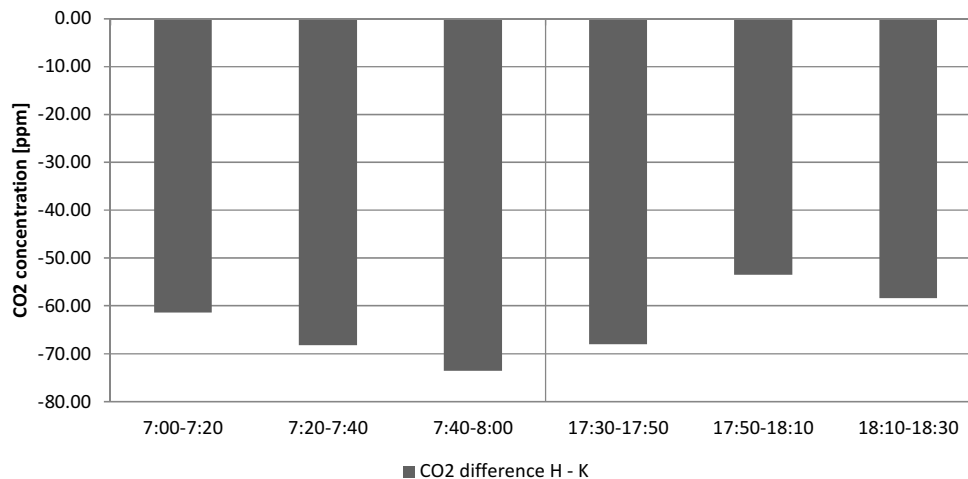
Figure 4.16 Mean CO_2 differences between Herbststrasse and Koppstrasse

The conducted short-term mobile measurements indicated a meaningful difference between micro climates in an unvegetated and a vegetated urban canyon. Some of the monitored parameters, for example air temperatures, wind speed and global solar radiation, confirmed the expected results about the impact of shade trees. Others, like absolute humidity, remained almost unaffected from this factor. The collected CO_2 data completely contradicted the statements that vegetation reduces CO_2 levels (Oke 1987; Akbari et al. 1990; Kleerekoper et al. 2012). Apparently micro-climate conditions in street canyons differ significantly from other urban contexts and have to be observed with particular prudence. For the identification of the exact reasons more details are needed. In this case the reason could be the higher traffic flow at the vegetated street, Koppstrasse, that affects air conditions substantially. Trees may have entrapped the exhaust gases from vehicles and in this way elevated CO_2 concentrations remained within the canyon.

A certain trend is discernible in the graphs of mobile measurements – with exception of the CO_2 values evening differences are always higher than the morning ones. That tendency relates also to the long-term data analysis where heat island highest expression begins mostly a few hours before sunset. At that time urban surfaces are slowly reaching their "saturation" with heat and are supposed to give that absorbed heat away at night. However, dense geometries in urban canyons constitute obstacles for this radiative heat loss and the long-wave emissions remain within the canyon boundaries. In the current situation trees could be also taken as barriers for these heat fluxes. Nevertheless, during the day they play a significant role for the reduction of air temperatures. As reported by Shashua-Bar and Hoffman (2000) 80% of the total cooling provided by trees is due to shading. This appearance is confirmed at Koppstrasse when considering the monitored global solar radiation and temperature values.

Although the measurements supported the statement by Shashua-Bar and Hoffman (2000) that trees prevent most of the short-wave radiation from reaching the ground, their large crowns and dense foliage also trap the gathered heat and exhaustion gases within the canyon and diminish the air exchange. High traffic levels and reduced wind speed at Koppstrasse create favourable conditions for the retaining of pollutants. This is a reasonable explanation for the higher CO_2 concentrations monitored in the vegetated street. A possible solution for this case is presented by Gromke and Ruck (2007) in their experiment with different tree spacing in urban canyons. The study showed that larger tree spacing decreases harmful concentrations and ensures better street ventilation if tree crowns are far enough, and not interlacing.

The absence of trees on the other street, Herbststrasse, was expected to provide lower humidity levels and higher CO2 concentrations. Despite of the higher air temperatures and solar radiation collected humidity data did not show any considerable variation compared to the vegetated street. The small differences indicated in the graphs could be a result of equipment differences or the more intensive air exchange due to absence of trees. The significantly lower carbon dioxide values at the unvegetated street can be explained with the lower traffic level, the better natural street ventilation and the lack of obstacles that would normally prevent pollutants dilution.

4.3 ENVI-met simulation results

Simulated cases in the computational model can be seen in Table 4.2. For the amount of mitigation in each simulated situation in ENVI-met improvement values are subtracted from base case values. For a more reasonable comparison with the mobile measurements only

Table 4.2

Simulated ENVI-met cases

SIMULATION CASE	KOPPSTRASSE	HERBSTSTRASSE
Base Case (BC)	Current situation	
Improvement Case 1 (C1)	Black asphalt materials replaced with white concrete	
Improvement Case 2 (C2)	Increased albedo of building facades	
Improvement Case 3 (C3)	Larger tree spacing	Trees added
Improvement Case 4 (C4)	C1, C2 and C3 cases combined	

the values at a height of 1.8 m are taken from the output files. The calculated results for air temperatures are displayed in the following Figures 4.17 – 4.20. The improvement values for absolute humidity and surface temperatures can be found in the appendix (Appendix: Figures 9.18 – 9.22). The surface temperature results were significant only in the first improvement case and therefore results for the other simulated cases are not included in the study. For the analysis of each case an average wind speed value is taken for the whole simulation period.

The first improvement of the current situation – replacement of black asphalt with white concrete, made considerable changes to the micro -climate of both canyons. Temperatures at both streets decreased with up to 0.83 K (Figure 4.17). Highest differences are noticed at 9:00 and 10:00 in the morning for Herbststrasse, at 13:00 and 14:00 for Koppstrasse, and lowest ones in the hours after sunset. Pavement surface temperatures decreased with up to 4.8 K at Herbststrasse (Appendix: Figure 9.20). Surface temperature decreases for Koppstrasse were not essential, but still evident. The replacement of the black asphalt with grey concrete did not influence the wind speed. The absolute humidity levels on the other side are affected, as expected from the lower temperature values, and increased at both streets with up to 1.5 g/kg dry air (Appendix: Figure 9.16).

Applying the second mitigation method – increasing the albedo of building facades, brought the expected positive results, i.e. temperatures at both streets have decreased after altering the solar reflectance of the surrounding structures. Temperature values became lower with up to 0.8 K at 9:00 in the morning and between 0.3 and 0.4 K during the rest of the day for both streets (Figure 4.18). Absolute humidity values were not affected substantially from this method. However there is a slight positive change, i.e. slightly increased absolute humidity that is visible in the graph (Appendix: Figure 9.17). Wind speed remained unchanged.

After the third improvement – adding of tree vegetation at the unvegetated street and re-spacing the trees at the vegetated one, temperatures at Herbststrasse have slightly

decreased, reaching a difference of 0.54 K at 16:00 in the afternoon (Figure 4.19). The increase of sky obstruction with up to 27% because of tree crowns made the main contribution in this case. In the early hours and after sunset however differences are negative, but too small to be considered as significant. Wind speed on the other side has decreased with an average of 1.2 m/s that may be the reason for the negative temperature differences, i.e. temperatures are higher. Absolute humidity values changed with up to 1.2 g/kg dry air, which makes trees influence on humidity in this canyon significant.

Temperatures at Koppstrasse slightly increased after re-spacing the trees (Figure 4.19). Highest increase is noticed by the first position, where the tree from base case right next to the receptor point was placed further away in the improvement case and SVF increased
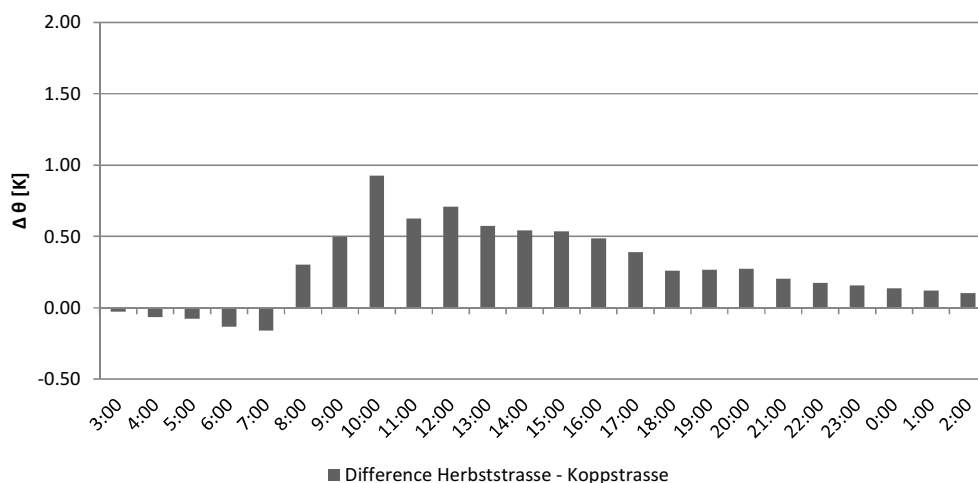
Figure 4.16 Mean air temperature differences between Herbststrasse and Koppstrasse in BC
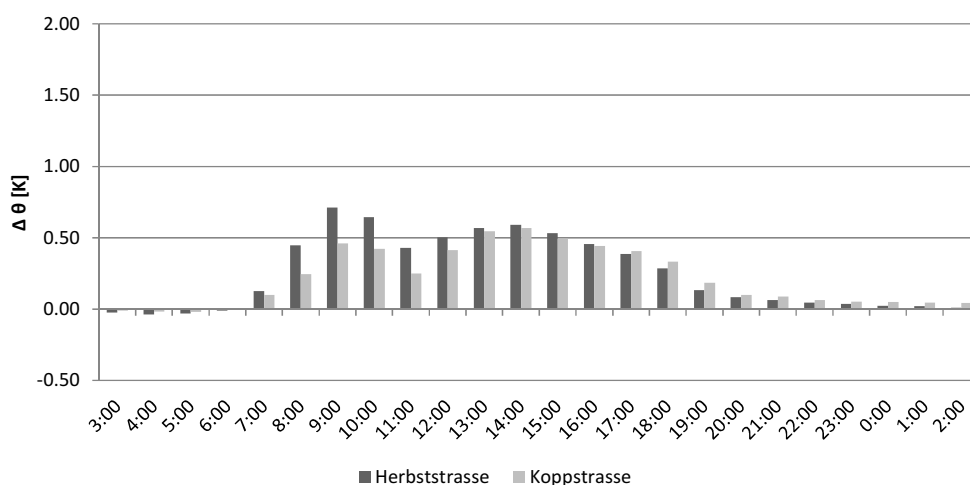
Figure 4.17 Mean air temperature differences between BC and C1 (white concrete case)

58

with 25%. Thus almost no shading is provided at this spot after 10:00 in the morning. The temperature values by the other 2 spots did not change substantially. Air velocity at Koppstrasse increased with an average of 0.5 m/s. The lower amount of trees appeared to have an important effect on absolute humidity levels – they decreased with up to 1 g/kg.

The simulated combined cases altered the micro-climates of both street canyons substantially. It is noticeable that differences at Koppstrasse are slightly lower than at Herbststrasse (Figure 4.20). However, they are always positive with only few exceptions. The same is valid for Herbststrasse, where negative values appear in the early morning. Temperatures during the day have decreased with up to 1.69 K at Herbststrasse and up to 1.35 K at Koppstrasse. Considerable changes appear in absolute humidity values as well, reaching an increase of 2.6 g/kg dry air at Koppstrasse and 3.2 g/kg dry air at
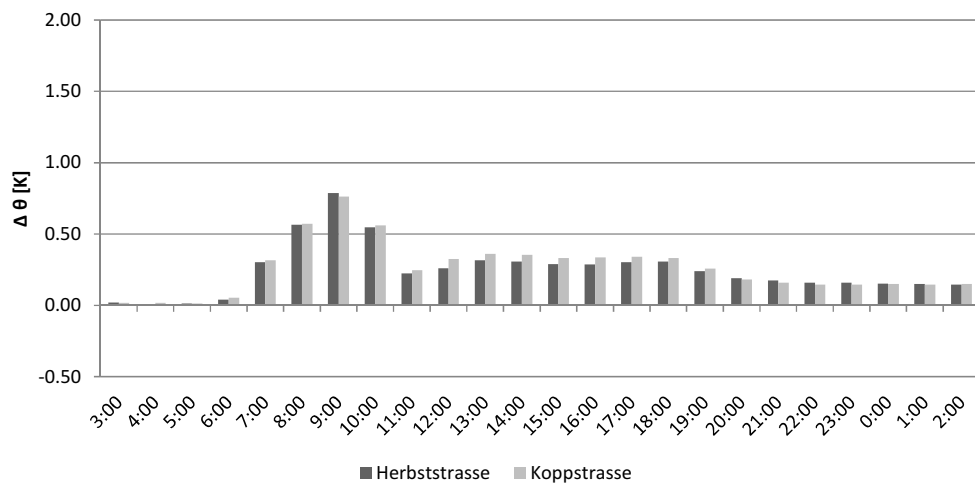
Figure 4.18 Mean air temperature differences between BC and C2 (increased albedo case)
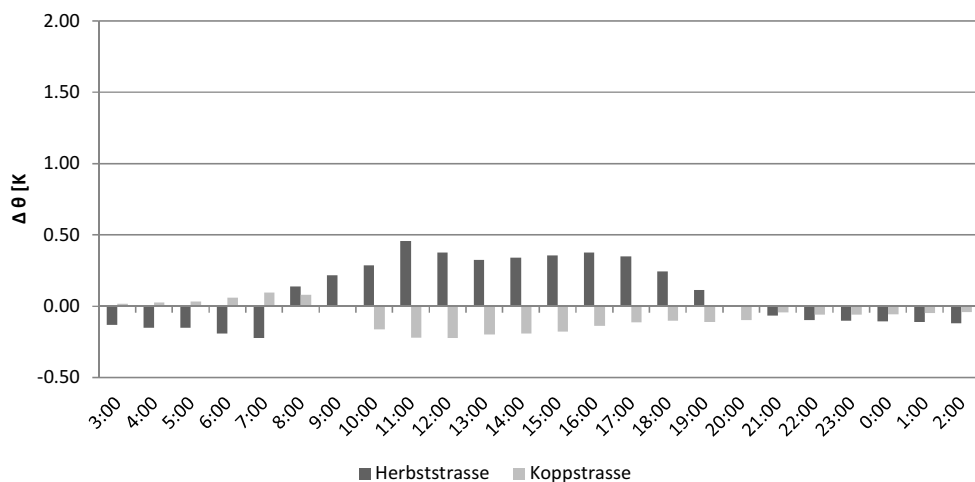
Figure 4.19 Mean air temperature differences between BC and C3 (trees case)
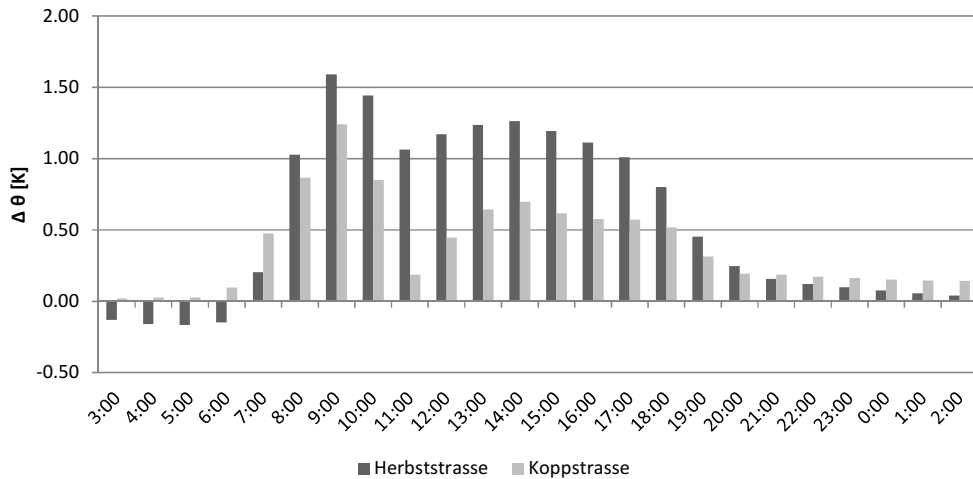
Figure 4.20 Mean air temperature differences between BC and C4 (combined case)

Herbststrasse (Appendix: Figure 9.21).

The simulated mitigation methods predicted considerable alleviation of the UHI effect. The first strategy applied in the computational model improved the base case conditions in bothstreets. Air temperatures decreased with up to 0.83 K and surface temperatures with more than 4.8 K at Herbststrasse. Additional positive effect is noticed in the absolute humidity levels with an increase of up to 3.2 g/kg dry air. The amount of improvement shows that increasing the albedo of pavements has a significant role in altering the micro climate of urban canyons.

Changing the albedo of building facades also predicted certain mitigation. Temperature differences with base-case are not as essential as after the first improvement, but they still remain above the zero line. The more reflective facades reduce the heat accumulation during the day and thus the long-wave radiation flux to the surroundings. This UHI reduction method is of great importance for human thermal satisfaction outdoors as well as indoors.

Third improvement of ENVI-met base case situation – adding and respectively re-spacing of trees, underlines the importance of tree vegetation for shading in hot summer days. According to the results trees lower the air temperatures as long as they constitute obstacles for short-wave radiation. Objects that stand under the shadow of tree crowns (e.g. 1.Spot at Herbststrasse C3) experience a slight alleviation in the surrounding temperature conditions and therefore an increased comfort. However, those that stand outside the shaded area (e.g. 1.Spot at Koppstrasse C3) do not experience any difference in temperature from the neighbouring tree. Concerning the wind speed tree vegetation has

a significant influence. It increased slightly at Koppstrasse and substantially hindered the natural ventilation at Herbststrasse, which is a great disadvantage for pollutants dispersion and air temperatures in hot summer days.

The magnitude of mitigation for both street canyons after applying the methods together is eminent. Significant air and surface temperature decreases, and absolute humidity increases emphasize the huge potential of reflective materials and tree vegetation for the alleviating of micro-climates. Applying these strategies in the real urban context is able to bring not only an improved outdoor comfort, but also essential energy savings and thermal comfort for building users indoors.

5. CONCLUSION

In this study the effect of UHI for Vienna, Austria, was examined. The detailed background exploration of this phenomenon and related reduction strategies indicated that different urban contexts need different climate adaptation procedures. The particular context in Vienna was determined with the aid of long-term measurement data and their analysis on a spatial, seasonal and hourly basis. The occurrence of a heat island in the city was evidenced. Distributed from the center to the outskirts the phenomenon is found to be most pronounced in autumn and winter seasons. A definite nocturnal expression is indicated on a daily basis.

For an examination at a pedestrian level two parallel urban canyons near the city center were adopted for short-term measurements – one of them with (Koppstrasse) and the other one without vegetation (Herbststrasse). The collected data underlined the importance of trees for alleviating of extreme summer conditions. However, measured levels of CO_2 were higher at the vegetated street. To identify the reasons for that more details are needed. Contributing factors may be in this case a) reduced air flow in Koppstrasse due to presence of trees and b) higher traffic density in the same canyon. Both streets were modeled in 3D-computational software to predict the amount of micro-climate improvement after application of several mitigation methods. The results of the simulations presented a significant potential for amelioration of current conditions. Modifications in land cover and adding of vegetation turned to be a key factor for the UHI mitigation.

Increased urban temperatures and thermal discomfort are major issues that need to be considered with responsibility and support by designers and urban planners. The correct application of the discussed complex solutions is able to provide healthy outdoor conditions for urban occupants, decrease carbon footprint of local processes and significantly improve surrounding buildings performance.

6. REFERENCES

Akbari, H., Rosenfeld, A.H., Taha, H. 1990. Summer heat islands, urban trees, and white surfaces. University of California-Berkeley.

Akbari, H., Pomerantz, M., Taha, H. 2001. Cool surfaces and shade trees to reduce energy use and improve air quality in urban areas. *Solar Energy* 70: 275-310.

Akbari, H., Menon, S., Rosenfeld, A. 2009. Global Cooling: increasing world-wide urban albedos to offset CO2. *Climatic Change* 94: 275-286.

Alexandri, E., Jones, P. 2008. Temperature decreases in an urban canyon due to green walls and green roofs in diverse climates. *Building and Environment* 43: 480–493.

Ali-Toudert, F., Mayer, H. 2007. Effects of asymmetry, galleries, overhanging facades and vegetation on thermal comfort in urban street canyons. Solar Energy 81: 742–754.

Andreou, E. 2013. Thermal comfort in outdoor spaces and urban canyon microclimate. Renewable Energy 55: 182-188.

ASHRAE. 2001. *ASHRAE Fundamentals Handbook 2001* (SI Edition) American Society of Heating, Refrigerating, and Air-Conditioning Engineers, ISBN: 1883413885.

Conti, S., Meli, P., Minelli, G., Solimini, R., Toccaceli, V., Vichi, M., Beltrano, C., Perini, L. 2005. Epidemiologic study of mortality during the Summer 2003 heat wave in Italy. *Environmental Research* 98: 390–399.

Doshi, H., Banting, D., Li, J., Missios, P., Au, A., Currie, B., Verrati, M. 2005, 10. Report on the environmental benefits and costs of green roof technology for the City of Toronto. Ryerson University, Toronto, Ontario.

Doulos, L., Santamouris, M., Livada, I. 2004. Passive cooling of outdoor urban spaces. The role of materials. *Solar Energy* 77: 231-249.

Drlik, S. 2010. *Klimawandelanpassung der Pflege und Erhaltung öffentlicher Grünanlagen in Grosstädten unter Berücksichtigung des Konzepts der nachhaltigen Entwicklung, untersucht am Fallbeispiel Wien.* Ph.D. diss., University of Natural Resources and Life Sciences, Vienna.

Ferguson, B., Fisher, K., Golden, J., Hair, L., Haselbach, L., Hitchcock, D., Kaloush, K., Pomerantz, M., Tran, N., Waye, D. 2008. Reducing Urban Heat Islands: Compendium

of Strategies. Cool Pavements. *Environmental Protection Agency*. Internet. Available from http://www.epa.gov/hiri/resources/pdf/CoolPavesCompendium.pdf; accessed June 2005.

Formayer, H., Haas, P., Hofstätter, M., Radanovics, S., Kromp-Kolb, H. 2007. *Räumlich und zeitlich hochaufgelöste Temperaturszenarien für Wien und ausgewählte Analysen bezüglich Adaptionsstrategien*. Vienna: University of Natural Resources and Life Sciences.

Gartland, L. 2008. *Heat islands*. London: Cromwell Press, Trowbridge.

Gromke, C., Ruck, B. 2007. Influence of trees on the dispersion of pollutants in an urban street canyon - experimental investigation of the flow and concentration field. *Atmospheric Environment* 41: 3287–3302.

Guan, B., Ma, B., Qin, F. 2011. Application of asphalt pavement with phase change materials to mitigate urban heat island effect. *Water Resource and Environmental Protection* 3: 2389 – 2392.

Gui, J., Phelan, P. E., Kaloush, K. E., Golden, J. S. 2007. Impact of pavement thermophysical properties on surface temperatures. *Journal of materials in civil engineering* 19: 683–690.

Gulias, A., Unger, J., Matzarakis, A. 2006. Assessment of the microclimatic and human comfort conditions in a complex urban environment: Modelling and measurements. *Building and Environment* 41: 1713-1722.

Hamada, S.; Ohta, T. 2010. Seasonal variations in the cooling effect of urban green areas on surrounding urban areas. *Urban Forestry & UrbanGreening* 9: 15-24.

Harlan, S.L., Ruddell, D.M. 2011. Climate change and health in cities: impacts of heat and air pollution and potential co-benefits from mitigation and adaptation. *Current Opinion in Environmental Sustainability* 3: 126-134.

Holmer, B. 1992. A simple operative method for determination of sky view factors in complex urban canyons from fisheye photographs. Meteorol. Zeitschrift N.F.1: 236-239.

Holmer, B., Postgard, U., Eriksson, M. 2001. Sky view factors in forest canopies calculated with DRISI. *Theoretical and Applied Climatology* 68: 33–40.

Howard, L. 1818. The climate of London: deduced from meteorological observations, made at different places in the neighbourhood of the metropolis, Volume 1. London: J. and A. Arch, 1818.

Howard, L. 1833. The climate of London: deduced from meteorological observations made in the metropolis and at various places around it, Volume 1. London: Harvey and Darton, J. and A. Arch, Longman, Hatchard, S. Highley [and] R. Hunter, 1833.

Hoyois, P., Below, R., Scheuren, J-M., Guha-Sapir, D. 2007. Annual Disaster Statistical Review: Numbers and Trends 2006. Centre for Research on the Epidemiology of Disasters (CRED), School of Public Health, Catholic University of Louvain Brussels, Belgium, Brussels, 2007.

Kinouchi, T, Yoshinaka, T., Fukae, N., Kanda, M. 2004. Development of cool pavement with dark colored high albedo coating. In: Fifth Conference for the Urban Environment, Vancouver, Canada, 2004.

Kleerekoper, I., Van Esch, M., Salcedo, T. B. 2012. How to make a city climate-proof, addressing the urban heat island effect. *Resources, Conservation and Recycling* 64: 30-38.

Kolokotroni, M., Giridharan, R. 2008. Urban heat island intensity in London: An investigation of the impact of physical characteristics on changes in outdoor air temperature during summer. *Solar energy* 82: 986–998.

Kosareo,L., Ries, R. 2007. Comparative environmental life cycle assessment of green roofs. *Building and environment* 42: 2606–2613.

Krüger, E.L., Minella, F.O., Rasia, F. 2011. Impact of urban geometry on outdoor thermal comfort and air quality from field measurements in Curitiba, Brazil. *Building and Environment* 46: 621-634.

Kwok, A.G., Rajkovich, N.B. 2010. Addressing climate change in comfort standards. *Building and environment* 45: 18-22.

Lin, T., Matzarakis, A., Hwang, R. 2010. Shading effect on long-term outdoor thermal comfort. *Building and Environment* 45: 213-221.

Liu, C., Shi, B., Tang, C., Gao, L. 2011. A numerical and field investigation of underground temperatures under Urban Heat Island. *Building and environment* 46: 1205–1210.

Mallick, R. B., Chen, B., Bhowmick, S. 2009. Harvesting energy from asphalt pavements and reducing the heat island effect. *International Journal of Sustainable Engineering* 2: 214-228.

Matzarakis, A., Muthers, S., Koch, E. 2011. Human biometeorological evaluation of heat-related mortality in Vienna. *Theoretical and Applied Climatology* 105: 1-10.

Mitchell, B. C. 2011. *Urbanization and Land Surface Temperature in Pinellas County, Florida*. Master thesis, University of South Florida, U.S.

Montavez, J.P., Rodriguez, A., Jimenez, J.I. 2000. A study of the urban heat island of Granada. *International journal of climatology* 20: 899-911.

Nakayama, T., Fujita, T. 2010. Cooling effect of water-holding pavements made of new materials on water and heat budgets in urban areas. *Landscape and Urban Planning* 96: 57–67.

Nikolopoulou, M., Lykoudis, S. 2006. Thermal comfort in outdoor urban spaces: Analysis across different European countries. *Building and environment* 41: 1455–1470.

Oke, T. R. 1981. Canyon geometry and the nocturnal Urban Heat Island. *International Journal of Climatology* 10: 237–245.

Oke, T. R. 1987. *Boundary layer climates*. Second Edition. London and New York: Routledge.

Ottele, M., Perini, K., Fraaij, A.L.A., Haas, E.M., Raiteri, R. 2011. Comparative life cycle analysis for green facades and living wall systems. *Energy and Buildings* 43: 3419–3429.

Papadopoulos, A. M. 2001.The influence of street canyons on the cooling loads of buildings and the performance of air conditioning systems. *Energy and Buildings* 33: 601-607.

Radhi, H., Fikry, F., Sharples, S. 2013. Impacts of urbanisation on the thermal behaviour of new built up environments: A scoping study of the urban heat island in Bahrain. *Landscape and Urban Planning* 113: 47-61.

Santero, Nicholas J., Masanet, E., Horvath, A. 2011. Life-cycle assessment of pavements Part II: Filling the research gaps. *Resources, Conservation and Recycling* 55: 810–818.

Shahmohamadi, P., Che-Ani, A.I., Etessam, I., Maulud, K.N.A., Tawil, N.M. 2011. Healthy Environment: The Need to Mitigate Urban Heat Island Effects on Human Health. *Procedia Engineering* 20: 61-70.

Shashua-Bar, L., Hoffman, M. E. 2000. Vegetation as a climatic component in the design of an urban street. An empirical model for predicting the cooling effect of urban green areas with trees. *Energy and Buildings* 31: 221–235.

Scholz, M., Grabowiecki, P. 2007. Review of permeable pavement systems. *Building and Environment* 42: 3830–3836.

Schwab, U., Steinicke, W. 2003. *Stadtklimauntersuchung Wien*. Vienna: SPACETEC Steinicke & Streifeneder, Umweltuntersuchungen GbR.

Taha, H., Sailor, D., Akbari, H. 1992. *High albedo materials for reducing cooling energy use.* Lawrence Berkeley Lab Rep. 31721. Berkeley, CA: University of California.

Vardoulakis, E., Karamanis, D., Fotiadi, A., Mihalakakou, G. 2013. The urban heat island effect in a small Mediterranean city of high summer temperatures and cooling energy demands. Solar Energy 94: 128-144.

Wan, W.C., Hien, W.N., Ping, T.P., Aloysius, A.J.W. 2009. A study on the effectiveness of heat mitigating pavement coatings in Singapore. In: Second International Conference on Countermeasures to Urban Heat Islands, Berkeley, California, September, 2009.

Xu, T., Sathaye, J., Akbari, H., Garg, V., Tetali, S. 2012. Quantifying the direct benefits of cool roofs in an urban setting: Reduced cooling energy use and lowered greenhouse gas emissions. *Building and environment* 48: 1-6.

Zinzi, M., Agnoli, S. 2012. Cool and green roofs. An energy and comfort comparison between passive cooling and mitigation urban heat island techniques for residential buildings in the Mediterranean region. *Energy and Buildings* 55: 66-76.

7. INTERNET SOURCES

ENVI-met:

http://www.envi-met.com/ (accessed August 2012)

Google Maps:

http://www.maps.google.com/ (accessed August 2012)

The International Organization for Standardization (ISO):

http://www. iso.org/iso/home/store/catalogue_tc/ (accessed December 2013)

Organization for Economic Co-operation and Development (OECD):

http://www.oecd.org/ (accessed December 2012)

Stadt Wien:

http://www.wien.gv.at/stadtplan/ (accessed July 2012)

Statistik Austria:

http://www.statistik.at/web_de/statistiken/ (accessed July 2012)

World Maps of Köppen-Geiger Climate Classification:

http://www.koeppen-geiger.vu-wien.ac.at/ (accessed December 2012)

Zentralanstalt für Meteorologie und Geodynamik (ZAMG):

http://www.zamg.ac.at/ (accessed August 2012)

8. INDEX

8.1 List of tables

8.2 List of figures

8.3 List of formulas

9. APPENDIX

9.1 Abbreviations

CET   Central European Time

GHG   Greenhouse gas

ISO   The International Organization for Standardization

LCA   Life cycle assessment/analysis

LWS   Living wall system

NAAQS   National Atmospheric Air Quality Standard

NIR   Near-infrared (spectrum)

OECD   Organization for Economic Co-operation and Development

PCM   Phase - change materials

PET   Physiological Equivalent Temperature

PMV   Predicted Mean Vote

PPS   Permeable pavement system

RH   Relative humidity

SVF   Sky view factor

UHI   Urban heat island

UHII   Urban heat island intensity

WS   Wind speed

ZAMG   Zentralanstalt für Meteorologie und Geodynamik

9.2 Vienna – facts

Population growth for a period of 20 years and completed dwellings in Vienna for the years with the steepest growth can be seen in Figure 9.1 and Table 9.1, respectively.
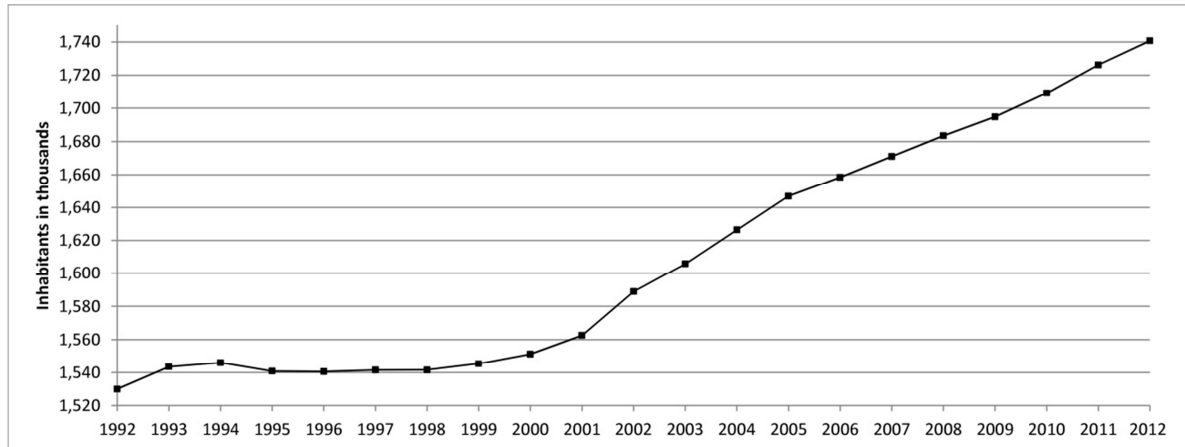
Figure 9.1 Population growth in Vienna for the last 20 years (according to Statistik Austria 2012)

Table 9.1

Residential dwellings completed in Vienna (according to Statistik Austria 2012)

YEAR	DWELLINGS COMPLETED IN VIENNA
1998	9.363
1999	12.878
2000	11.713
2001	6.329
2002	5.628

9.3 Mobile measurements

The monitored data from all days of measurements is averaged for each street and parameter and a reference measuring period is created. Obtained distributions can be seen in Figures 9.2 – 9.6. Differences of minimum and maximum monitored values from mobile measurements are depicted in Figures 9.7 – 9.15. Tables 9.2 – 9.7 show average, minimum and maximum values for each measuring period of 20min. Hemispherical sky images and SVF of both streets can be seen in Figure 9.16.
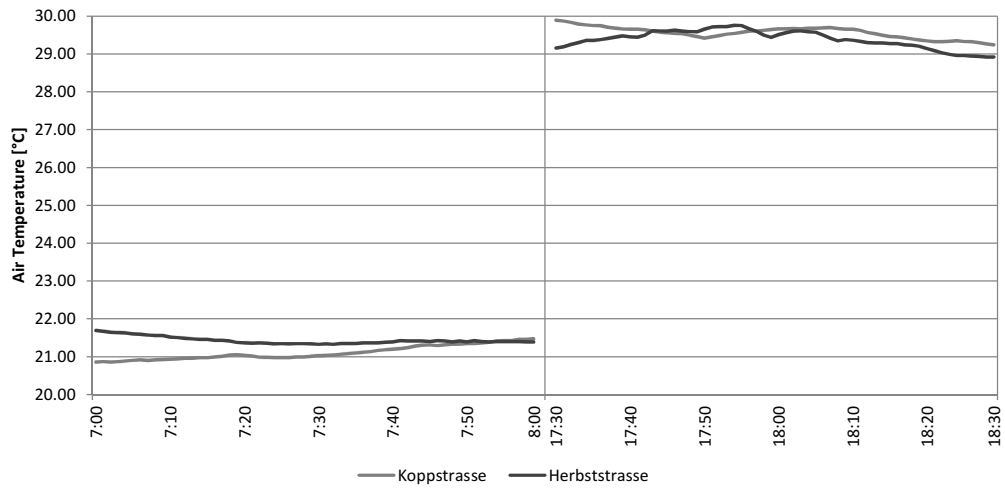
Figure 9.2 Distribution of mean air temperatures at Koppstrasse and Herbststrasse
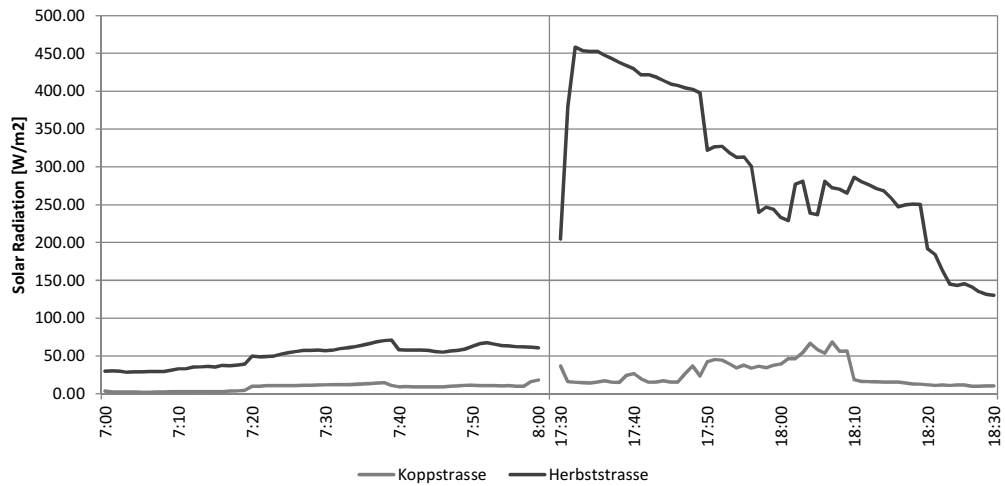
Figure 9.3 Distribution of mean solar radiation at Koppstrasse and Herbststrasse
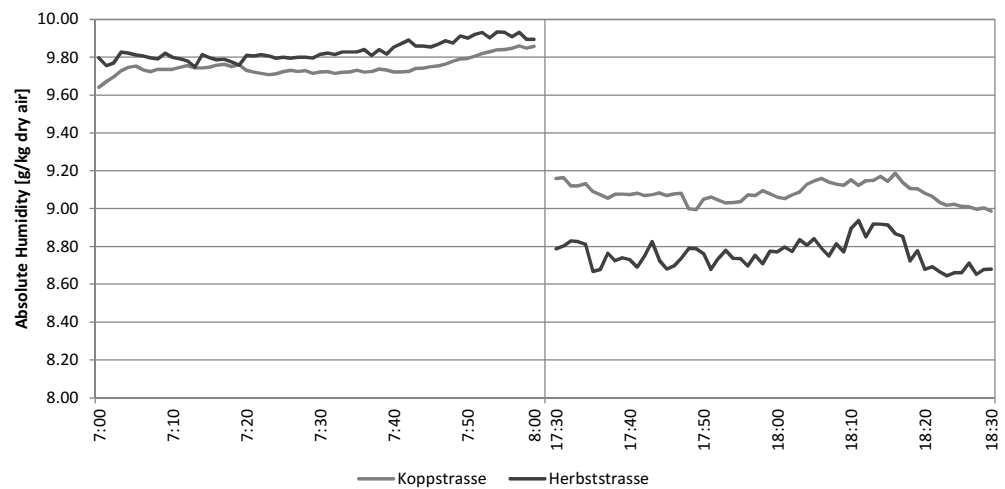
Figure 9.4 Distribution of mean absolute humidity at Koppstrasse and Herbststrasse
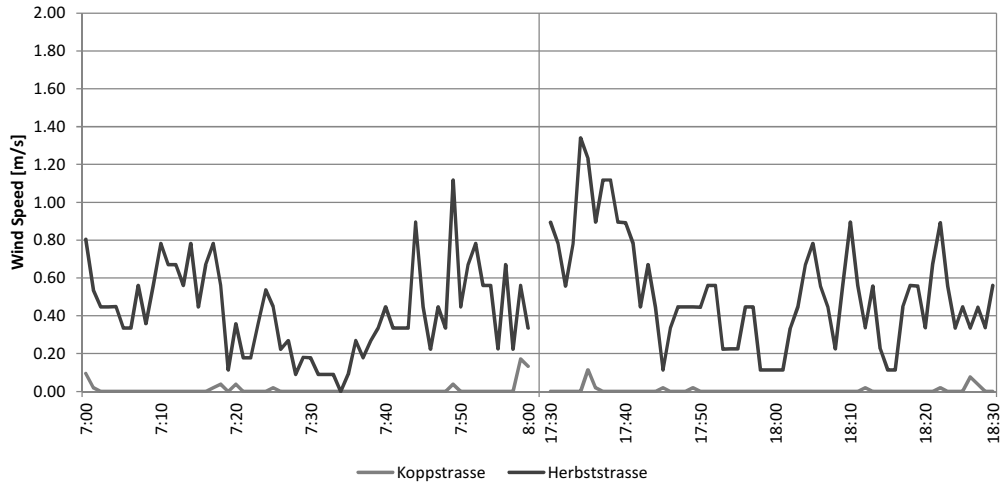
Figure 9.5 Distribution of mean wind speed at Koppstrasse and Herbststrasse
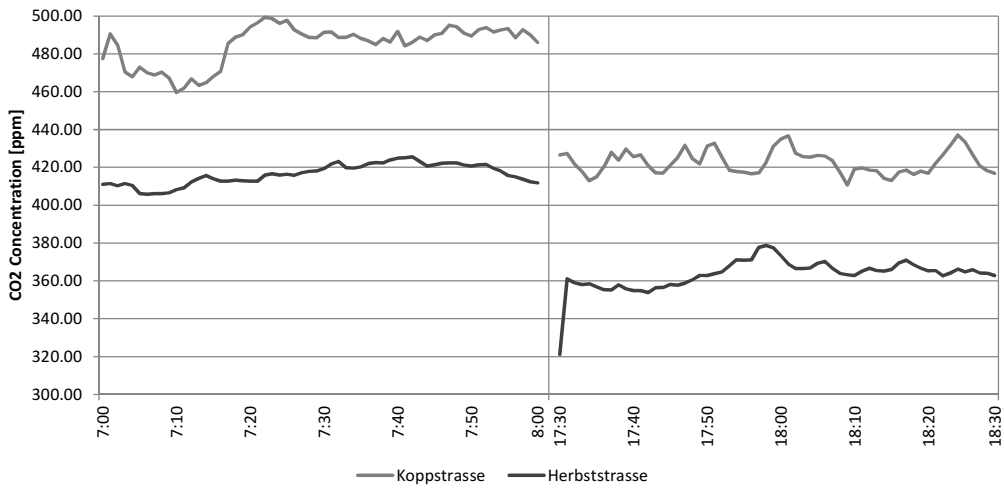
Figure 9.6 Distribution of mean CO$_2$ concentrations at Koppstrasse and Herbststrasse
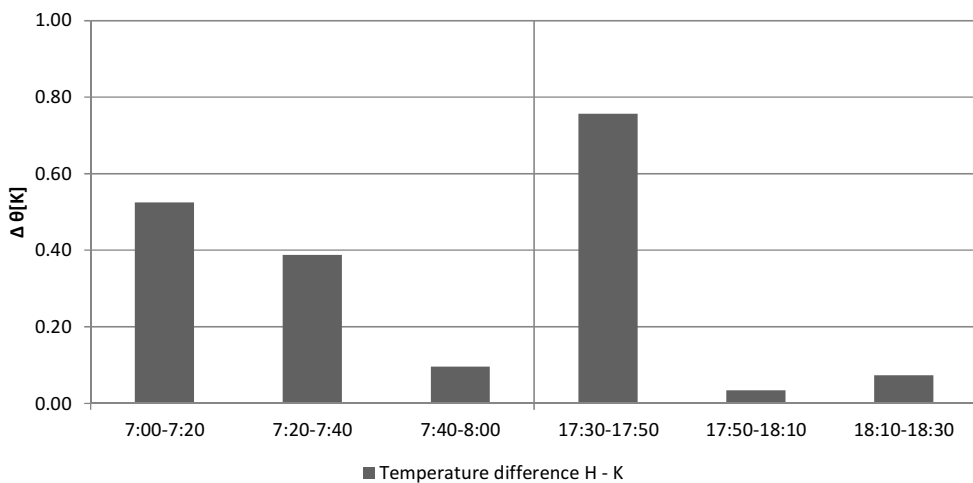
Figure 9.7 Differences of minimum air temperatures between Herbststrasse and Koppstrasse

78
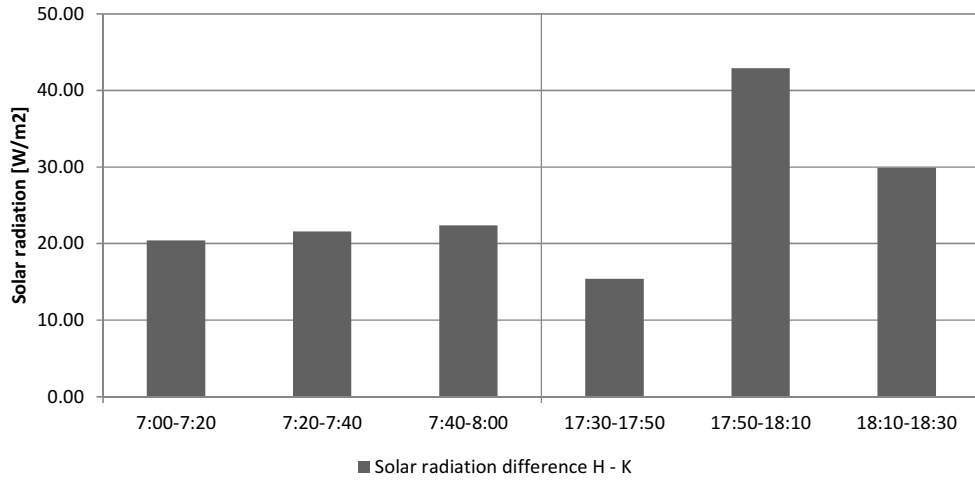
Figure 9.8 Differences of minimum solar radiation between Herbststrasse and Koppstrasse
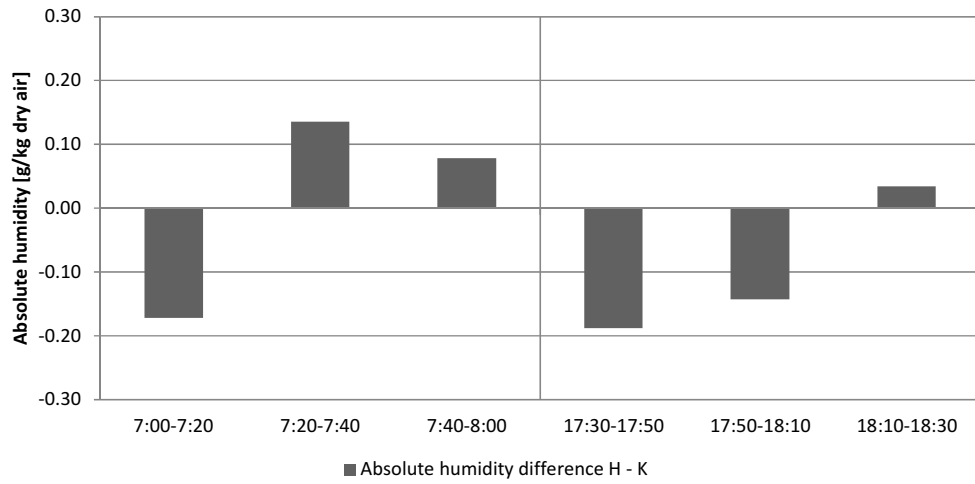
Figure 9.9 Differences of minimum absolute humidity between Herbststrasse and Koppstrasse
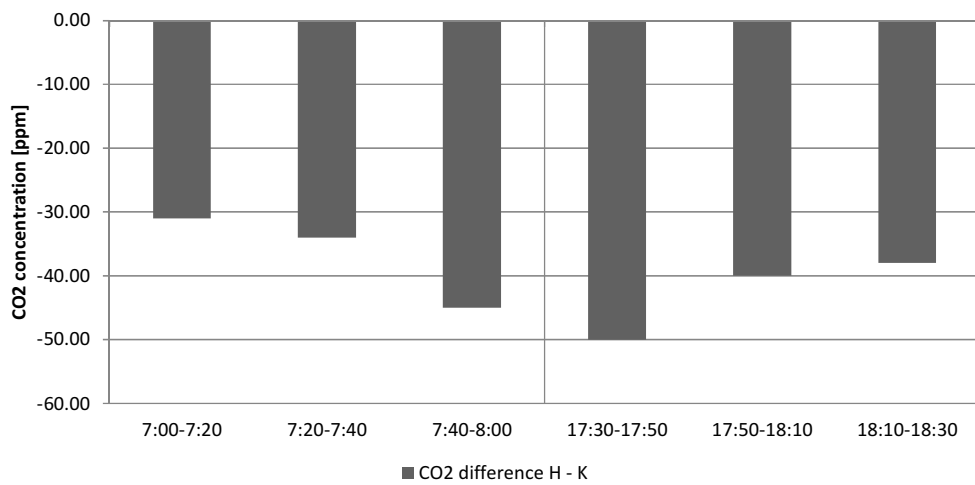
Figure 9.10 Differences of minimum CO2 concentrations between Herbststrasse and Koppstrasse
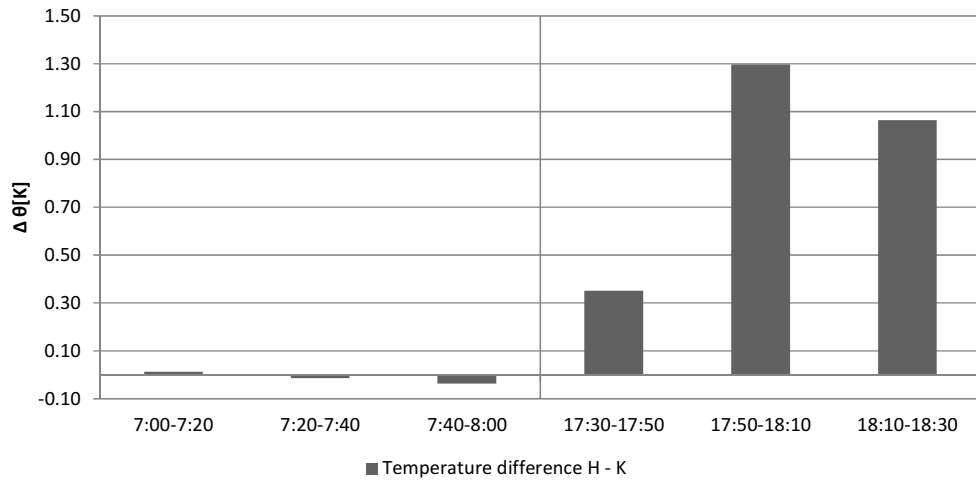
Figure 9.11 Differences of maximum air temperatures between Herbststrasse and Koppstrasse
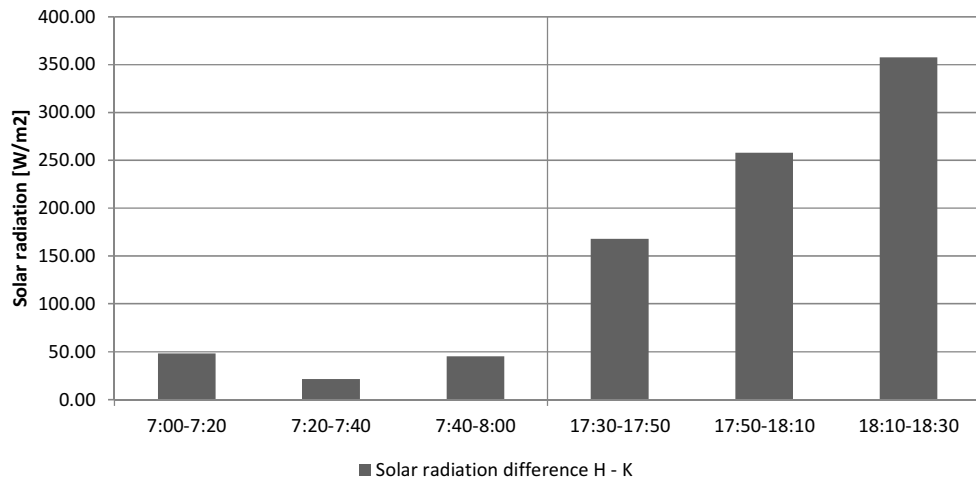
Figure 9.12 Differences of maximum solar radiation between Herbststrasse and Koppstrasse
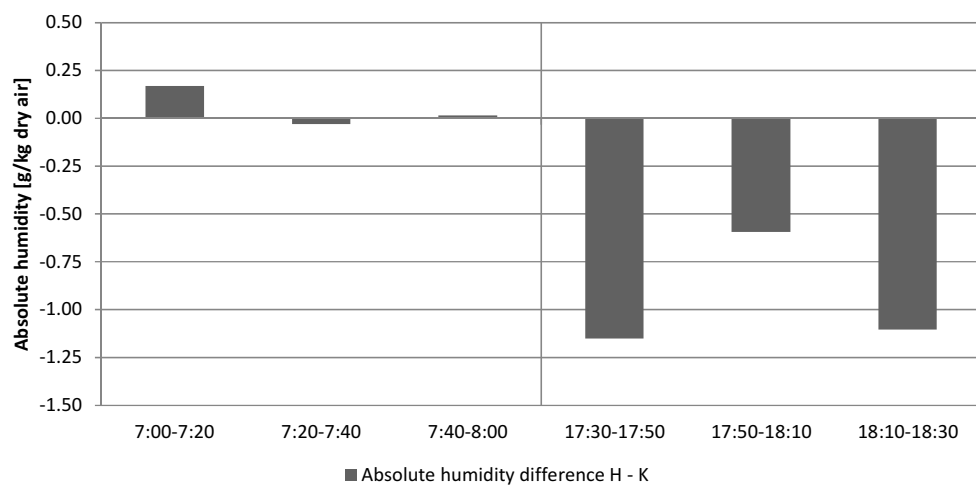
Figure 9.13 Differences of maximum absolute humidity between Herbststrasse and Koppstrasse
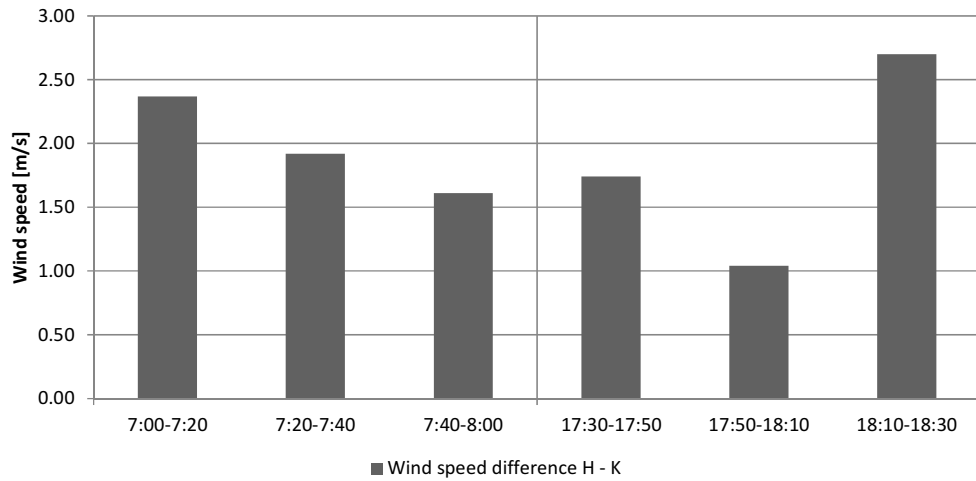
Figure 9.14 Differences of maximum wind speed between Herbststrasse and Koppstrasse
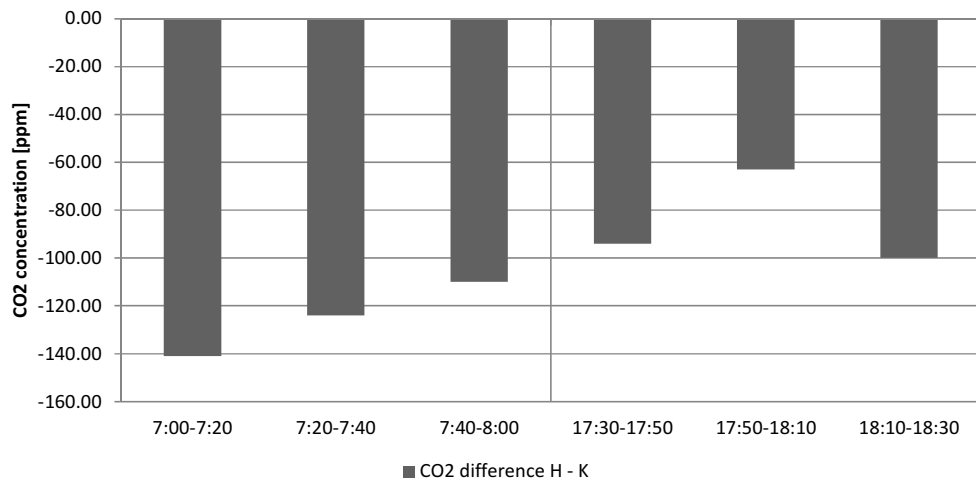
Figure 9.15 Differences of maximum CO₂ concentrations between Herbststrasse and Koppstrasse

Table 9.2

Exact dates and time of mobile measurements with averaged values for the monitored parameters at Koppstrasse

DATE	PLACE	TIME	Koppstrasse - Average Values					
			Air Temperature [°C]	Solar Radiation [W/m2]	Relative Humidity [%]	Absolute Humidity [g/kg dry air]	Wind Speed [m/s]	CO2 [ppm]
17 July 2012	1.Spot	7:00-7:20	16.55	3.77	61.83	7.43	0.01	439.37
	2.Spot	7:20-7:40	16.53	16.07	61.57	7.39	0.00	441.85
	3.Spot	7:40-8:00	16.47	13.19	63.40	7.58	0.08	439.22
	1.Spot	17:30-17:50	21.13	24.93	52.11	8.21	0.43	410.22
	2.Spot	17:50-18:10	21.42	37.28	51.50	8.25	0.32	412.46
	3.Spot	18:10-18:30	21.07	14.50	52.60	8.26	0.36	412.29
7 Aug 2012	1.Spot	7:00-7:20	/	/	/	/	/	/
	2.Spot	7:20-7:40	/	/	/	/	/	/
	3.Spot	7:40-8:00	/	/	/	/	/	/
	1.Spot	17:30-17:50	25.29	23.92	43.88	8.76	0.00	393.84
	2.Spot	17:50-18:10	25.65	30.78	43.33	8.83	0.00	409.05
	3.Spot	18:10-18:30	25.09	8.51	44.02	8.69	0.00	393.80
8 Aug 2012	1.Spot	7:00-7:20	/	/	/	/	/	/
	2.Spot	7:20-7:40	/	/	/	/	/	/
	3.Spot	7:40-8:00	/	/	/	/	/	/
	1.Spot	17:30-17:50	25.27	17.16	44.68	8.91	0.00	431.38
	2.Spot	17:50-18:10	25.42	84.58	43.80	8.81	0.00	413.70
	3.Spot	18:10-18:30	25.33	16.28	44.52	8.91	0.00	413.84
9 Aug 2012	1.Spot	7:00-7:20	19.61	4.07	59.72	8.61	0.00	432.63
	2.Spot	7:20-7:40	19.63	18.01	59.07	8.52	0.00	430.17
	3.Spot	7:40-8:00	20.17	9.40	57.97	8.63	0.00	424.77
	1.Spot	17:30-17:50	/	/	/	/	/	/
	2.Spot	17:50-18:10	/	/	/	/	/	/
	3.Spot	18:10-18:30	/	/	/	/	/	/
19 Aug 2012	1.Spot	7:00-7:20	/	/	/	/	/	/
	2.Spot	7:20-7:40	/	/	/	/	/	/
	3.Spot	7:40-8:00	/	/	/	/	/	/
	1.Spot	17:30-17:50	31.25	23.46	30.99	8.58	0.00	399.77
	2.Spot	17:50-18:10	30.88	39.01	32.75	8.89	0.00	403.13
	3.Spot	18:10-18:30	30.82	15.87	33.54	9.07	0.00	410.90
20 Aug 2012	1.Spot	7:00-7:20	20.70	1.44	63.16	9.71	0.00	535.15
	2.Spot	7:20-7:40	21.10	4.49	62.20	9.78	0.00	561.05
	3.Spot	7:40-8:00	21.86	7.02	60.59	9.95	0.00	566.64
	1.Spot	17:30-17:50	35.60	14.40	28.24	9.82	0.04	442.20
	2.Spot	17:50-18:10	35.18	37.48	27.76	9.45	0.00	443.73
	3.Spot	18:10-18:30	34.95	11.65	26.98	9.08	0.00	445.91
21 Aug 2012	1.Spot	7:00-7:20	25.32	2.64	57.61	11.52	0.01	414.48
	2.Spot	7:20-7:40	25.31	12.01	57.76	11.54	0.01	444.30
	3.Spot	7:40-8:00	25.36	14.67	57.63	11.56	0.01	458.91
	1.Spot	17:30-17:50	30.94	21.20	34.36	9.35	0.00	450.20
	2.Spot	17:50-18:10	30.95	41.49	34.66	9.44	0.00	461.02
	3.Spot	18:10-18:30	30.81	13.03	35.75	9.66	0.03	457.66
22 Aug 2012	1.Spot	7:00-7:20	22.50	2.44	66.91	11.41	0.00	534.85
	2.Spot	7:20-7:40	22.65	8.20	66.12	11.37	0.00	565.07
	3.Spot	7:40-8:00	22.86	9.38	64.51	11.22	0.00	565.11
	1.Spot	17:30-17:50	/	/	/	/	/	/
	2.Spot	17:50-18:10	/	/	/	/	/	/
	3.Spot	18:10-18:30	/	/	/	/	/	/

Table 9.3

Exact dates and time of mobile measurements with averaged values for the monitored parameters at Herbststrasse

DATE	PLACE	TIME	Herbststrasse - Average values					
			Air Temperature [°C]	Solar Radiation [W/m2]	Relative Humidity [%]	Absolute Humidity [g/kg dry air]	Wind Speed [m/s]	CO2 [ppm]
17 July 2012	1.Spot	7:00-7:20	17.46	34.81	59.10	7.50	0.45	394.75
	2.Spot	7:20-7:40	16.81	51.52	61.48	7.50	0.13	409.79
	3.Spot	7:40-8:00	16.60	78.14	64.29	7.75	0.94	413.41
	1.Spot	17:30-17:50	21.81	457.24	50.86	8.33	2.87	342.05
	2.Spot	17:50-18:10	21.52	286.00	51.41	8.28	3.07	366.41
	3.Spot	18:10-18:30	21.25	209.24	52.38	8.31	3.90	360.18
7 Aug 2012	1.Spot	7:00-7:20	/	/	/	/	/	/
	2.Spot	7:20-7:40	/	/	/	/	/	/
	3.Spot	7:40-8:00	/	/	/	/	/	/
	1.Spot	17:30-17:50	26.09	205.50	41.63	8.69	1.45	358.89
	2.Spot	17:50-18:10	25.56	147.81	42.81	8.68	0.59	357.39
	3.Spot	18:10-18:30	24.96	79.63	43.88	8.60	1.93	355.11
8 Aug 2012	1.Spot	7:00-7:20	/	/	/	/	/	/
	2.Spot	7:20-7:40	/	/	/	/	/	/
	3.Spot	7:40-8:00	/	/	/	/	/	/
	1.Spot	17:30-17:50	26.51	425.06	41.50	8.87	0.73	342.05
	2.Spot	17:50-18:10	25.87	330.31	42.19	8.70	0.50	356.05
	3.Spot	18:10-18:30	25.65	239.88	43.69	8.90	0.31	351.89
9 Aug 2012	1.Spot	7:00-7:20	20.52	40.06	57.63	8.76	0.03	380.52
	2.Spot	7:20-7:40	20.30	82.25	58.00	8.70	0.00	381.16
	3.Spot	7:40-8:00	20.23	63.25	58.00	8.67	0.42	363.18
	1.Spot	17:30-17:50	/	/	/	/	/	/
	2.Spot	17:50-18:10	/	/	/	/	/	/
	3.Spot	18:10-18:30	/	/	/	/	/	/
19 Aug 2012	1.Spot	7:00-7:20	/	/	/	/	/	/
	2.Spot	7:20-7:40	/	/	/	/	/	/
	3.Spot	7:40-8:00	/	/	/	/	/	/
	1.Spot	17:30-17:50	31.56	413.75	29.00	8.16	0.48	342.68
	2.Spot	17:50-18:10	32.01	272.00	30.06	8.66	0.39	382.52
	3.Spot	18:10-18:30	31.41	216.25	31.13	8.69	0.25	374.00
20 Aug 2012	1.Spot	7:00-7:20	21.21	28.75	62.00	9.81	0.03	451.16
	2.Spot	7:20-7:40	21.17	37.38	62.88	9.93	0.00	465.61
	3.Spot	7:40-8:00	21.70	28.00	61.88	10.07	0.08	467.95
	1.Spot	17:30-17:50	36.26	386.19	26.00	9.36	1.20	357.34
	2.Spot	17:50-18:10	36.32	245.69	24.94	9.00	0.48	359.05
	3.Spot	18:10-18:30	35.91	195.44	24.31	8.59	0.70	376.25
21 Aug 2012	1.Spot	7:00-7:20	25.39	35.88	58.06	11.66	2.15	387.30
	2.Spot	7:20-7:40	25.39	58.00	58.00	11.64	0.98	391.70
	3.Spot	7:40-8:00	25.35	75.25	58.00	11.62	1.62	386.16
	1.Spot	17:30-17:50	31.33	398.50	32.38	9.00	0.50	376.45
	2.Spot	17:50-18:10	32.10	238.31	31.81	9.21	0.08	400.48
	3.Spot	18:10-18:30	31.26	138.63	33.19	9.19	0.48	366.58
22 Aug 2012	1.Spot	7:00-7:20	23.05	29.94	64.00	11.26	0.00	436.00
	2.Spot	7:20-7:40	23.08	67.81	64.00	11.28	0.03	453.05
	3.Spot	7:40-8:00	23.19	58.81	64.00	11.35	0.00	456.11
	1.Spot	17:30-17:50	/	/	/	/	/	/
	2.Spot	17:50-18:10	/	/	/	/	/	/
	3.Spot	18:10-18:30	/	/	/	/	/	/

Table 9.4

Exact dates and time of mobile measurements with minimum values for the monitored parameters at Koppstrasse

DATE	PLACE	TIME	Koppstrasse - Minimum values					
			Air Temperature [°C]	Solar Radiation [W/m2]	Relative Humidity [%]	Absolute Humidity [g/kg dry air]	Wind Speed [m/s]	CO_2 [ppm]
17 July 2012	1.Spot	7:00-7:20	16.42	1.90	61.30	7.31	0.00	412.00
	2.Spot	7:20-7:40	16.39	6.90	61.30	7.30	0.00	433.00
	3.Spot	7:40-8:00	16.34	6.90	61.70	7.32	0.00	433.00
	1.Spot	17:30-17:50	20.91	20.60	51.40	8.00	0.00	402.00
	2.Spot	17:50-18:10	21.25	14.40	51.00	8.09	0.00	405.00
	3.Spot	18:10-18:30	20.82	3.10	52.00	8.04	0.00	394.00
7 Aug 2012	1.Spot	7:00-7:20	/	/	/	/	/	/
	2.Spot	7:20-7:40	/	/	/	/	/	/
	3.Spot	7:40-8:00	/	/	/	/	/	/
	1.Spot	17:30-17:50	25.04	5.60	43.00	8.47	0.00	380.00
	2.Spot	17:50-18:10	25.16	13.10	42.30	8.39	0.00	377.00
	3.Spot	18:10-18:30	24.70	3.10	42.50	8.21	0.00	386.00
8 Aug 2012	1.Spot	7:00-7:20	/	/	/	/	/	/
	2.Spot	7:20-7:40	/	/	/	/	/	/
	3.Spot	7:40-8:00	/	/	/	/	/	/
	1.Spot	17:30-17:50	25.09	15.60	43.90	8.67	0.00	385.00
	2.Spot	17:50-18:10	25.23	39.40	43.00	8.56	0.00	390.00
	3.Spot	18:10-18:30	25.19	11.90	44.10	8.75	0.00	402.00
9 Aug 2012	1.Spot	7:00-7:20	19.51	1.90	58.90	8.44	0.00	418.00
	2.Spot	7:20-7:40	19.48	14.40	58.00	8.30	0.00	408.00
	3.Spot	7:40-8:00	19.87	6.90	57.50	8.41	0.00	404.00
	1.Spot	17:30-17:50	/	/	/	/	/	/
	2.Spot	17:50-18:10	/	/	/	/	/	/
	3.Spot	18:10-18:30	/	/	/	/	/	/
19 Aug 2012	1.Spot	7:00-7:20	/	/	/	/	/	/
	2.Spot	7:20-7:40	/	/	/	/	/	/
	3.Spot	7:40-8:00	/	/	/	/	/	/
	1.Spot	17:30-17:50	30.67	13.10	30.10	8.08	0.00	380.00
	2.Spot	17:50-18:10	30.62	36.90	31.50	8.43	0.00	392.00
	3.Spot	18:10-18:30	30.72	11.90	33.20	8.93	0.00	380.00
20 Aug 2012	1.Spot	7:00-7:20	20.41	0.60	62.50	9.44	0.00	490.00
	2.Spot	7:20-7:40	20.96	4.40	61.40	9.58	0.00	542.00
	3.Spot	7:40-8:00	21.44	5.60	60.10	9.64	0.00	545.00
	1.Spot	17:30-17:50	35.29	13.10	27.90	9.55	0.00	422.00
	2.Spot	17:50-18:10	34.97	34.40	27.10	9.12	0.00	415.00
	3.Spot	18:10-18:30	34.86	9.40	26.50	8.87	0.00	424.00
21 Aug 2012	1.Spot	7:00-7:20	25.14	1.90	57.20	11.32	0.00	398.00
	2.Spot	7:20-7:40	25.23	9.40	57.30	11.41	0.00	410.00
	3.Spot	7:40-8:00	25.31	9.40	57.40	11.47	0.00	438.00
	1.Spot	17:30-17:50	30.90	13.10	33.70	9.15	0.00	435.00
	2.Spot	17:50-18:10	30.82	35.60	33.90	9.17	0.00	420.00
	3.Spot	18:10-18:30	30.57	8.10	34.50	9.21	0.00	413.00
22 Aug 2012	1.Spot	7:00-7:20	22.37	1.90	65.30	11.05	0.00	516.00
	2.Spot	7:20-7:40	22.61	5.60	65.40	11.22	0.00	538.00
	3.Spot	7:40-8:00	22.68	8.10	63.80	10.99	0.00	539.00
	1.Spot	17:30-17:50	/	/	/	/	/	/
	2.Spot	17:50-18:10	/	/	/	/	/	/
	3.Spot	18:10-18:30	/	/	/	/	/	/

Table 9.5

Exact dates and time of mobile measurements with minimum values for the monitored parameters at Herbststrasse

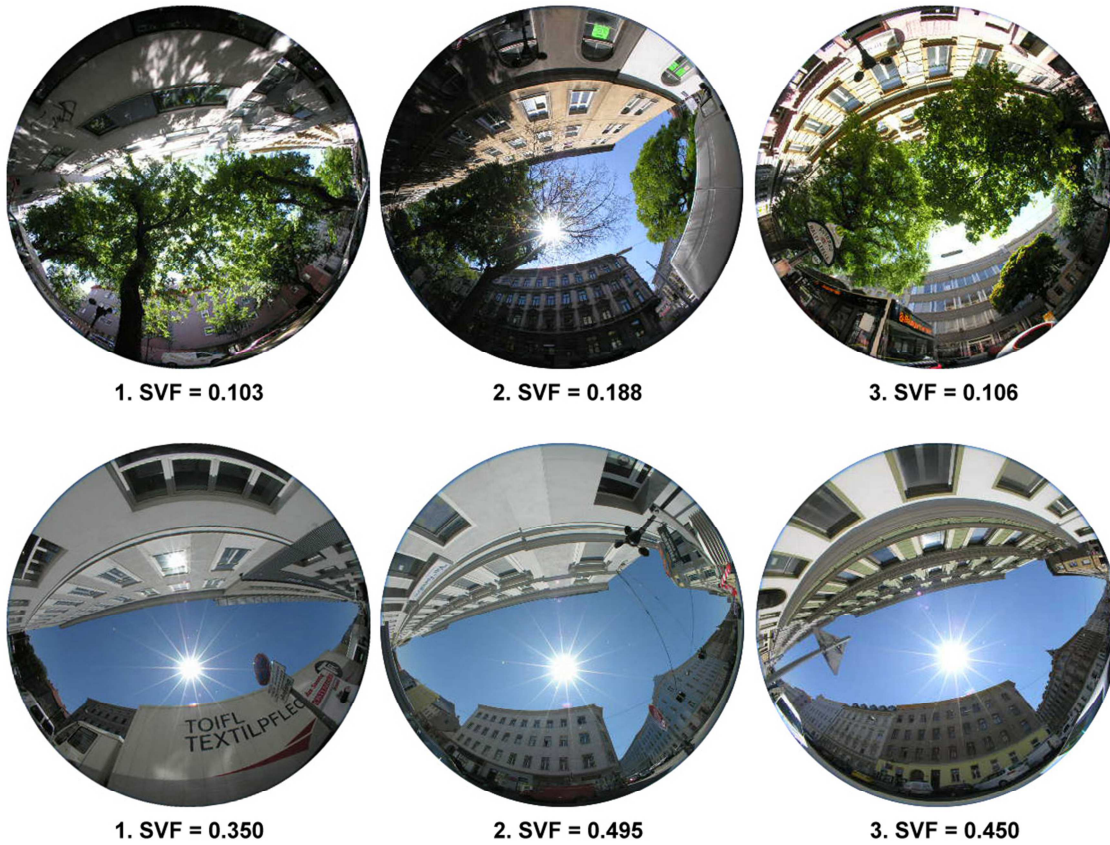| DATE	PLACE	TIME	Herbststrasse - Minimum values					
			Air Temperature	Solar Radiation	Relative Humidity	Absolute Humidity	Wind Speed	CO2
			[°C]	[W/m2]	[%]	[g/kg dry air]	[m/s]	[ppm]
17 July 2012	1.Spot	7:00-7:20	16.94	26.00	58.00	7.14	0.00	389.00
	2.Spot	7:20-7:40	16.78	26.00	61.00	7.43	0.00	395.00
	3.Spot	7:40-8:00	16.44	65.00	62.00	7.40	0.45	404.00
	1.Spot	17:30-17:50	21.67	21.00	50.00	8.13	1.79	335.00
	2.Spot	17:50-18:10	21.28	67.00	50.00	7.94	1.79	339.00
	3.Spot	18:10-18:30	20.89	33.00	52.00	8.08	2.68	355.00
7 Aug 2012	1.Spot	7:00-7:20	/	/	/	/	/	/
	2.Spot	7:20-7:40	/	/	/	/	/	/
	3.Spot	7:40-8:00	/	/	/	/	/	/
	1.Spot	17:30-17:50	25.89	63.00	41.00	8.47	0.45	352.00
	2.Spot	17:50-18:10	25.33	56.00	42.00	8.41	0.00	348.00
	3.Spot	18:10-18:30	24.83	35.00	43.00	8.37	0.45	351.00
8 Aug 2012	1.Spot	7:00-7:20	/	/	/	/	/	/
	2.Spot	7:20-7:40	/	/	/	/	/	/
	3.Spot	7:40-8:00	/	/	/	/	/	/
	1.Spot	17:30-17:50	26.06	396.00	40.00	8.34	0.00	337.00
	2.Spot	17:50-18:10	25.28	292.00	41.00	8.18	0.00	337.00
	3.Spot	18:10-18:30	25.39	211.00	43.00	8.63	0.00	342.00
9 Aug 2012	1.Spot	7:00-7:20	20.44	21.00	57.00	8.63	0.00	367.00
	2.Spot	7:20-7:40	20.28	70.00	58.00	8.70	0.00	374.00
	3.Spot	7:40-8:00	20.11	56.00	58.00	8.61	0.00	359.00
	1.Spot	17:30-17:50	/	/	/	/	/	/
	2.Spot	17:50-18:10	/	/	/	/	/	/
	3.Spot	18:10-18:30	/	/	/	/	/	/
19 Aug 2012	1.Spot	7:00-7:20	/	/	/	/	/	/
	2.Spot	7:20-7:40	/	/	/	/	/	/
	3.Spot	7:40-8:00	/	/	/	/	/	/
	1.Spot	17:30-17:50	31.39	387.00	28.00	7.81	0.00	330.00
	2.Spot	17:50-18:10	31.56	253.00	29.00	8.16	0.00	360.00
	3.Spot	18:10-18:30	31.28	188.00	31.00	8.59	0.00	358.00
20 Aug 2012	1.Spot	7:00-7:20	21.06	28.00	62.00	9.73	0.00	442.00
	2.Spot	7:20-7:40	21.06	35.00	62.00	9.73	0.00	457.00
	3.Spot	7:40-8:00	21.50	28.00	61.00	9.82	0.00	445.00
	1.Spot	17:30-17:50	36.17	359.00	26.00	9.32	0.00	350.00
	2.Spot	17:50-18:10	36.06	223.00	24.00	8.55	0.00	353.00
	3.Spot	18:10-18:30	35.67	167.00	24.00	8.38	0.00	352.00
21 Aug 2012	1.Spot	7:00-7:20	25.33	32.00	58.00	11.61	0.45	383.00
	2.Spot	7:20-7:40	25.33	49.00	58.00	11.61	0.00	384.00
	3.Spot	7:40-8:00	25.33	70.00	58.00	11.61	0.00	383.00
	1.Spot	17:30-17:50	31.22	374.00	32.00	8.84	0.00	366.00
	2.Spot	17:50-18:10	31.83	186.00	31.00	8.85	0.00	378.00
	3.Spot	18:10-18:30	31.06	46.00	33.00	9.04	0.00	363.00
22 Aug 2012	1.Spot	7:00-7:20	23.00	25.00	64.00	11.23	0.00	429.00
	2.Spot	7:20-7:40	23.06	56.00	64.00	11.26	0.00	443.00
	3.Spot	7:40-8:00	23.11	51.00	64.00	11.30	0.00	449.00
	1.Spot	17:30-17:50	/	/	/	/	/	/
	2.Spot	17:50-18:10	/	/	/	/	/	/
	3.Spot	18:10-18:30	/	/	/	/	/	/

Table 9.6

Exact dates and time of mobile measurements with maximum values for the monitored parameters at Koppstrasse

DATE	PLACE	TIME	Koppstrasse - Maximum values					
			Air Temperature	Solar Radiation	Relative Humidity	Absolute Humidity	Wind Speed	CO2
			[°C]	[W/m2]	[%]	[g/kg dry air]	[m/s]	[ppm]
17 July 2012	1.Spot	7:00-7:20	16.70	8.10	62.50	7.58	0.76	504.00
	2.Spot	7:20-7:40	16.70	69.40	61.90	7.51	0.00	521.00
	3.Spot	7:40-8:00	16.70	61.90	65.00	7.88	1.52	450.00
	1.Spot	17:30-17:50	21.37	43.10	52.80	8.43	2.28	430.00
	2.Spot	17:50-18:10	21.58	191.90	52.00	8.41	3.43	421.00
	3.Spot	18:10-18:30	21.27	25.60	53.50	8.50	2.66	424.00
7 Aug 2012	1.Spot	7:00-7:20	/	/	/	/	/	/
	2.Spot	7:20-7:40	/	/	/	/	/	/
	3.Spot	7:40-8:00	/	/	/	/	/	/
	1.Spot	17:30-17:50	25.62	129.40	44.70	9.09	0.00	408.00
	2.Spot	17:50-18:10	25.84	46.90	44.80	9.23	0.00	421.00
	3.Spot	18:10-18:30	25.77	15.60	45.20	9.27	0.00	415.00
8 Aug 2012	1.Spot	7:00-7:20	/	/	/	/	/	/
	2.Spot	7:20-7:40	/	/	/	/	/	/
	3.Spot	7:40-8:00	/	/	/	/	/	/
	1.Spot	17:30-17:50	25.45	19.40	45.60	9.19	0.00	454.00
	2.Spot	17:50-18:10	25.55	203.10	44.50	9.02	0.00	439.00
	3.Spot	18:10-18:30	25.55	29.40	44.90	9.10	0.00	426.00
9 Aug 2012	1.Spot	7:00-7:20	19.79	8.10	60.30	8.79	0.38	466.00
	2.Spot	7:20-7:40	19.84	20.60	59.60	8.71	0.00	469.00
	3.Spot	7:40-8:00	20.32	11.90	58.40	8.77	0.00	484.00
	1.Spot	17:30-17:50	/	/	/	/	/	/
	2.Spot	17:50-18:10	/	/	/	/	/	/
	3.Spot	18:10-18:30	/	/	/	/	/	/
19 Aug 2012	1.Spot	7:00-7:20	/	/	/	/	/	/
	2.Spot	7:20-7:40	/	/	/	/	/	/
	3.Spot	7:40-8:00	/	/	/	/	/	/
	1.Spot	17:30-17:50	31.71	88.10	32.20	9.13	0.00	444.00
	2.Spot	17:50-18:10	31.10	41.90	33.30	9.14	0.00	437.00
	3.Spot	18:10-18:30	31.00	20.60	34.00	9.28	0.38	433.00
20 Aug 2012	1.Spot	7:00-7:20	20.94	11.90	63.90	9.95	0.00	562.00
	2.Spot	7:20-7:40	21.39	5.60	62.70	10.03	0.00	570.00
	3.Spot	7:40-8:00	22.20	8.10	61.30	10.27	0.00	600.00
	1.Spot	17:30-17:50	36.04	15.60	28.60	10.18	1.52	480.00
	2.Spot	17:50-18:10	35.26	46.90	28.20	9.64	0.00	455.00
	3.Spot	18:10-18:30	35.00	14.40	27.50	9.27	0.00	462.00
21 Aug 2012	1.Spot	7:00-7:20	25.43	3.10	58.20	11.71	0.38	463.00
	2.Spot	7:20-7:40	25.40	15.60	58.10	11.68	0.76	468.00
	3.Spot	7:40-8:00	25.43	19.40	57.80	11.63	0.38	491.00
	1.Spot	17:30-17:50	31.03	363.10	35.20	9.63	0.00	470.00
	2.Spot	17:50-18:10	31.08	80.60	35.60	9.76	0.00	487.00
	3.Spot	18:10-18:30	31.03	16.90	37.00	10.12	0.76	495.00
22 Aug 2012	1.Spot	7:00-7:20	22.63	4.40	68.10	11.70	0.00	601.00
	2.Spot	7:20-7:40	22.68	9.40	66.90	11.52	0.00	600.00
	3.Spot	7:40-8:00	22.97	10.60	65.50	11.47	0.00	578.00
	1.Spot	17:30-17:50	/	/	/	/	/	/
	2.Spot	17:50-18:10	/	/	/	/	/	/
	3.Spot	18:10-18:30	/	/	/	/	/	/

Table 9.7

Exact dates and time of mobile measurements with maximum values for the monitored parameters

at Herbststrasse

DATE	PLACE	TIME	Herbststrasse - Maximum values					
			Air Temperature [°C]	Solar Radiation [W/m2]	Relative Humidity [%]	Absolute Humidity [g/kg dry air]	Wind Speed [m/s]	CO_2 [ppm]
17 July 2012	1.Spot	7:00-7:20	18.00	40.00	60.00	7.86	0.89	412.00
	2.Spot	7:20-7:40	16.89	77.00	62.00	7.61	1.79	417.00
	3.Spot	7:40-8:00	16.78	107.00	66.00	8.04	1.79	420.00
	1.Spot	17:30-17:50	21.94	531.00	52.00	8.58	4.02	385.00
	2.Spot	17:50-18:10	21.94	461.00	52.00	8.58	4.47	379.00
	3.Spot	18:10-18:30	21.39	387.00	54.00	8.63	5.36	379.00
7 Aug 2012	1.Spot	7:00-7:20	/	/	/	/	/	/
	2.Spot	7:20-7:40	/	/	/	/	/	/
	3.Spot	7:40-8:00	/	/	/	/	/	/
	1.Spot	17:30-17:50	26.28	381.00	42.00	8.86	2.24	370.00
	2.Spot	17:50-18:10	25.78	202.00	43.00	8.82	1.34	369.00
	3.Spot	18:10-18:30	25.22	148.00	44.00	8.75	2.68	367.00
8 Aug 2012	1.Spot	7:00-7:20	/	/	/	/	/	/
	2.Spot	7:20-7:40	/	/	/	/	/	/
	3.Spot	7:40-8:00	/	/	/	/	/	/
	1.Spot	17:30-17:50	27.06	457.00	43.00	9.48	2.68	352.00
	2.Spot	17:50-18:10	26.22	357.00	44.00	9.25	2.24	398.00
	3.Spot	18:10-18:30	26.06	265.00	44.00	9.17	1.34	370.00
9 Aug 2012	1.Spot	7:00-7:20	20.61	60.00	58.00	8.86	0.45	391.00
	2.Spot	7:20-7:40	20.33	91.00	58.00	8.72	0.00	389.00
	3.Spot	7:40-8:00	20.33	69.00	58.00	8.72	1.34	384.00
	1.Spot	17:30-17:50	/	/	/	/	/	/
	2.Spot	17:50-18:10	/	/	/	/	/	/
	3.Spot	18:10-18:30	/	/	/	/	/	/
19 Aug 2012	1.Spot	7:00-7:20	/	/	/	/	/	/
	2.Spot	7:20-7:40	/	/	/	/	/	/
	3.Spot	7:40-8:00	/	/	/	/	/	/
	1.Spot	17:30-17:50	31.89	439.00	30.00	8.59	1.34	373.00
	2.Spot	17:50-18:10	32.61	294.00	31.00	9.22	1.34	404.00
	3.Spot	18:10-18:30	31.61	246.00	32.00	9.03	0.89	384.00
20 Aug 2012	1.Spot	7:00-7:20	21.33	30.00	62.00	9.88	0.45	460.00
	2.Spot	7:20-7:40	21.28	39.00	63.00	10.01	0.00	476.00
	3.Spot	7:40-8:00	21.89	28.00	62.00	10.20	0.45	490.00
	1.Spot	17:30-17:50	36.39	418.00	26.00	9.42	2.24	363.00
	2.Spot	17:50-18:10	36.56	267.00	26.00	9.50	1.34	375.00
	3.Spot	18:10-18:30	36.06	223.00	25.00	8.91	1.79	395.00
21 Aug 2012	1.Spot	7:00-7:20	25.44	39.00	59.00	11.88	3.13	392.00
	2.Spot	7:20-7:40	25.39	72.00	58.00	11.65	2.68	402.00
	3.Spot	7:40-8:00	25.39	76.00	58.00	11.65	3.13	390.00
	1.Spot	17:30-17:50	31.44	431.00	33.00	9.23	1.34	386.00
	2.Spot	17:50-18:10	32.22	279.00	33.00	9.62	0.89	424.00
	3.Spot	18:10-18:30	31.61	248.00	34.00	9.59	1.34	387.00
22 Aug 2012	1.Spot	7:00-7:20	23.06	39.00	64.00	11.26	0.00	447.00
	2.Spot	7:20-7:40	23.17	76.00	64.00	11.34	0.45	461.00
	3.Spot	7:40-8:00	23.28	72.00	64.00	11.41	0.00	465.00
	1.Spot	17:30-17:50	/	/	/	/	/	/
	2.Spot	17:50-18:10	/	/	/	/	/	/
	3.Spot	18:10-18:30	/	/	/	/	/	/

Figure 9.16 Fisheye pictures at Koppstrasse (upper figure) and Herbststrasse (down figure) taken at noon on 16th June 2012 (ordered: first, second and third spot). Sky view factors calculated according to Holmer et al. (2001)
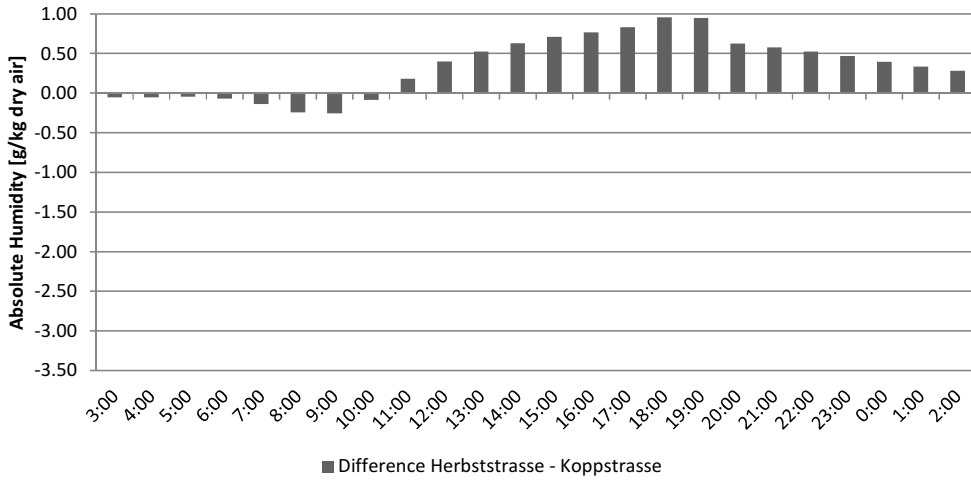
9.4 Computer simulations

Mean absolute humidity differences between Herbststrasse and Koppstrasse in Base Case are shown in Figure 9.17. Absolute humidity differences between Base Case and Improvement cases can be seen in Figures 9.18 - 9.21. Differences of surface temperatures for case C1 (white concrete) are displayed in Figure 9.22.

Figure 9.17 Mean absolute humidity differences between Herbststrasse and Koppstrasse in BC
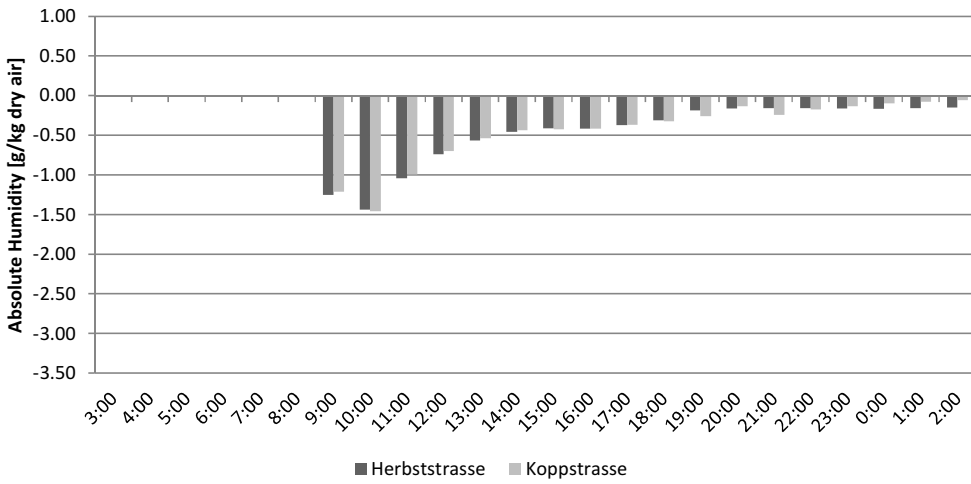
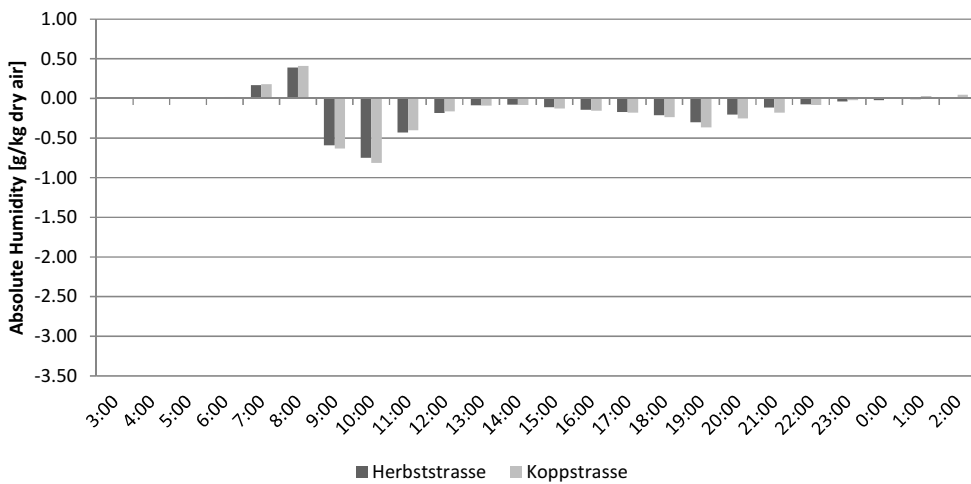*Figure 9.18 Mean absolute humidity differences between BC and C1 (white concrete case)*

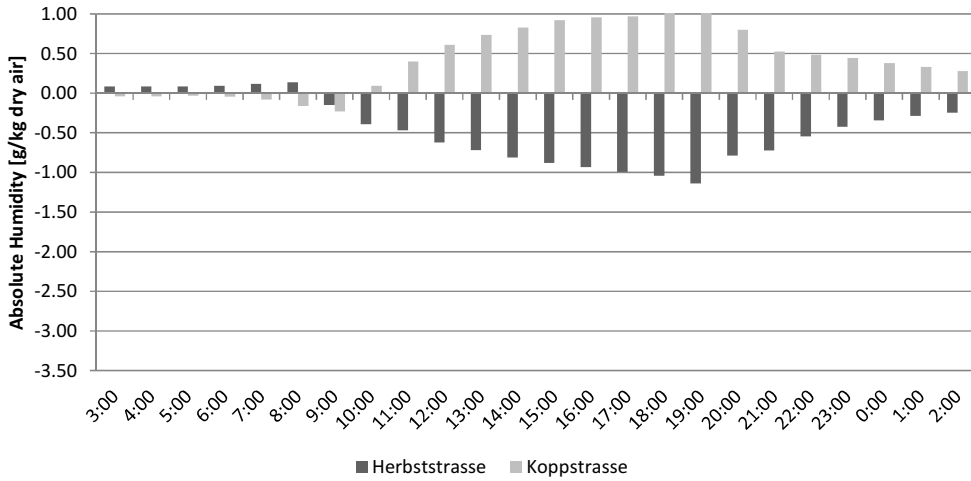*Figure 9.19 Mean absolute humidity differences between BC and C2 (increased albedo case)*

Figure 9.20 Mean absolute humidity differences between BC and C3 (trees case)
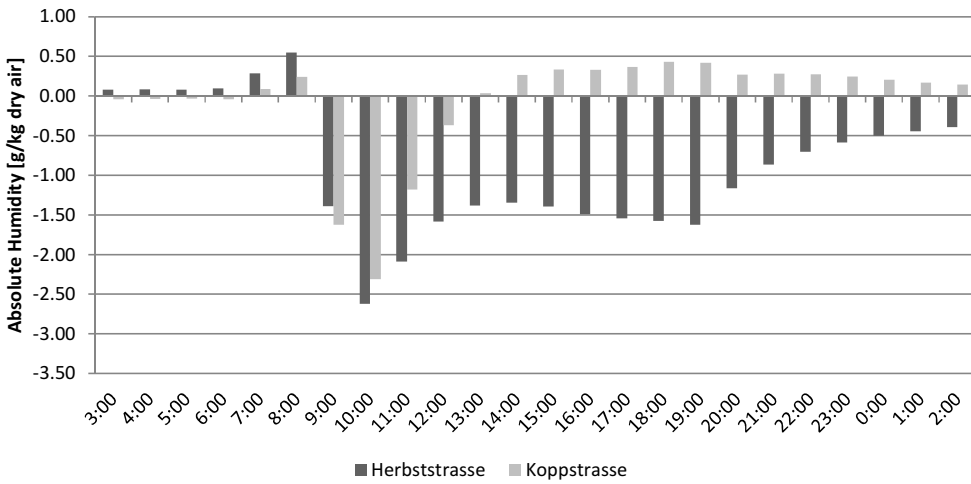

Figure 9.21 Mean absolute humidity differences between BC and C4 (combined cases)
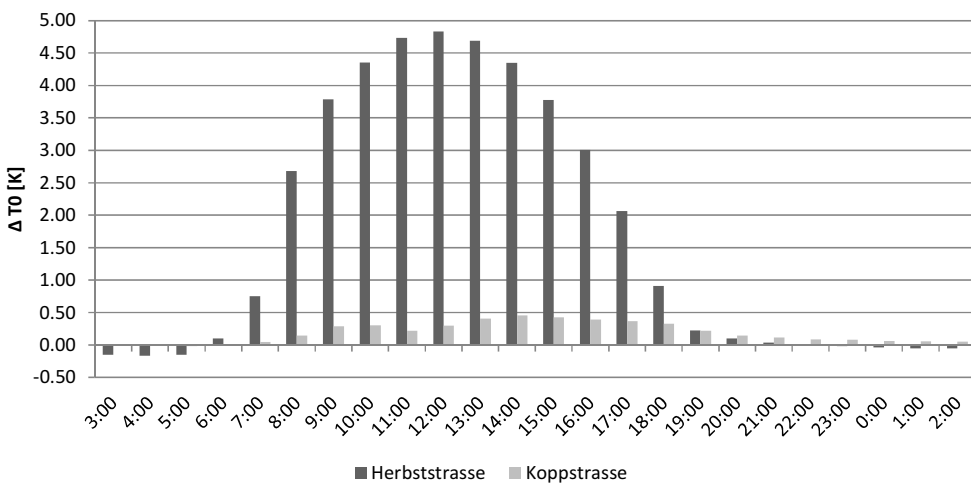

Figure 9.22 Mean surface temperature differences between BC and C1 (white concrete case)